Electron Transport Chain Coupled Protoporphyrinogen IX Oxidase from *Escherichia coli*

Von der Fakultät für Lebenswissenschaften
der Technischen Universität Carolo-Wilhelmina
zu Braunschweig
zur Erlangung des Grades eines
Doktors der Naturwissenschaften
(Dr. rer. nat.)
genehmigte
D i s s e r t a t i o n

von Kalle Möbius
aus Wolfsburg

1. Referent: Prof. Dr. Dieter Jahn
2. Referent: Prof. Dr. Michael Steinert
eingereicht am: 14.05.2008
mündliche Prüfung (Disputation) am: 23.06.2008

Druckjahr 2008

VORVERÖFFENTLICHUNGEN DER DISSERTATION

Teilergebnisse aus dieser Arbeit wurden mit Genehmigung der Fakultät für Lebenswissenschaften, vertreten durch den Mentor der Arbeit, in folgenden Beiträgen vorab veröffentlicht:

EINGEREICHTE PUBLIKATION

Kalle Möbius, Daniela Breckau, Rodrigo Arias, Anna-Lena Hännig, Claudia Schulz, Katrin Riedmann, Rebekka Biedendieck, Dörte Becher, Axel Magalon, Jürgen Moser and Dieter Jahn: Cofactor Biosynthesis is coupled to the Electron Transport mediated Energy Conservation. *Under review.*

TAGUNGSBEITRÄGE

Kalle Möbius, Corinna Lüer, Jürgen Moser, Dieter Jahn. The oxygen-independent magnesium protoporphyrin IX monomethyl ester oxidative cyclase of *Chlorobaculum tepidum* (Poster) ICTPPO, Luzern, Schweiz (2005)

Kalle Möbius, Daniela Breckau, Anna-Lena Hännig, Jürgen Moser and Dieter Jahn. The oxygen-independent Protoporphyrinogen IX Oxidase HemG of *E. coli* couples to aerobic and anaerobic electron transfer chains (Poster) TPDG, Lund, Schweden (2007)

TABLE OF CONTENTS

Abbreviations

A	Ampere
A_λ	absorption at wavelength λ nm
ALA	5-aminolevulinic acid
amp	ampicillin
amp_r	ampicillin resistance
approx.	approximately
APS	ammonium peroxodisulfate
ATP	adenosine triphosphate
AU	absorption units
bp	base pair
BSA	bovine serum albumin
BCIP	5-brom-4-chloro-3-indolylphosphate
CHAPS	3-[(3-Cholamidopropyl)dimethylammonio]propanesulfonic acid
CPI	chloroform phenol isoamyl alcohol
C_V	column volume
Da	Dalton
DCIP	dichloroindophenol
DEAE	diethylaminoethyl
dFU	difference in fluorescence units
H_2O_{deion}	deionised water
DMF	N,N-dimethylformamide
DNA	deoxyribonucleic acid
(d)dNTP	(di)deoxynucleotide
DTT	1,4-dithio-D,L-threitol
e.g.	*exempli gratia* (for instance)
et al.	*et alteri* (and others)
EDTA	ethylenediaminetetraacetic acid
F	Farad
FAD	flavin adenine dinucleotide
FMN	flavin mononucleotide
fig.	figure
Fp	flavoprotein subunit of the fumarate reductase
FPLC	fast performance liquid chromatography
FRD	fumarate reductase
for	forward
FU	fluorescence units
GPC	gel permeation chromatography
h	hour
HemG	protoporphyrinogen IX oxidase
HEPES	4-(2-hydroxyethyl)-piperazine-1-ethane sulfonic acid
Ip	fumarate reductase subunit containing iron-sulfur clusters
IPTG	isopropyl-ß galactopyranosid
kb	kilo base pair (1 kb = 1,000 bp)
λ	wavelength
LC-MS	liquid chromatography – mass spectrometry
l	liter
LB	Luria broth
MCS	multiple cloning site
MOPS	3-morpholinopropanesulfonic acid
M_r	relative moleculare mass
n	nano
NAD(P)H	nicotinamide adenine dinucleotide (phosphate), reduced form

NBT	nitro blue tetrazolium
n.d.	not detectable
Ω	Ohm
OD_{λ}	optical density at wavelength λ nm
ORF	open reading frame
Pa	Pascal
PBS	phosphate buffered saline
PCR	polymerase chain reaction
PEG	polyethylene glycol
pH	negative decadic logarithm of the H^+ concentration in a solution
PPO	protoporphyrinogen IX oxidase
proto	protoporphyrin IX
proto'gen	protoporphyrinogen IX
p.s.i.	pounds per square inch
PVDF	polyvinylidendifluorid
rev	reverse
RNase	ribonuclease
rpm	rotations per minute
RT	room temperature
s.a.	see above
s.b.	see below
SDS	sodium dodecyl sulfate
SDS-PAGE	sodium dodecyl sulfate-polyacrylamide gel electrophoresis
sec	second
ss	single stranded
tab.	table
TAE	TRIS-acetate-EDTA
TB	terrific broth
TE	TRIS-EDTA
TEMED	N,N,N',N',-tetramethyl ethylen diamine
Thesit®	2-dodecoxyethanol
(t)RNA	(transfer) ribonucleic acid
Triton® X-100	t-octylphenoxypolyethoxyethanol
TRIS	Tris-(hydroxymethyl)-aminomethane
TTC	2,3,5- triphenyl-tetrazolium chloride
Tween	Polyoxyethylensorbitanmonolaurat
U	unit
Uro´gen	Uroprophyrinogen III
UV-VIS	ultra violet and visible spectrum of light
V	volt
W	watt
v/v	volume per volume
w/v	weight per volume
℃	centigrade

Glossary

His-tag an amino acid motif consisting of at least six histidine residues
BLAST basic local alignment search tool (*NCBI*-database)

1 Introduction

1.1 Tetrapyrroles

Some dominant colours in nature point towards fundamental biochemical processes which dominate life on earth like the green colour of leaves and the red colour of blood. A class of molecules known as tetrapyrroles is responsible for these phenomenons. Tetrapyrroles are distributed ubiquitously, being indispensable components of the metabolism of almost all organisms on earth.

Tetrapyrroles play a central role in electron transfer-dependent energy generating processes such as photosynthesis and respiration. Further, they function as prosthetic groups for a variety of enzymes. Due to their strong colours, they have been referred to as "pigments of life" (Battersby, 2000). The most commonly found tetrapyrrole in nature is the green, magnesium-containing chlorophyll. It is essential for light harvesting and energy transduction during photosynthesis and responsible for the green colour of plants. Iron-chelating tetrapyrroles such as hemes represent the prosthetic group of hemoglobin and myoglobin (Panek and O'Brian, 2002). They are involved in the transport of oxygen and are responsible for the red colour of blood. More importantly, as prosthetic groups of cytochromes they are indespensable for photosynthesis and oxidative phosphorylation.

1.2 Structure and Functions of Tetrapyrroles

All tetrapyrroles consist of four pyrrole derived groups, linked to each other by single carbon bridges either in linear or in a cyclic arrangement. The basic cyclic structure is termed porphyrin, with four pyrrole rings being covalently connected via methine bridges.

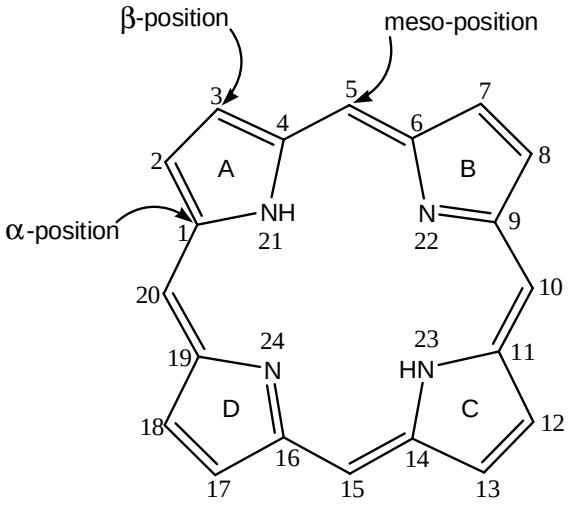

Fig. 1: Basic structure of cyclic tetrapyrroles, the porphyrin ring.
Pyrrole rings are denoted A to D, carbon and nitrogen atoms are numbered. α-position: carbon atoms next to nitrogen atoms. β-positiion: carbon atoms without a direct bond to nitrogen. Meso-position: Bridging carbon atoms between pyrrole rings.

The pyrrole rings of the porphyrin are denoted A to D in a clockwise orientation. Numbering of the carbon and nitrogen atoms is also clockwise and illustrated in figure 1. Carbon atoms adjacent to the nitrogen atoms are termed α-carbons (e.g. C1 and C4 in ring A), while carbon atoms without a direct bond to a nitrogen atom are termed β-carbons (e.g. C2 and C3 in ring A). The methine bridges between the pyrrole rings are constituted of carbon atoms in meso-position (e.g. C5 between ring A and B). During the past 100 years, more and more structural information about these molecules became available (Battersby, 2000). The first structures - those of heme and chlorophyll - were determined in the beginning of the 20th century.

Today, seven different groups of cyclic tetrapyrroles are known. The individual functional properties of each group are determined by the nature of the metal ion chelated by the nitrogen atoms in the center of the ring system as well as by the oxidation state of the macrocycle and sidechain substituents (Frankenberg *et al.*, 2003; Jahn *et al.*, 1996). Figure 2 shows the structures of representatives of the different groups of tetrapyrroles.

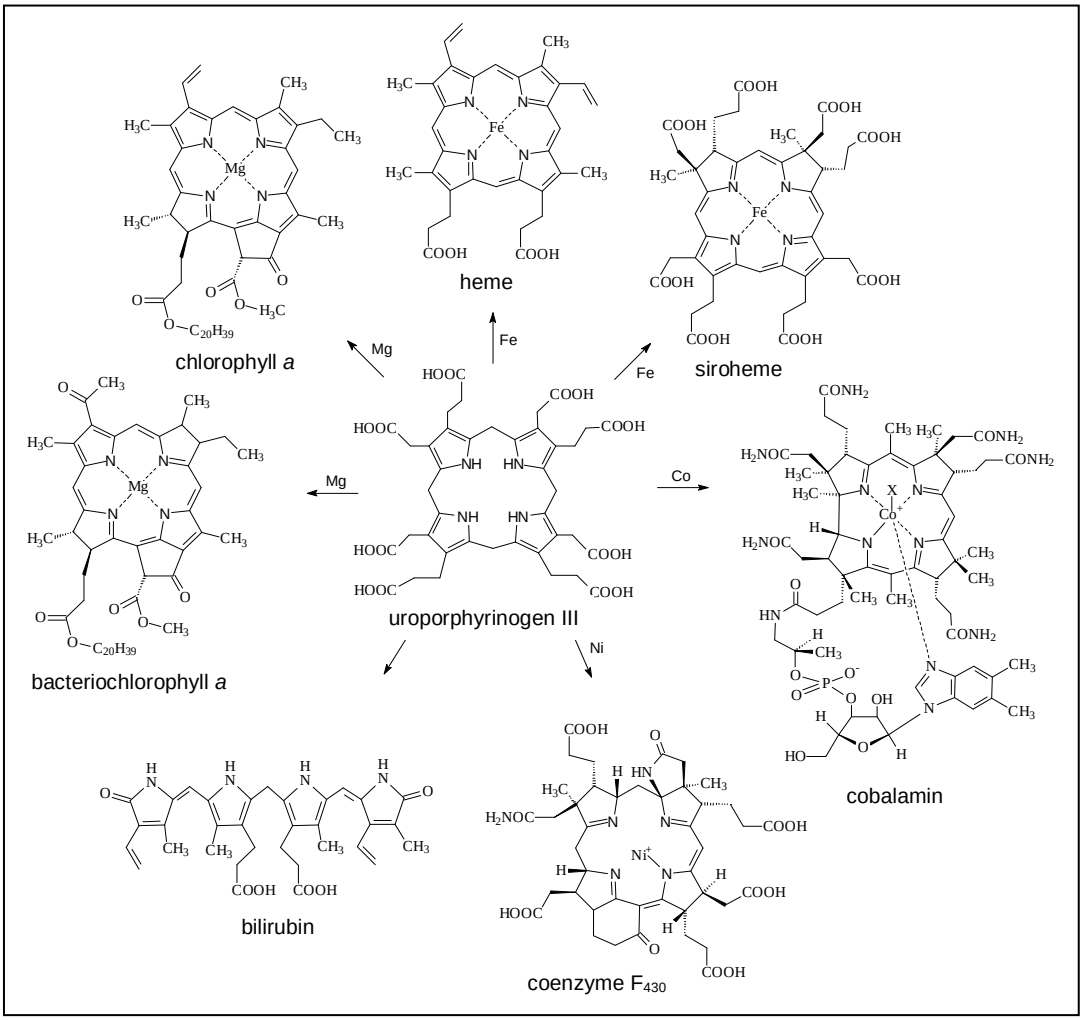

Fig. 2: Structures of important representatives of the seven tetrapyrrole groups.
Depicted are naturally occurring tetrapyrroles and their common precursor molecule uroporphyrinogen III. A = acetate side chain; P = propionate side chain; M = methyl group; V = vinyl group.

Hemes are true porphyrins. They function as prosthetic groups of e.g. hemoglobin and myoglobin, but also of cytochromes, catalases and peroxidases. Heme, an iron-chelating tetrapyrrole, possesses characteristic spectroscopic properties and a red colour due to a complete aromatic ring system. Variations of the basic porphyrin structure lead to tetrapyrroles known as porphinoids, e.g. chlorophylls (chlorins) and bacteriochlorophylls (bacteriochlorins). These molecules contain magnesium as central atom and function as photoreceptors during photosynthesis (Beale 1999). Siroheme (an isobacteriochlorin) and heme d_1 are the cofactors of assimilatory sulfite and nitrite reductase and of dissimilatory nitrite reductase, respectively (Chang, 1994; Warren *et al*., 1994). Like hemes, both contain iron as central atom. Cofactor F_{430} - the tetrapyrrole discovered most recently -

chelates nickel and serves as prosthetic group of methyl coenzyme M reductase, an enzyme involved in archaeal methanogenesis (Friedmann *et al*., 1990; Thauer and Bonacker, 1994). Finally, coenzyme B_{12} belongs to the class of corrinoids, cobalt-containing tetrapyrroles which are characterized by a missing methine bridge (C20) between pyrrole rings A and D (Scott *et al*., 1987). Members of the corrinoids are e.g. cofactors for enzymes catalyzing various transfer and radical - dependent reactions. The seventh group is formed by linear tetrapyrroles such as bilirubin. Like corronoids, they also contain only three bridging carbons. They derive from oxidatively cleaved cyclic tetrapyrroles. The cleavage product of heme, biliverdin, serves as a precursor for the biosynthesis of phycobilins and phytochrome chromophores (Beale and Yeh, 1999). The variety of functions fulfilled by tetrapyrroles underscores their importance in nature. Life without tetrapyrroles would be very different from what we know.

1.3 Biosynthesis of Hemes and Chlorophylls

The shared structural core of tetrapyrroles implies a highly conserved biosynthetic pathway. All tetrapyrroles derive from a common precursor 5-aminolevulinic acid (ALA). This molecule is the exclusive source of all carbon and nitrogen atoms required for the formation of the tetrapyrrole macrocycle. The initial steps of the biosynthetic pathway from ALA are conserved throughout the different biosynthetic routes until the formation of the first cyclic intermediate, uroporphyrinogen III (uro´gen III). This intermediate is the last common precursor for two distinct groups of tetrapyrroles: the porphinoids (siroheme, coenzyme F_{430} and vitamin B_{12}), and the porphyrins (hemes and chlorophylls).

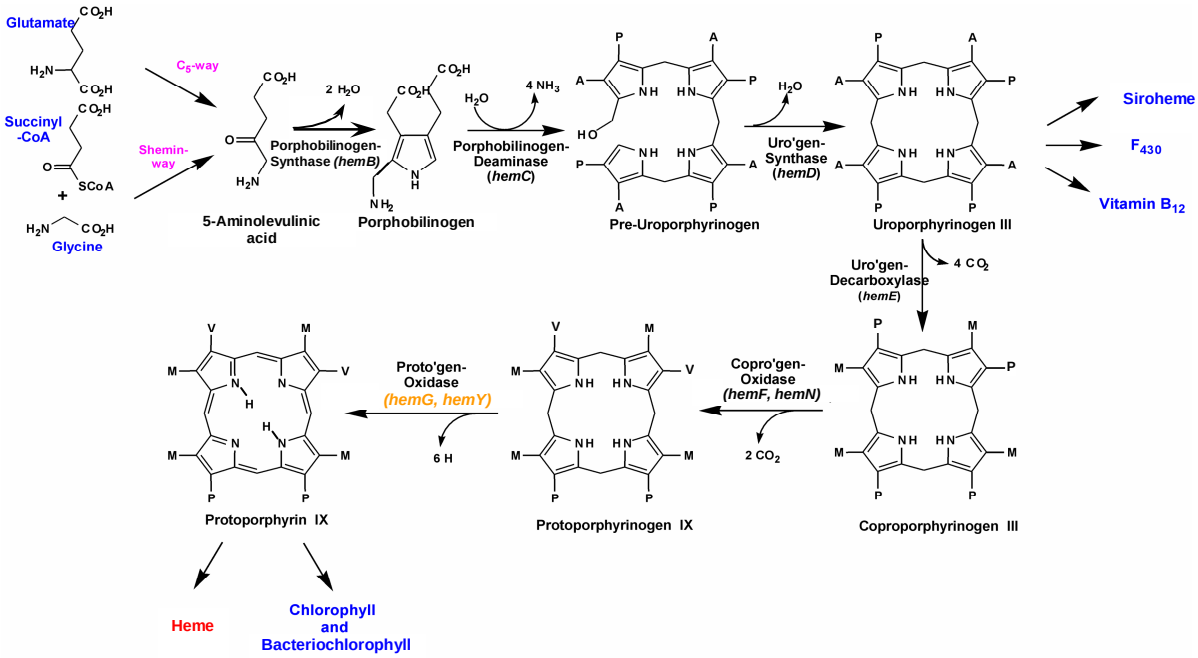

Fig. 3: The biosynthesis of tetrapyrroles.
The names of the enzymes and their respective genes (bacterial) are given above the arrows. A = acetate side chain; P = propionate side chain; M = methyl group; V = vinyl group.

The precursors of chlorophylls and hemes are synthesised by the successive decarboxylation of the four acetate side chains of uro´gen III to produce coproporphyrinogen III. Uro´gen III decarboxylase catalyses this decarboxylation in clockwise direction beginning with the acetate side chain of ring D (Luo and Lim, 1993). In the next step, coproporphyrinogen III oxidases catalyse the conversion of coproporphyrinogen III into protoporphyrinogen IX. Then, protoporphyrinogen IX is converted by the protoporphyrinogen IX oxidase into the aromatic and coloured protoporphyrin IX. The latter step will be described in detail in section 1.4. Protoporphyrin IX represents the branching point of heme and chlorophyll biosynthesis. Insertion of iron into protoporphyrin IX catalysed by ferrochelatase directs the intermediates towards heme biosynthesis (Dailey, 2002), whereas the chelation of magnesium into protoporphyrin IX leads towards the biosynthesis of chlorophylls and bacteriochlorophylls (Willows, 2003).

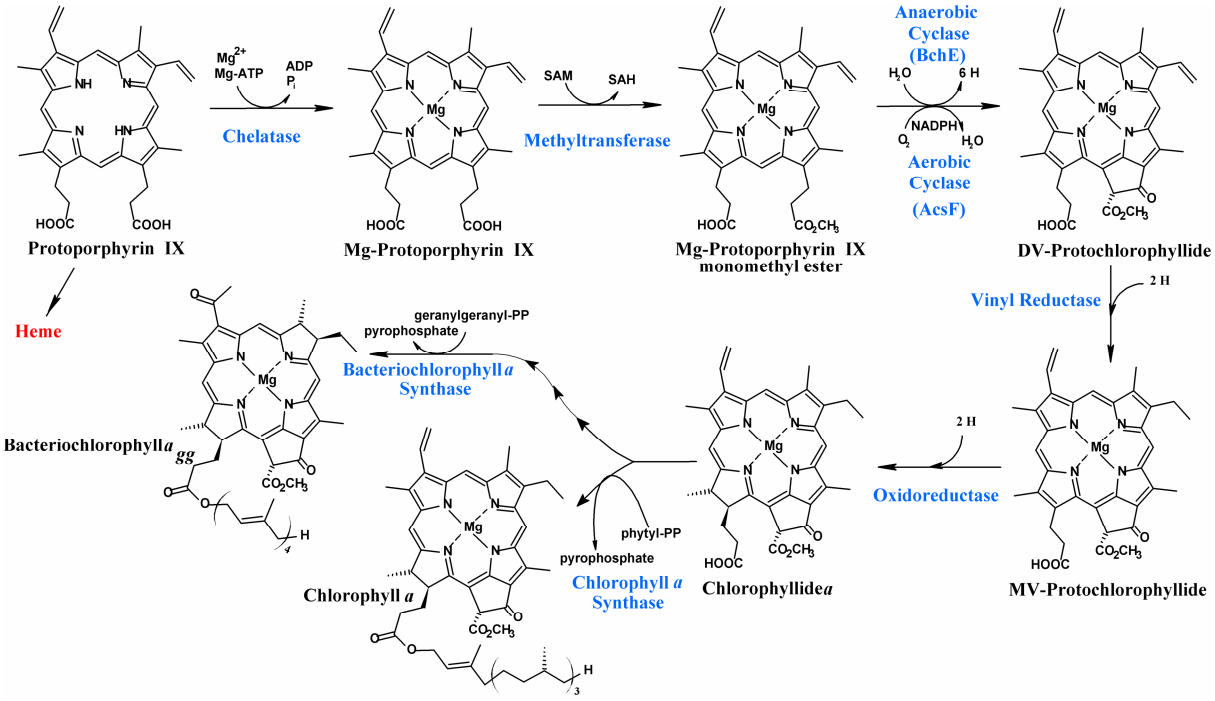

Fig. 4: The biosynthesis of (bacterio-)chlorophyll from protoporphyrin IX
Short names of the enzymes are shown in blue. The branch point towards heme (red) is depicted as well. MV: monovinyl; DV: divinyl

The insertion of magnesium into the macrocycle is catalysed by magnesium protoporphyrin chelatase in an ATP - dependent manner (Viney *et al.*, 2007). Subsequently, magnesium protoporphyrin IX is converted into magnesium protoporphyrin IX monomethyl ester by S-adenosyl-L-methionine (SAM) dependent magnesium protoporphyrin IX methyl transferase (Shepherd and Hunter, 2004). Conversion of magnesium protoporphyrin IX monomethyl ester into 3,8-protochlorophyllide introduces an isocyclic fifth ring to the porphyrin macrocycle which is characteristic for all chlorophylls and bacteriochlorophylls and is described in detail in section 1.6. After this reaction, being performed by magnesium protoporphyrin IX monomethyl ester oxidative cyclases (Bollivar and Beale, 1996), the reduction of the 8-vinyl side chain occurs. It is catalysed by 3,8-divinyl protochlorophyllide *a* 8-vinyl reductase and leads to 3-monovinyl protochlorophyllide. This compound is the substrate for protochlorophyllide oxidoreductases which can be divided into two classes. In angiosperms, the reaction giving chlorophyllide is facilitated from a light - dependent enzyme (McFarlane *et al.*,

2005). On the other hand, in bacteria performing anoxygenic photosynthesis, the reaction is catalysed by a multi-subunit protein complex in a light-independent manner (Nomata *et al*., 2006). Cyanobacteria, algae and gymnosperms possess both types of enzymes. Esterification of chlorophyllide with phytol by chlorophyll a synthase leads to chlorophyll in plants and cyanobactieria. The pathway towards bacteriochlorophyll includes further modifications at the tetrapyrrole backbone until phytol is attached by bacteriochlorophyll synthase (Rüdiger *et al*., 2005).

1.4 Formation of Protoporphyrin IX

The penultimate step of heme biosynthesis – the conversion of protoporphyrinogen IX (proto'gen) into protoporphyrin IX (proto) – is catalysed by protoporphyrinogen IX oxidases (PPO). During this reaction, two of the four imino groups of the pyrrole and the four bridging carbons (C5, C10, C15 and C20) are oxidised (Dailey, 2002). This six electron oxidation gives rise to a completely conjugated, planar and coloured macrocycle (fig. 5).

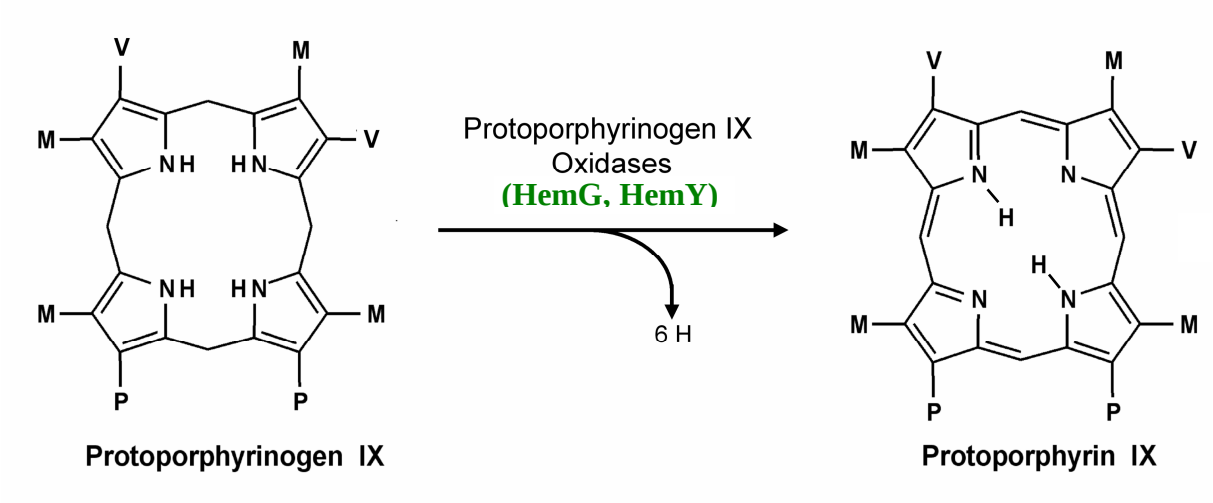

Fig. 5: Conversion of protoporphyrinogen IX into protoporphyrin IX.
P = propionate side chain; M = methyl group; V = vinyl group.

1.4.1 The Oxygen-Dependent Protoporphyrinogen IX Oxidase

The oxygen-dependent protoporphyrinogen IX oxidase (O_2-dependent PPO) is encoded by the gene *hemY* and mainly produced in eukaryotes. It is also found in procaryots like

Myxobacteria (Dailey and Dailey, 1996) and Gram positive bacteria (Hansson and Hederstedt, 1994). During the formation of proto, molecular oxygen serves as the terminal electron acceptor. It is proposed that three moles of dioxygen are consumed per mole of substrate, yielding three moles of H_2O_2 (Koch *et al*., 2004).

Most investigated HemYs in plants, animals and α-*Proteobacteria* occur as a dimeric enzyme. Only HemY of *Bacillus subtilis* has been reported to exist as monomer (Dailey *et al*., 1994). The relative molecular masses of PPO monomers range from M_r = 36,000 (barley) to M_r = 65,000 (cattle). Two isoforms have been found in plants: plastidal PPO I and mitochondrial PPO II (Jacobs and Jacobs, 1984; Jacobs and Jacobs, 1987). PPO I and II from *Nicotiana tabacum* share a sequence identity of only 27 % (Lermontova *et al*., 1997). PPO II is located in the inner mitochondrial membrane with the active site facing the cytosolic face of the membrane (Ferreira *et al*., 1988).

The O_2-dependent PPO belongs to the superfamily of flavin-containing oxidases (Dailey and Dailey, 1998) and utilizes FAD as a cofactor (Camadro *et al*., 1994; Siepker *et al*., 1987). PPO II of *N. tabacum* was the first PPO for which the crystal structure was solved (Koch *et al*., 2004). The structure reveals a homodimeric conformation in which each monomer consists of a FAD-, a substrate- and a membrane-binding domain. The structure was successfully modelled onto the structure of the subsequent enzyme, the human ferrochelatase (Wu *et al*., 2001). Together with experimental data this points towards a possible physical interaction of the two enzymes. During this interaction, the intermediate substrate proto is channelled from PPO directly to ferrochelatase (Ferreira *et al*., 1988). Possibly coproporphyrinogen III oxidase, the antepenultimate enzyme of heme biosynthesis, is also part of this protein complex (Koch *et al*., 2004).

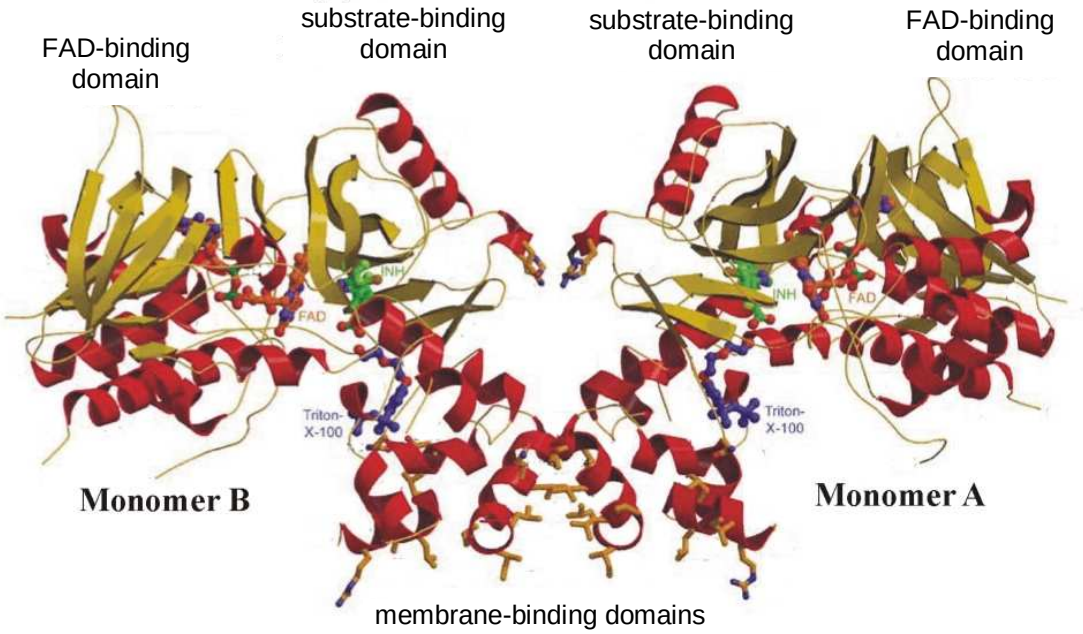

Fig. 6: Structure of the mitochondrial protoporphyrinogen IX oxidase (PPO II) of *Nicotiana tabacum*.
The tobacco mitochondrial PPO is a homodimer. Monomers consist of FAD-, substrate- and membrane-binding domains. The inhibitor phenylpyrazole (green), the FAD-cofactor (orange) and bound Triton® X-100 (blue) are also shown. (Koch *et al.*, 2004)

A prokaryotic HemY from *Myxococcus xanthus* has been co-crystallised with the common herbicide Acifluorfen, a potent inhibitor of HemY (Corradi *et al*., 2006). Aciflourfen is a diphenylether that inhibits investigated HemY´s by blocking the substrate binding site (Table 1).

Table 1: HemY´s of specified organisms and their acifluorfen IC_{50} values
The organisms are grouped in eucaryots and procaryots. The concentrations of acifluorfen where half of the activity is diminished (IC_{50} values) are given except for *Bacillus subtilis*.

cucumber:	500 nM	} (Camadro *et al*., 1991)
yeast:	7 nM	
mouse	250 nM	
Myxococcus xanthus:	2 µM	(Dailey and Dailey, 1996)
Porphyromonas gingivalis:	6 µM	(Kusaba *et al*., 2002)
Bacillus subtilis:	18% at 100 µM	(Dailey *et al*., 1994)

Bilirubin has also been reported to possess an inhibitory effect on murine HemY with a K_i of 25 µM (Ferreira *et al*., 1988).

1.4.2 The Oxygen-Independent Oxidation of Protoporphyrinogen IX

O_2-dependent HemY is found in eukaryotes as well as in many Gram positive bacteria, but not in anaerobic or facultative bacteria like the *Enterobacteriaceae*. For these organisms, a second, oxygen-independent (O_2-independent) system must exist in nature. O_2-independent PPO activity was solubilised from cytoplasmic membranes of *Desulfovibrio gigas* (Klemm and Barton, 1987). The enzyme was described as a complex of three polypeptides with relative molecular masses of M_r = 12,000, 18,500 and 57,000, respectively. In activity assays performed, the artificial electron acceptor dichloroindophenol (DCIP) was used. For this molecule auto-oxidation of the substrate has been demonstrated previously (Breckau, 2005). Therefore, it remains unclear if the purified enzyme complex indeed possessed PPO activity.

O_2-independent PPO activity was also detected in cell-free extracts of *Escherichia coli* when nitrate or fumarate served as electron acceptors. It was suggested that electrons evolving from the oxidation of protoporphyrinogen IX are transferred via the respiratory chains to these molecules (Jacobs and Jacobs, 1975; Jacobs and Jacobs, 1976). Proto formation was sensitve to ultra-violet irradiation and could be restored by adding menadione. Cell-free extracts treated with 2-heptyl-4-hydroxy quinoline-N-oxide (HQNO), an electron transport inhibitor, uncoupled protoporphyrinogen oxidation from fumarate reduction. Taken together, these findings suggest that the overall PPO-reaction in *E. coli* is dependent upon quinones as electron transport carriers (Jacobs and Jacobs, 1978).

The chemically mutated *E. coli* K12 strain SASX38 accumulates proto and is reduced in anaerobic PPO-activity. The accumulation of product was explained with the nonenzymatical conversion of substrate. The phenotype was tracked down to a mutation of the gene *hemG* (Sasarman *et al.*, 1979). Complementation of SASX38 with *hemG* restores PPO-activity, suggesting that the gene product is involved in the O_2-independent PPO-reaction (Sasarman *et al.*, 1993). Due to the small size of HemG (M_r = 21'200 in *E. coli*) and the fact that PPO-activity could not be clearly attributed to the recombinantly

produced protein, it was been assumed that *E. coli* HemG may be a subunit of a larger PPO complex (Dailey and Dailey, 1996; Panek and O'Brian, 2002).

In our laboratory, Dr. Daniela Breckau was able to establish a reproducible activity test for the anaerobic PPO from *E. coli*. Therein, PPO activity is monitored by the formation of the fluorescent product proto. A 60-fold increase of proto formation was found in purified membrane fractions of *E. coli* compared to whole cell lysates. In accordance to Sasarman (1993) and Klemm (1987) it was concluded that the oxygen-independent PPO is either membrane-integral or -associated (Breckau, 2005). A screen for electron acceptors with cell-free extracts of *E. coli* showed that O_2-independent PPO acitivity involves an electron transfer to fumarate. This was in agreement with previous findings (Jacobs & Jacobs, 1975). The fumarate reductase (FRD) deficient E*. coli* strain DW35 was impaired in proto formation. It was concluded that FRD, which oxidises quinones to reduce fumarate, is involved in the flow of electrons from PPO to fumarate. Therefore, fumarate may act as the physiological electron acceptor while the menaquinone pool serves as a redox carrier. Apart from fumarate, triphenyl tetrazoliumchloride (TTC) was found to act as an artificial electron acceptor. This compound has previously been shown to interact with respiratory chains (Rich *et al*., 2001). The postulated flow of electrons from proto'gen via the menaquinone pool to FRD is shown in figure 7.

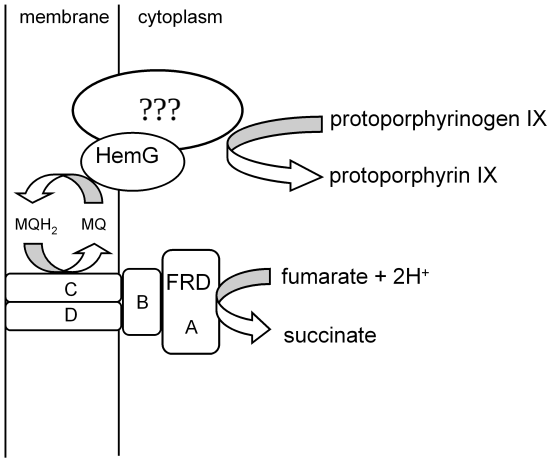

Fig. 7: Working hypothesis of the electron flow during oxidation of protoporphyrinogen IX.
Electrons from the protoporphyrinogen IX oxidase are transferred via the quinone pool to fumarate reductase. HemG is assumed to be a component for the proto´gen oxidation process. **PPO**, protoporphyrinogen IX oxidase; **FRD**, fumarate reductase (subunits A-D); **MQ**, menaquinone; **MQH_2**, reduced menaquinone (Breckau, 2005).

1.5 Respiratory Chains of Escherichia coli

In *E. coli*, the respiratory chains and the aerobic and anaerobic regulation of the corresponding genes are well characterised (Darwin *et al*., 1996; Unden and Bongaerts, 1997). The various electron-transport chains of the facultative anaerobic bacterium involve numerous dehydrogenases and quinone-linked terminal oxidases. The three quinones of *E. coli* are ubiquinone (Q), menaquinone (MQ) and demethylmenaquinone (DMQ). During aerobic respiration, Q serves as the main electron carrier. When O_2 is not present, *E. coli* is capable of utilising other molecules as terminal electron acceptors. If fumarate or dimethyl sulfoxide (DMSO) function as terminal electron acceptors, Q is largely replaced by MQ in anaerobic respiration. Nitrate-dependent growth mainly requires the electron carrier DMQ.

The presence of terminal electron acceptors regulate the expression of six terminal oxido-reductases. O_2 is the preferred electron acceptor producing the highest energy yield. *E. coli* possesses two cytochrome oxidases which are produced differentially depending on the availability of O_2. At high O_2 tensions in the growth medium, cytochrome *bo*3 oxidase dominates over all other terminal oxidases. This enzyme is constituted of four subunits and belongs to the heme-copper superfamily of proton-pumping respiratory oxidases (Rumbley *et al*., 1997). At low O_2 tensions, the second cytochrome oxidase, termed *bd,* is present in the cytoplasmic membrane. It is composed of two subunits and three heme prosthetic groups (Kaysser *et al*., 1995).

Nitrate stimulates the synthesis of nitrate reductase (NarGHI). This enzyme consists of three subunits and possesses molybdo and heme cofactors as well as iron-sulphur-clusters. It is efficiently inhibited by pentachlorophenol (PCP) (Bertero *et al*., 2005).

Fumarate reductase (FRD) from *E. coli* is a membrane-bound flavoprotein catalysing the cytoplasmic reduction of fumarate to succinate, as well as the oxidation of quinones in the membrane (Luna-Chavez *et al*., 2000). The enzyme consists of four polypeptides encoded by the *frdABCD* operon (Jones and Gunsalus, 1985). The gene *frdA* encodes a flavoprotein subunit (FrdA) that binds a FAD cofactor. FrdB contains three iron-sulphur

clusters. The FrdAB-dimer represents the catalytic portion of the complex and is attached to the inner membrane of *E. coli* by the hydrophobic gene products *of frdC* and *frdD*. Subunits C and D are required for the interaction with quinones which serve as proton carriers during the reaction (Cecchini *et al*., 2003). It should be noted that although preferring a specific quinone (see above), fumarate reductase as well as nitrate reductase are able to utilize MQ as well as Q_1 as electron donor (Giordani and Buc, 2004; Maklashina *et al*., 2006).

The hierarchy of terminal electron acceptor utilisation by *E. coli* is O_2 > nitrate > DMSO > TMAO > fumarate.

1.6 Formation of Protochlorophyllide during Chlorophyll Biosynthesis

The addition of the isocyclic, fifth ring to magnesium protoporphyrin IX monomethyl ester (MgPME) is catalysed by MgPME oxidative cyclases (cyclases). This step leads to the formation of protochlorophyllide. To date, two cyclases are known: AcsF (Aerobic enzyme Fe-containing subunit), which, as the name suggests, is dependent on O_2, while the cyclase BchE is O_2-independent. Some organisms contain both enzymes, as shown for *Rubrivivax gelatinosus* (Ouchane *et al*., 2004). However, the anaerobic enzyme is usually found in anaerobic organisms like *Chlorobaculum tepidum*.

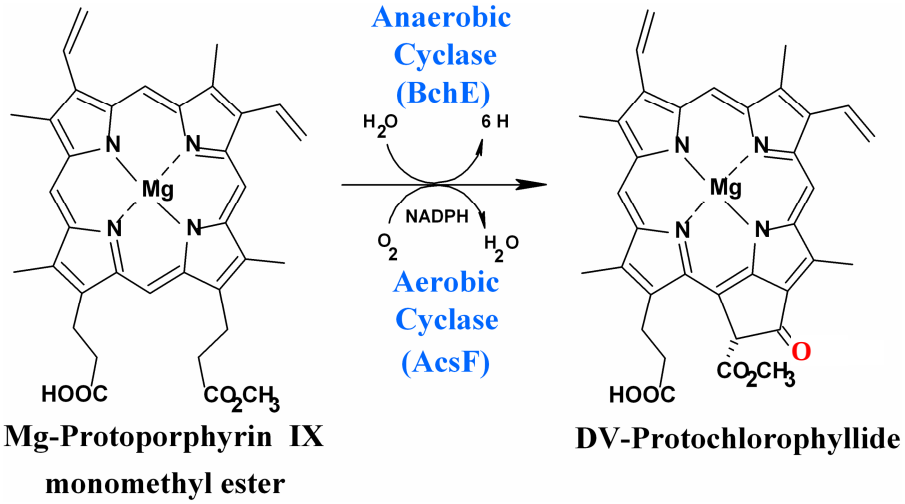

Fig. 8: Conversion of magnesium protoporphrin IX monomethyl ester to protochlorophyllide
O_2-dependent and -independent cyclases (marked in blue) catalyse the conversion of magnesium protoporphrin IX monomethyl ester to protochlorophyllide. The arising oxygen atom at the 13^2 carbon atom (marked in red) is derived from molecular oxygen (AcsF) or from water (BchE).

1.6.1 The Oxygen-Dependent oxidative Cyclisation of Mg-Protoporphyrin IX monomethyl ester

Activity of the O_2-dependent cyclase was detected in chloroplasts of *Chlamydomonas reinhardtii* and cucumber (Chereskin *et al*., 1982), in Barley (Rzeznicka *et al*., 2005) and in cell lysates of *Synechocystis* PCC 6803 (Bollivar and Beale, 1996). As shown in figure 8, the oxygen at position 13^2 of the tetrapyrrole derives from molecular oxygen. For all organisms investigated, cyclase activity was only detectable if cytosolic and membrane fraction were combined. In all the experiments carried out so far, the AcsF subunit was found in the membrane fraction. This points towards a multi-subunit arrangement of the O_2-dependent cyclase (Walker *et al*., 1991). To date, none of the cytosolic subunits could be identified.

1.6.2 The Oxygen-Independent Mg-Protoporphyrin IX monomethyl ester oxidative Cyclase

Organisms performing anoxygenic photosynthesis possess an O_2-independent enzyme system for the cyclisation of MgPME. A *Rhodobacter capsulatus* mutant deficient in *bchE* was found to accumulate MgPME (Biel and Marrs, 1983). Homologs of *bch*E are only

found in phototrophs (Ouchane *et al*., 2004). Consequently, BchE was annotated as O_2-independent cyclase (Bollivar *et al*., 1994). Isotope labelling experiments with the O_2-independent cyclase showed that the oxygen at the 13^2 position of protochlorophyllide was derived from water (Porra *et al*., 1995).

All orthologous BchE sequences show a highly conserved motif containing three cysteines (CXXXCXXC). This sequence motif is also found in enzymes containing [4Fe-4S] clusters. UV-Vis spectra of the purified BchE protein from *R. gelatinosus* were obtained exhibiting properties typical for proteins coordinating [4Fe-4S] clusters (Ouchane *et al*., 2004). These clusters are found in proteins of the radical-SAM family. Members of this family are involved in radical reaction mechanisms associated with the cleavage of (SAM) (Sofia *et al*., 2001). Hence, SAM has been postulated as cofactor for BchE which, however, has not been experimentally verified. The amino-terminus of *R. capsulatus* BchE shares similarities with cobalamin binding domains, e.g from P-methylase from *Streptomyces hygroscopicus*. Indeed, mutants of *R. capsulatus*, deficient in vitamin B_{12} biosynthesis have been shown to accumulate MgPME. This effect was abolished by the addition of exogenous cobalamin or vitamin B_{12} (Gough *et al*., 2000). On the basis of these results, the following reaction mechanism for the formation of the fifth ring was postulated (fig. 9).

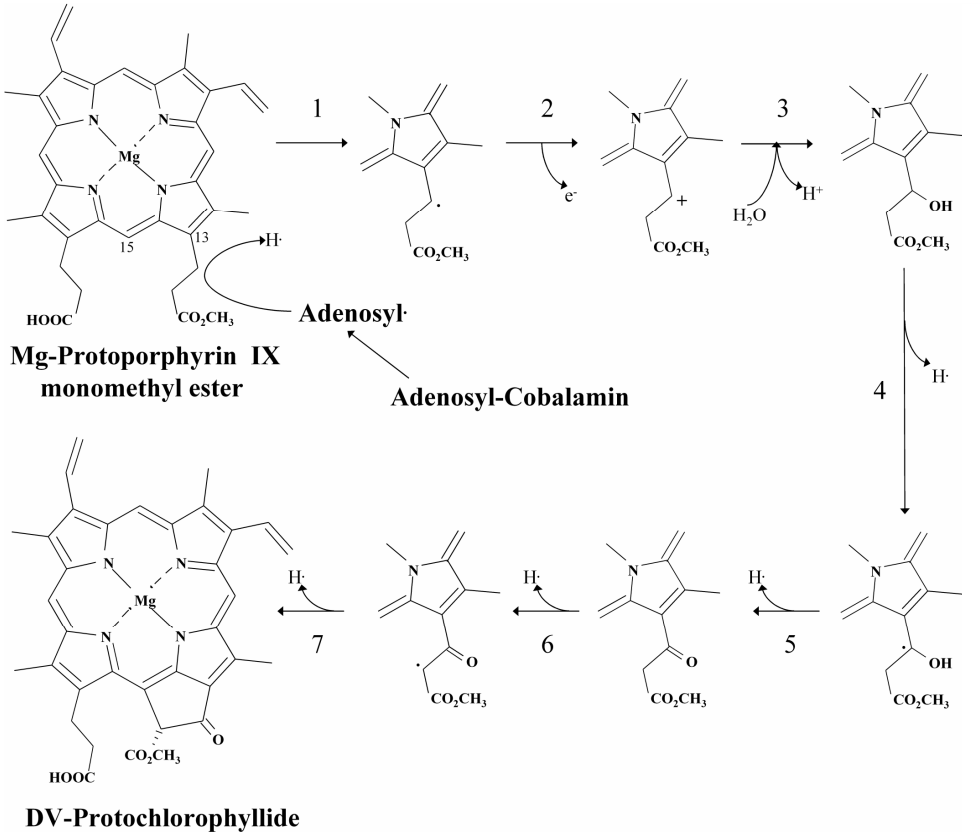

Fig. 9: Proposed reaction mechanism for the formation of protochlorophyllide by O_2-independent cyclase (Gough *et al.*, 2000).

In this reaction, six hydrogen atoms are formally removed from the substrate and from water. It is proposed that the enzyme catalyses the formation of an adenosyl radical from adenosyl-cobalamin. Possibly by a protein radical, a free electron is transferred onto the substrate. Hydrogen is abstracted (fig. 9,1), forming the 13^1-radical of the methyl propionate side chain of MgMPE. Withdrawal of an electron (2) leads to the 13^1-cation of MgMPE, which is attacked by OH^- derived from water (3) yielding the 13^1-hydroxy derivative of MgMPE.

Abstraction of a hydrogen gives the 13^1-OH radical (4) which is postulated to attack the Fe(III)-ion of the FeS-cluster of the enzyme. 13^1-keto-MgMPE is formed by intermolecular electron transfer (5), removal of an hydrogen atom leads to the 13^2-radical (6). This radical attacks the adjacent 15-methene carbon. A last abstraction of a hydrogen gives the isocyclic ring of Pchlide (7). If a radical termination occurs during the reactions, regenerated adenosyl radical reinitiates the process.

1.7 Aim of this study

The penultimate step of heme biosynthesis – the conversion of protoporphyrinogen IX into protoporphyrin IX – is catalysed by two different protoporphyrinogen IX oxidases. To date only the O_2-dependent enzyme system of eukaryotes and Gram positive bacteria has been extensively characterised. Many prokaryotes, as obligate or facultative anaerobes, make use of an O_2-independent PPO. The objective of this work was to identify the O_2-independent PPO. For this purpose, a chromatographic purification strategy for the O_2-independent PPO had to be developed. Once identified, the O_2-independent PPO should be recombinantly produced, purified and biochemically characterised. Beyond the biochemical analysis of this O_2-independent enzyme itself, its integration into various electron transport chains had to be clarified.

An additional aim was to study the O_2-independent conversion from magnesium protoporphyrin IX monomethyl ester to protochlorophyllide during (bacterio-)chlorophyll biosynthesis. For this purpose, the polypeptide BchE was recombinantly produced, purified and biochemically analysed.

2 Materials and Methods

2.1 Instruments and Chemicals

2.1.1 Instruments

agarose gel electrophoresis	Agargel	Biometra
agarose gel documentation	GelDoc	Bio-Rad
anaerobic workstations	Type B Flexible vinyl chamber	COY Laboratory Products Inc.
autoclave	LVSA 50/70	Zirbus
centrifuges	Centrifuge 5415 C	Eppendorf
	Centrifuge 5804	Eppendorf
	Minispin	Eppendorf
	RC 5B Plus	Sorvall
	L8 70M Ultracentrifuge	Beckmann
DNA sequencing	ABI Prism™ 310 Genetic Analyser	Applied Biosystems
electroporation	Gene-Pulser™ II	Bio-Rad
FPLC	ÄKTApurifier™	GE Healthcare
French® Press	French® Pressure Cell	SLM Aminco
HPLC	Jasco 1500	Jasco
luminescence (fluorescence) spectrometer	LS50B	Perkin Elmer
pH determination	pH-Meter C 6840 B	Schott
photometer	Ultrospec 2000	Pharmacia
scales	SBA 52	Scaltec
	BP61S	Sartorius
SDS-PAGE	Mini Protean III	Bio-Rad
thermocycler	Tpersonal	Biometra
thermomixer	Thermomixer 5436	Eppendorf
UV/Visible spectrophotometer	Lambda 2	Perkin Elmer
vortex	Vortex-Genie 2	Scientific Industries
water purification	Milli-Q System	Millipore
western blotting	Semidry-Blot Trans-Blot®SD	Bio-Rad

2.1.2 Materials

cannulas “Sterican”	Braun
DEAE-Sepharose Fast Flow HR 5/5	GE Healthcare
dialysis Visking, type 27/32 exclusion 14,000	Roth
Filter Minisart SRP4	Sartorius
"Gel Blotting Papers”	Roth
glutathione sepharose 4 Fast Flow	GE Healthcare
gravity flow column “Poly-Prep”, 0.8 x 4 cm	Bio-Rad
Ni-NTA Superflow	Qiagen
Precision cuvettes 115F-QS	Hellma
“Roti-PVDF-membrane”	Roth
sterile filter	Millipore, Sartorius
Superdex 200 HR 10/30	GE Healthcare
syringes (1 ml, 5 ml)	Braun

2.1.3 Chemicals, Enzymes and Kits

Antarctic Phosphatase	New England Biolabs
anti-goat HRP-conjugate (rabbit)	Sigma
anti-GST-antibody (goat)	GE Healthcare
anti-His-antibody (mouse)	GE Healthcare
anti-mouse HRP-conjugate FC specific	Sigma
Benzonase	Merck
Bio-Rad Protein Assay	Bio-Rad
Biotherm™ DNA polymerase	Biotherm
FAD	Fluka
FMN	Fluka
GelStar® Nucleic Acid Gel Stain	Cambrex
magnesium protoporphyrin IX monomethyl ester	Frontier Scientific
nucleotides (dNTPs)	Fermentas
Oligonucleotides	MWG Biotech, Biomers
PreScission™ Protease	GE Healthcare
protease inhibitor tablets mini complete EDTA free	Roche
protoporphyrin IX	Sigma
QIAquick Gel Extraction Kit	Qiagen
QIAquick PCR purification kit	Qiagen
QuikChange® Site-Directed Mutagenesis Kit	Stratagene
restriction enzymes and reaction buffers	New England Biolabs

size standard for agarose gels:	
-GeneRuler™ DNA Ladder Mix	Fermentas
-MassRuler™ DNA Ladder Mix	Fermentas
size standards for SDS-PAGE:	
-Protein Molecular Weight Marker	Fermentas
-PageRuler™ Prestained Protein Ladder	Fermentas
T4 ligase	New England Biolabs

Chemicals and reagents not specifically listed here were purchased from the following manufacturers: GE Healthcare, Fluka, Macherey-Nagel, Merck, Riedel-de Haën, Roche, Roth and Sigma.

2.2 Bacterial Strains, Plasmids and Primers

2.2.1 Bacterial Strains

All bacterial strains and plasmids used in this work are listed in table 2 and 3.

Table 2: Bacterial strains used in this work

Strain	Genotype	Reference/Source
Bacillus megaterium WH323	Mutant of WH320, *lac*$^-$ *xyl*$^-$ φ(*xylA1-spoVG-lacZ*)	(Rygus and Hillen, 1992)
Chlorobaculum tepidum TSL	wildtype	DSMZ
Rhodobacter capsulatus DSM 938	wildtype	DSMZ
Escherichia coli strains:		
BL21 (λDE3)	F$^-$*ompZ r*$^-$*m*$^-$ λ_{lys}P*lac*UV5-T7-*GenIPlac*^{q}-*lac*I	Stratagene
DH5α	F$^-$ Φ80d*lacZ*ΔM15(*lac*ZYA-A*rg*F) U169 *rec*A1 *end*A1 *hsd*R17(rk$^-$, mk$^+$) *pho*A *sup*E44 λ$^-$ *thi*-1 *gyr*A96 *rel*A1	Invitrogen
DW35	*Zjd*::Tn10Δ*(frdABCD)*18 *sdh*C::Kan *araD139*Δ*(argF-lac)U169 rpsL150 relA1 flbB5301 deoC1 pfsF25 rbsR*	G. Cecchini, University of California
DS 253	W3110 Δ*lac*U169 *tna*-2 Δ*cyd*::cam Δ*cyo*::kan	D. Siegele, Texas A + M

FB20172	MG1655 *cyoB*::Tn5KAN-2, -pKD46	Blattner Laboratories, U of Wisconsin
FB20228	MG1655 *cydA*::Tn5KAN-2, - pKD46	Blattner Laboratories, U of Wisconsin
GO105	Δ(*cydAB'*)*455 zbg-2200*::*kan cyo-123 recA srlC300*::Tn*10* pRG110	R. Gennis, U of Illinois
JCB4023	RK4353 *narG*::ery D*napA-B narZ*::W	Potter *et al*., 1999

2.2.2 Plasmids

Table 3: Plasmids used in this work

Plasmid	Description	Reference/Source
pC-His1622	Shuttle vector for cloning in *E. coli* (*Amp*^{r}) and gene expression under xylose control in *B. megaterium* (*Tet*^{r}) for the intracellular production of C-terminal His_6-tagged proteins in *B. megaterium*; P_{xylA}-MCS-His_6-Tag-Stop	Biedendieck *et al*., 2007
pC-His1622 *hemG*	*E. coli hemG* cloned into *SphI* and *BglII* of pC-HIS1622 creating P_{xylA}-His_6-Tag-*hemG*-Stop	this work
pETDuet 1 *hemG*	Expression vector encoding the sequence for His_{6x}-*E. coli* HemG fusion protein under the control of a *lac* promoter, Amp^r	Schröder, 2006
pH3	*frdA*$^+$*B*$^+$*C*$^+$*D*$^+$ Amp^r	G. Cecchini, Universtiy of California
pJRHisA	*cyoA*$^+$, *cyoB-histag*$^+$, *cyoC*$^+$, *cyoD*$^+$	R. Gennis, Universtiy of Illinois
pTK1	*cydA*$^+$, *cydB*$^+$	R. Gennis, Universtiy of Illinois

pGEX-6P-1 *bchE*	Expression vector encoding *lac* promoter and sequence for: N-terminal fusion protein of GST from *Schistosoma japonicum*, PreScission™ Protease cleavage site and BchE from *C. tepidum*, *amp*^{r}	this work
pGEX-6P-1 *bchE* His_{4x}	Derivative from pGEX-6P-1 *bchE* with an additional sequence for a C-terminal His-tag	this work

2.2.3 Primers

Oligonucleotide primers for the amplification and cloning of *E. coli hemG* and *C. tepidum bchE* into different vectors were designed. All oligonucleotide primers used in this work are listed below. Recognition sequences of restriction endonucleases are cursive and the extensions homologous to the *E. coli* genome and the *C.tepidum* chromosome are underlined. Primers were purchased from MWG Biotech AG or biomers.net GmbH.

Primers for the cloning of *E. coli hemG* into pCHis1622

HemG for Bmfor GCAAGC*AGATCTC*TAAAACATTAATTCTTTTCTC

HemG for Bmrev AGTAGT*GCATGC*TTCAGCGTCGGTTTG

Primers for the cloning of *C. tepidum* into pGEX-6P-1

CTpGEXCT G*GAATTC*ATGAAAATTCTGATGATTC

CTpGEX/ACYCrev CAT*GTCGAC*TCAGCAGTTGCGG

Primers for the insertion of a C-terminal His_{4x}-tag sequence

2FCtBchEHisF

ACCGTCCGCAACTGCGCGCTCGAACATCATCATCATTGAGTCGACTCGAGCGGC

2RCtBchEHisR

GCCGCTCGAGTCGACTCAATGATGATGATGTTCGAGCGCGCAGTTGCGGACGGT

2.3 Media and Additives

2.3.1 Media

As a standard medium for growth of all bacterial strains Luria broth (LB) medium was used unless indicated otherwise (Sambrook *et al*., 1989). For the production of fumarate reductase glycerol-fumarate-medium was employed (Luna-Chavez *et al*., 2000). Some *E. coli* mutants deficient in

components of respiration chains where cultivated in modified glycerol-fumarate or -nitrate media. For solid media 1.5 % (w/v) agar-agar was added before sterilization.

Luria Bertani (LB)	yeast extract	5.0 g/l
	NaCl	10.0 g/l
	tryptone	10.0 g/l
glycerol-fumarate-medium	KH_2PO_4	5.44 g/l
	K_2HPO_4	10.49 g/l
	$(NH_4)_2SO_4$	2.0 g/l
	$MgSO_4$ x 7 H_2O	50 mg/l
	$FeSO_4$ x 7 H_2O	125 µg/l
	$CaCl_2$	500 µg/l
	glucose	2.0 g/l
	glycerol	3.96 g/l
	casamino acids	500 mg/l
	tryptone	2.0 g/l
	yeast extract	1.0 g/l
	sodium fumarate	6.4 g/l
modified glycerol medium	Tris-HCl pH 7.5	25 mM
	glucose	0.3 % (w/v)
	casaminoacids	1 % (w/v)
	yeast extract	0.1 % (w/v)
	glycerol	40 mM
	sodium fumarate	0.6 % (w/v)
	or	
	KNO_3	0.2 % (w/v)

2.3.2 Additives

Antibiotics and other additives were prepared as concentrated stock solutions, sterilised by filtration (pore width 0.2 µm) and added to the medium after autoclaving. Solutes and concentrations are summarised in Table 4.

Table 4: Media additives

Substance	Solute	Concentration of stock solution	Final concentration
ampicillin	H_2O	100 mg/ml	50 or 100 µg/ml
tetracycline	ethanol (70 % (v/v))	5 mg/ml	10 µg/ml
IPTG	H_2O	1M	50 µM – 1 mM

2.4 Microbiological Techniques

2.4.1 Sterilisation

All media were vapour sterilised at 121 °C and 1 bar positive pressure for 20 min. Other substances and solutions were either vapour sterilised or – if temperature sensitive – sterilised by filtration (pore width 0.2 µm).

2.4.2 Cultivation of Bacteria

Cells for recombinant protein production were cultivated aerobically as described under "Aerobic Cultivation". *E. coli* mutants where first grown under conditions where substantial cell growth was possible. Once cell mass was achieved, cells were shifted to conditions for 45 min where a strong phenotype was expected.

Aerobic Cultivation

Aerobic precultures of *E. coli* were inoculated from glycerol-stocks or single colonies from a plate culture with a sterile toothpick or pipette tip in 100 ml of LB containing the respective antibiotic and grown overnight at 37 °C and 200 rpm in baffled flasks. Aerobic cultures of 100 - 500 ml of LB containing the respective antibiotic were incubated at 37 °C and 200 rpm in baffled flasks after inoculation with 1/100th volume of preculture.

LB-agar plates containing the corresponding antibiotic were utilised for plating 10 - 100 µl of a bacterial cell suspension with a Drygalski spatula. They were incubated aerobically at 37 °C overnight.

For a *B. megaterium* preculture, a volume of 100 ml of LB supplemented with tetracycline was inoculated with a single colony and grown overnight at 37 °C and 100 rpm in baffled flasks. For the main culture, 100 ml of LB containing tetracycline were inoculated with 1/50th volume of preculture and grown at 37 °C and 250 rpm in baffled flasks.

Anaerobic Cultivation

Hundred ml of modified glycerol-medium in rubber-stoppered flasks where inoculated with *E. coli* mutants and flushed with sterile nitrogen. Cultures were then incubated at 37 °C and 100 rpm.

2.4.3 Determination of Cell Density

The cell density of liquid cultures was determined by measuring the optical density (OD) at a wavelength of 578 nm. For cell densities with an $OD_{578\ nm} \geq 0.6$ dilutions with the respective cultivation-medium were prepared before measurement. An $OD_{578\ nm}$ of 1 corresponds to approximately 1 x 10^9 cells/ml.

2.4.4 Storage of Bacterial Strains

Strains were kept on agar plates at 4 °C for up to f our weeks. For long term storage glycerol-stocks were prepared. Therefore 700 µl of an overnight-culture were mixed with 300 µl of sterile glycerol (80 % (v/v)). Stocks were immediately frozen and kept at -80 °C.

2.4.5 Harvesting of Bacterial Cells

Cells were sedimented by centrifugation for 15 min at 5,000 rpm and 4 °C (Sorvall RC 5B Plus, rotor: SLA-3,000) and washed with 50 mM HEPES (pH 7.5). Cell sediments were stored at -20 °C until use.

2.4.6 Disruption of Cells

Sedimented cells were suspended in the lysis-buffer appropriate for the respective enzyme preparation (see sections 2.9 - 2.12 below). Then cells were disrupted by a single anaerobic passage or by multiple aerobic passages (where applicable) through a French® Press at 1,200 p.s.i.. Benzonase (Merck, Darmstadt, Germany) was added in a ratio of 1 : 2,000 and incubated for 30 min at 17 °C.

2.5 Molecular Biological Techniques

2.5.1 Preparation of Plasmid DNA (Miniprep)

Cells of a 2 ml overnight culture were harvested by centrifugation (5 min, 7,000 x g). The sedimented cells were resuspended in 150 µl of buffer P1. 300 µl of buffer P2 were added. The sample was carefully mixed by inverting the tube and incubated at RT for 2 min. 225 µl of buffer P3 were added and the sample was carefully mixed again. After centrifugation (25 min at 15,000 x g) 600 µl of the supernatant were added to 600 µl isopropanol in a fresh tube. Precipitation of plasmid DNA was allowed during a 30 min centrifugation step at 4 °C (15,000 x g). The precipitated DNA was washed with 70 % (v/v) ethanol. After all traces of ethanol had evaporated, the DNA was solubilised in 50 µl H_2O.

P1 buffer	Tris-HCl, pH 8.0	50 mM
	EDTA	10 mM
	RNase	200 µg/ml
P2 buffer	NaOH	200 mM
	SDS	1 % (w/v)
P3 buffer	sodium acetate pH 4.8	3 M

2.5.2 Electrophoretic Separation of DNA

For the analytical separation of DNA-fragments agarose gels (1 % (w/v) agarose in TAE-buffer) were prepared. DNA samples were mixed with DNA loading dye to facilitate loading and to indicate the progress of the samples in the gel. GeneRuler™ DNA Ladder Mix or MassRuler™ DNA Ladder Mix (MBI Fermentas; St. Leon-Rot; Germany) were used as size standards according to the manufacturer's instructions. Depending on the size of the gel, a voltage of 80 – 100 V was applied. The DNA fragments migrate towards the anode with a velocity that is proportional to the negative logarithm of their length. After electrophoresis, gels were incubated in an ethidium bromide solution for 30 min and briefly rinsed with H_2O_{deion}. The DNA was detected via the fluorescence under UV light (λ = 312 nm).

TAE buffer (pH 8.0)	Tris-acetate	40 mM
	EDTA	1 mM
	dissolved in H_2O_{deion}	
DNA loading dye	Bromophenol blue	350 µM
	Xylene cyanol FF	450 µM
	glycerol	50 % (w/v)
	dissolved in H_2O_{deion}	
ethidium bromide solution	ethidium bromide	0.1 % (w/v)
	dissolved in H_2O_{deion}	

2.5.3 Determination of DNA Concentration

Two methods where used to determine the DNA concentration of the prepared plasmid DNA.
The plasmid was enzymatically linearised and visualised on an agarose gel (see 2.5.2). Using the software for gel documentation (Quantity One; Bio-Rad; Munich; Germany), the concentration of the respective band in the agarose gel was determined in comparison to two bands of known concentration.
The concentration and purity was also determined by measuring the absorbance at 260 nm and additionally at 280 nm to account for protein impurities. For a pure DNA solution, an A_{260nm} of 1

corresponded to a concentration of dsDNA of 50 µg/ml. The quality of the DNA solution is deduced from the ratio of A_{260nm} to A_{280nm}. With A_{260nm}/A_{280nm} = 1.8 – 2.0, the DNA can be considered as pure.

2.5.4 Amplification of DNA Fragments by Polymerase Chain Reaction

E. coli hemG was amplified by polymerase chain reaction (PCR). The PCR was performed at 50 µl scale with 5 µl of polymerase specific 10x buffer, 0.5 µl dNTP-mix (10 mM of each dNTP), 5 µl forward and reverse primer each (10 pmol/µl, section 2.2.3), 12.5 U of Biotherm® polymerase, and 20 ng of pETDuet 1 *hemG* as DNA-template. After an initial DNA denaturation step (95 °C), a cycle consisting of denaturation, primer ann ealing (55 °C), and primer elongation (72 °C) was completed 30 times. The reaction was terminated by a final elongation period.

Thermocycler program:

5 min 95 °C		
1 min 95 °C	←	
1 min 55 °C	x 30	
45 sec 72 °C	—	
10 min 72 °C		

For the amplification of *bchE* of *C. tepidum*, 50 µl assays were set up with with 5 µl of polymerase specific 10x buffer, 1 µl dNTP-mix (10 mM each dNTP), 5 µl forward and reverse primer each (10 pmol/µl section 2.2.3), 12.5 U of Biotherm® polymerase, and 1 µl of *C. tepidum* cell suspension (OD_{578nm} of 0.5) as DNA template.

Thermocycler program:

5 min 95 °C		
20 sec 95 °C	←	
30 sec 59 °C	x 30	
2 min 72 °C	—	
5 min 72 °C		

During amplification of the DNA, recognition sequences for restriction endonucleases were inserted by the sequence of the specific primers at both ends of the DNA fragment. After PCR, an aliquot of the reaction mixture was analysed by agarose gel electrophoresis (2.5.2). The amplified DNA fragment was purified using the "QIAquick PCR Purification Kit" according to manufacturer's instructions.

2.5.5 Restriction of DNA

Restriction of double stranded DNA (vectors and PCR products) was carried out using restriction endonucleases. Reaction buffers, concentrations of enzymes, and DNA concentrations as well as incubation temperatures were chosen according to manufacturer's instructions. The restriction was

allowed to proceed for 5 h or overnight at 37 °C, followed by heat inactivation of the restriction endonucleases according to enzyme-dependent conditions.
Restriction enzymes in the entire sample were removed by gel electrophoresis (2.5.2). The DNA was visualised using the GelStar® Nucleic Acid Gel Stain (Biozym; Hessisch Oldendorf; Germany) on a blue light detector (Flu-O-blu) and a yellow filter. The DNA fragment was then excised from the gel and purified using the "QIAquick Gel Extraction Kit" according to manufacturer's instructions.

2.5.6 Ligation of DNA-Fragments

In order to avoid re-circularisation of digested vector DNA, the 5'-phosphate groups of linearised vectors were removed prior to the ligation reaction. This was achieved by adding Antarctic Phosphatase (New England Biolabs) to the sample immediately after restriction (1 U/µg DNA), incubation at 37 °C for 30 min followed by heat inactivation for 15 min at 65 °C.
In one ligation reaction, 25 – 200 ng of plasmid DNA were used. Insert-DNA was added in excess (insert to vector ratio with regard to molar concentrations of 2 : 1 to 10 : 1) to a final volume of 20 µl. Ligation of vector-, and insert-DNA was carried out according to the manufacturer's instructions using T4 Ligase (New England Biolabs) and the reaction buffer supplied by the manufacturer. Additionally, controls without insert and without ligase were carried out. All reactions were incubated for 20 min at 25 °C or at 17 °C overnight.

2.5.7 Transformation of *Escherichia coli* by the RbCl Method

E. coli DH5α or BL21 (λDE3) cells were grown aerobically in 500 ml vapor sterilised LB. When the culture reached an $OD_{578\ nm}$ of 0.6 cells were harvested by centrifugation (10 min at 6,000 x g and 4°C). The cells were suspended in 200 ml TFB1 and incubated on ice for 5 min. After subsequent centrifugation (5 min at 3,000 x g and 4°C) cells were suspended in 2 volumes of TFB2 (referring to the volume of the cell sediment). After being incubated on ice for 30 min they were divided into 40 µl aliquots. These were either immediately used for transformation or stored at -80 °C.

TFB1	potassium acetate	30 mM
	$CaCl_2$	10 mM
	$MnCl_2$	50 mM
	RbCl	100 mM
	glycerol	15 % (v/v)
	in H_2O_{deion}; pH 5.8	
TFB2	MOPS	10 mM
	$CaCl_2$	75 mM
	RbCl	10 mM

glycerol	15 % (v/v)
in H_2O_{deion}; pH 6.5	

Transformation of chemo-competent cells was applied as standard transformation method. 40 µl of RbCl-competent cells were mixed with 1 - 2 µl of DNA solution (50 µg/ml), incubated on ice for 20 min and subjected to a heat shock for 2 min at 42 °C. Immediately after the transformation the sample was cooled on ice for 2 min. Afterwards 1 ml of preheated LB was added and cells were incubated at 37 °C for 1 h.
Depending on the expected colony density, different volumes were streaked onto agar plates containing the appropriate antibiotics. Plates were incubated overnight at 37°C.

2.5.8 DNA Sequence Analysis of Plasmid DNA

The successful modification of DNA was confirmed by sequence determination of the respective DNA region based on the principle of the Sanger dideoxy-method (Sanger *et al*., 1977).
The sequencing reactions were conducted on site with an ABI PRISM 310 Genetic Analyser (Applied Biosystems; Perkin Elmer; Boston; USA). The required preparatory PCR with fluorescence-labelled ddNTPs and the purification of the PCR product were carried out as described by the manufacturer. The analysis of all sequencing results was done using the computer software Sequence Analysis v5.2 (Applied Biosystems), Chromas (technelysium, Austria) and Seqman (GATC Biotech; Konstanz; Germany).

2.5.9 Protoplast Transformation of *Bacillus megaterium* Cells

Fifty ml of LB was inoculated with an individual *B. megaterium* WH323 colony and grown overnight at 37 °C and 100 rpm in baffled flasks. 1 ml of this culture was used to inoculate 50 ml of LB. The culture was incubated at 37 °C and 250 rpm in a baffled flask until it reached an OD_{578nm} of 1.0. Cells were sedimented by centrifugation (2,600 x g; 15 min; 4 °C) and resuspended in 5 ml of SMMP. After adding 100 µl of freshly prepared sterile lysozyme solution (100 µg of lysozyme/ml SMMP), the protoplast suspension was incubated at 37 °C for 30 min and smooth shaking. Formation of protoplasts was monitored microscopically. When 80 % of the rod shaped bacterium cells had formed coccoid protoplasts, the protoplasts were harvested (1,300 x g; 10 min; RT). The supernatant was decanted carefully and the protoplasts were suspended in 5 ml of SMMP. After a second washing step, the protoplasts were suspended in 5 ml of SMMP and 750 µl of 87 % (w/v) glycerol. They were either used directly for transformation or were frozen and stored in aliquots of 500 µl at -80 °C for a period of no longer than 2 months .
Before transformation, protoplasts were tested for viability. Therefore, a 500 µl aliquot of protoplast solution was mixed with 2.5 ml of cR5-top agar as described below and was streaked onto a LB-agar plate without antibiotics. After incubation overnight, a thick film of *B. megaterium* cells should be seen.
For the transformation of protoplasts, 5 µg of dried plasmid DNA were dissolved in 10 µl of SMMP for 20 min at 37 °C. 500 µl of protoplast suspension were mixed with the DNA and transferred into 1.5 ml of PEG-P solution. 5 ml of SMMP were added after incubation for 2 min at RT and gently

mixed with the suspension. The protoplasts were sedimented by centrifugation (1,300 x g; 10 min; RT), carefully suspended in 500 µl of SMMP and incubated at 30 °C for 45 min without shaking followed by 45 min of smooth shaking at 300 rpm (Thermomixer compact; Eppendorf; Germany). Regenerated protoplasts were mixed with 2.5 ml of pre-warmed (42 °C) cR5-top agar and spread on a pre-heated LB-agar plate containing the required antibiotics. The plates were incubated at 30 °C for up to 24 h. Colonies observed after this period of incubation were streaked on new LB-agar plates containing the required antibiotics.

SMMP	2 x AB3 and 2 x SMM; mixed 1 : 1	
2 x AB3	Antibiotic medium No. 3 (Difco)	35 g/l
2 x SMM (pH 6.5)	malic acid	40 mM
	$MgCl_2$ x 6 H_2O	40 mM
	NaOH	80 mM
	sucrose	1 M
	dissolved in H_2O_{deion}, sterilised by filtration	
PEG-P solution	PEG 6000	40 % (w/v)
	dissolved in 1 x SMM (pH 6.5)	
cR5 top-agar (2.5 ml)	solution A	1.25 ml
	solution B	713 µl
	8 x cR5-salts	288 µl
	L-proline (12 % (w/v))	125 µl
	D-glucose (20 % (w/v))	125 µl
solution A (pH 7.3)	sucrose	602 mM
	MOPS	58 mM
	NaOH	30 mM
	dissolved in H_2O_{deion}, sterilised by filtration	
solution B	agar agar	4 % (w/v)
	Casamino acids	0.2 % (w/v)
	yeast extract	10 % (w/v)
	dissolved in H_2O_{deion}	
8 x cR5-salts	K_2SO_4	11 mM
	$MgCl_2$ x 6 H_2O	394 mM
	KH_2PO_4	3 mM
	$CaCl_2$	159 mM
	dissolved in H_2O_{deion}	

2.6 Protein Biochemical Methods

2.6.1 Determination of Protein-Concentration

Concentrations of protein solutions were determined using the Bio-Rad Protein Assay (Bio-Rad, Munich, Germany) following the manufacturer's instructions ("Microassay Procedure" for 1 - 20 µg protein). The assay is based on the colourimetric method developed by (Bradford, 1976). Bovine serum albumin was used as a standard.

2.6.2 Concentrating Protein Solutions

Protein solutions were concentrated using Vivaspin 15 ultrafiltration units (Sartorius Vivascience, Aubagne Cedex, France; designed for centrifugation) with a molecular weight cut off of 10,000 in accordance to the manufacturers instructions.

2.6.3 Dialysis

Buffer exchange was performed anaerobically at 4 °C using dialysis membranes with a molecular weight cut off of 14,000. Therefore, 5 ml of protein solution were dialysed for approx. 14 h and then twice for 2 h against 250 ml of the respective buffer.

2.6.4 Electrophoretic Separation of Proteins (SDS-PAGE)

The discontinuous sodium dodecyl sulfate-polyacrylamide gel electrophoresis (SDS-PAGE) was executed as previously described (Laemmli, 1970; Righetti *et al*., 1990). Protein samples were prepared by heating to 95 °C for 5 min in appropriate amounts of 6 x SDS loading dye. 2 to 18 µl samples were loaded onto the gel which was run at 45 mA until the band of bromophenol blue dye reached the lower end of the gel. During electrophoresis, proteins were first focussed in the stacking gel and subsequently separated according to their relative molecular mass in the running gel. The size standards usually employed was the Protein Molecular Weight Marker (MBI Fermentas; St. Leon-Rot; Germany). For immunochemical detection of the proteins (section 2.6.5), the size standard PageRuler Prestained Protein Ladder (MBI Fermentas; St. Leon-Rot; Germany) was used. Subsequently the gels were stained with Coomassie Brilliant Blue G250 and destained until distinct protein bands elaborated. For documentation, gels equilibrated in water were scanned (ScanMakerX12USI; ScanWizard 5; Microtek; Willich; Germany) and then dried between two cellophane foils for storage.

	running gel (12 % (v/v))	**stacking gel (6 % (v/v))**
acrylamide stock solution	2 ml	500 µl
buffer for running gel	1.25 ml	-
buffer for stacking gel	-	625 µl
$H_2O_{deion.}$	1.75 ml	1.375 ml
10 % (w/v) APS solution	5 µl	3 µl
TEMED	50 µl	30 µl

acrylamide stock solution	acrylamide	29 % (w/v)
	N,N'-methylenbisacrylamide	1 % (w/v)
buffer for running gel	Tris-HCl pH 8.8	1.5 M
	SDS	0.4 % (w/v)
buffer for stacking gel	Tris-HCl pH 6.8	500 mM
	SDS	0.4 % (w/v)
SDS loading dye	Tris-HCl pH 6.8	100 mM
	glycerol	40 % (v/v)
	β-mercaptoethanol	10 % (v/v)
	SDS	3.2 % (w/v)
	bromophenol blue	0.2 % (v/v)
electrophoresis buffer	Tris-HCl pH 8.4	50 mM
	glycine	380 mM
	SDS	0.1 % (w/v)
staining solution	acetic acid	10 % (v/v)
	ethanol	25 % (v/v)
Coomassie Brilliant Blue	G-250	0.25 % (v/v)
destaining solution	acetic acid	10 % (v/v)
	ethanol	30 % (v/v)

2.6.5 Western-Blot

To further analyse protein samples, proteins separated during SDS-PAGE were transferred in a semi-dry process onto a PVDF-membrane (Western-Blot).
Therefore, PVDF-membranes were incubated in methanol for 10 min. Afterwards, in parallel to the SDS-gel and blotting paper, they were incubated in transfer-buffer and assembled in the blotting apparatus as described by the manufacturer. For one gel, a current of 0.8 mA/cm^2 was applied for 30 min at 10 V.

transfer-buffer	Tris-HCl pH 8.5	25 mM
	glycine	192 mM
	methanol	20 % (v/v)
PBS (pH 7.4)	NaCl	137 mM
	KCl	27 mM
	Na_2HPO_4 x 7 H_2O	100 mM
	KH_2PO_4	20 mM

2.6.6 Immunodetection of Immobilised Proteins

Proteins immobilised on a PVDF-membrane (2.6.5) can be detected by antibodies. The primary antibody is directed against an epitope of the protein of interest. The secondary antibody, directed against the primary antibody, is coupled to an enzyme which catalyses a detectable reaction. For immunodetection of recombinant proteins, non-specific binding sites of the membrane were saturated overnight in blocking-solution at 4 °C and smooth shaking. Incubation with the primary antibody was carried out in blocking-solution for 1 h (RT) and slight shaking (Anti-His from mouse and Anti-GST from rabbit diluted 1 : 5,000 in blocking solution). The membranes were washed three times for 10 min each step with washing-solution. The secondary antibody (Anti-mouse and anti-rabbit diluted 1:3,000 in washing-buffer), which is coupled to an alkaline phosphatase, was applied and incubated for 45 min. After four washing steps with PBS/Tween®-buffer for 10 min each step, membranes were incubated for 5 min in alkaline phosphatase-buffer and exposed to staining-solution until bands became visible. During exposure, alkaline phosphatase, the enzyme bound to the secondary antibody, catalyses the reaction of 5-brom-4-chloro-3-indolylphosphate (BCIP) with nitroblue-tetrazolium (NBT). The resulting insoluble dye precipitates immediately on the membrane. Development was stopped with water and the membranes were air dried in the dark.

PBS (pH 7.4)	NaCl	137 mM
	KCl	27 mM
	Na_2HPO_4 x 7 H_2O	100 mM
	KH_2PO_4	20 mM

blocking-solution	skim milk powder	5 % (w/v)
	Tween® 20	0.1 % (v/v)
	PBS	10 % (v/v)
washing-solution	skim milk powder	0.5 % (w/v)
	Tween® 20	0.1 % (v/v)
	PBS	10% (v/v)
PBS/Tween®-buffer	Tween® 20	0.1 % (v/v)
	PBS	10 % (v/v)
alkaline phosphatase-buffer	Tris pH 9.5	100 mM
	NaCl	100 mM
	$MgCl_2$	5 mM
staining-solution	alkaline phosphatase buffer	10 ml
	NBT-solution (100 mg/ml in 70 % DMF)	33 µl
	BCIP-solution (50 mg/ml in DMF)	33 µl

2.6.7 Compliance of Anaerobic Conditions

To ensure strict anaerobic conditions, most work was carried out in an anaerobic chamber. All buffers and solutions were subjected to repeated cycles of evacuation and saturation with N_2 prior to use unless stated otherwise.

Table 5: Anaerobisation of buffers and solutions employed in anaerobic work.

volume [ml]	number of cycles of evacuation and saturation with N_2	interval [min]
5	10	1
200	30	2
500	60	2

2.6.8 UV-Vis Spectroscopy

UV-Visible Light Absorption Spectroscopy was performed using a V-550 spectrophotometer (Jasco, Groß Umstadt, Germany). Spectra from 700 to 250 nm with a scan speed of 200 nm/min were recorded.

2.7 Determination of Escherichia coli *Protoporphyrinogen IX Oxidase Activity*

2.7.1 Principle of the Activity-Assay

The protoporphyrinogen IX oxidase activity test was developed in our laboratory (Breckau, 2005). In this assay, the substrate protoporphyrinogen IX (proto'gen) is enzymatically converted into protoporphyrin IX (proto) by *E. coli* cell-free extract in the presence of fumarate or TTC as electron acceptors. Excitation of the product proto at a wavelength of 409 nm results in a fluorescence emission at 633 nm detectable by a luminescence spectrometer. Therefore, it is clearly distinguishable from the substrate proto'gen since this compound reveals no spectroscopic properties.

2.7.2 Preparation of the Substrate Protoporphyrinogen IX

2.7.2.1 Reduction of Protoporphyrin IX with Sodium Amalgam

The substrate proto'gen was obtained through the reduction of proto (Sigma-Aldrich, Taufkirchen, Germany) according to a modified published instruction (Sano and Granick, 1961): 840 µg proto were dissolved in 3 ml of 10 mM KOH, 20 % (v/v) of ethanol (final concentration of proto: 500 µM) in a stream of N_2 and finally reduced with 6 g of 3 % Na-amalgam. When the reaction mixture has discoloured after incubation for less than 2 min at 80 °C, it was filtered through glass wool. 50 mM of DTT was added and the pH was adjusted to 8 - 8.8 with 20 % (v/v) phosphoric acid. The proto´gen solution was aliquoted anaerobically and stored at -20 °C in the dark to avoid autooxidation by oxygen and light.

2.7.2.2 Palladium-catalysed Reduction of Protoporphyrin IX with Molecular Hydrogen

For this reduction method, a published instruction was modified (Phillips, 2007). All steps were performed under anaerobic conditions. 2 mg of proto and 5 mg of palladium (for hydroxylation reactions, 10 % on activated charcoal) were suspended in a mixture of 100 µl of H_2O and 1.8 ml of methanol. After flushing with argon, a hydrogen atmosphere was established. The assay was stirred for up to 40 min at RT with occasional notification of fluorescence emission. The colourless assay was filtered and the methanol was withdrawn by evacuation. 500 µl of buffer were added to the remaining fluid and the assay was frozen at -20 °C in portions of 70 µl.

2.7.3 Conditions for the Activity-Assay

Determination of *E. coli* PPO-activity was started under strictly anaerobic conditions at RT in all cases. The standard assay mixture contained 25 µl of 10 x assay-buffer and components listed in the respective figure legends in a total volume of 250 µl. The reaction was started with the addition of 1.5 or 5 µl of proto'gen solution (final concentration of proto'gen were 3 and 10 µM, respectively)

or as indicated in 3.8.3 B. To investigate the utilisation of cytochrome oxidases as terminal oxidases, the assays were aeriated immediately. The formation of proto at RT was recorded in real time for up to one hour with using a luminescence spectrometer.

10x assay-buffer	Tris-HCl pH 7.6	500 mM
	EDTA	10 mM
	glutathione	50 mM
	Triton® X-100	3 % (v/v)
	NaCl	1 M
proto'gen-solution	proto'gen	500 µM

Settings of the Luminescence Spectrometer

Excitation Wavelength 409 nm

Emission Scan Range 570 - 680 nm

Scan Speed 200 nm/min

Slit Width for Excitation 5 nm

Slit Width for Emission 5 nm

In order to quantify product formation, a calibration curve with different concentrations of chemically synthesised proto was prepared.

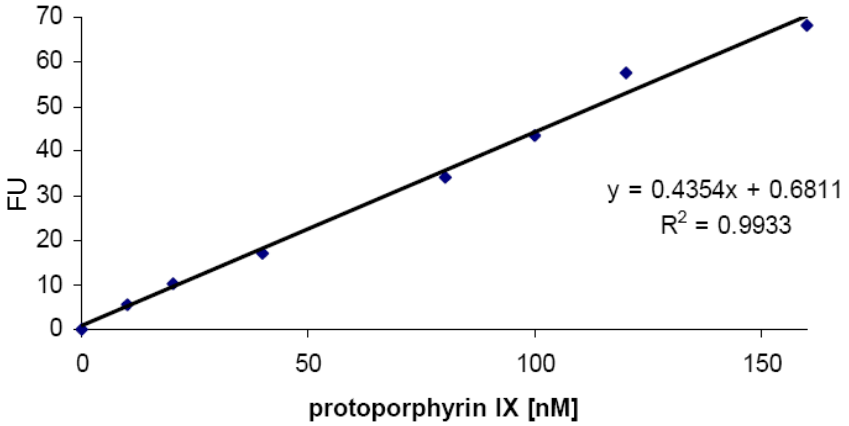

Figure 10: Calibration curve of the fluorescence intensities in relation to proto concentrations
Protoporphyrin IX was dissolved in assay-buffer. In accordance to the calibration curve, 1 nM proto resulted in 1.11 fluorescence intensity units.

2.8 Purification of the Oxygen-Independent Protoporphyrinogen IX Oxidase

2.8.1 Cultivation of *Escherichia coli* BL21 (λDE3)

Six liters of *E. coli* BL21 (λDE3) Cultures were grown aerobically as described under 2.4.2 and harvested as described under 2.4.5. All purification steps were performed under anaerobic conditions.

2.8.2 Isolation of Membrane Fractions of *Escherichia coli*

The cell sediment was suspended in 20 ml of 50 mM HEPES pH 7.5. After cell disruption (2.4.6), cell debris of crude cell extracts of *E. coli* was removed by centrifugation for 15 min at 20,000 x g and 4 °C. The resulting supernatant was subjected to an additional centrifugation step for 1 h at 120,000 x g and 4 °C to sediment the membrane fraction.

2.8.3 Purification of Membrane Fractions performing Sucrose Density Gradient Centrifugation

The membrane fraction of *E. coli* was further separated from soluble proteins by sucrose density gradient centrifugation. During centrifugation in a discontinuous 3 step sucrose gradient, protein fractions enriched in layers corresponding to their own density. The gradient was prepared by layering 3 ml of each sucrose solution (60, 40, and 20 % (w/v), respectively) onto each other. The sedimented membrane fraction was suspended in 2 ml of 20 % (w/v) sucrose-solution, layered onto the gradient and centrifuged for 2 h at 145,000 x g and 4 °C in a swing out rotor (Beckmann SW40Ti). The membrane fraction was enriched in a band on the boundary between the 40 % (w/v) and 60 % (w/v) sucrose solution. It was harvested with a Pasteur pipette.

sucrose solution	Tris-HCl (pH 7.3)	10 mM
	$MgCl_2$	100 mM
	sucrose	20 % (w/v)
	(added respectively)	40 % (w/v)
		60 % (w/v)

2.8.4 Solubilisation of Membrane Proteins

Extraction of proteins from membranes of *E. coli* was performed by suspending the membrane fraction in 10 ml solubilisation buffer. Therefore, the suspension was stirred at 4 °C overnight. Afterwards, it was centrifuged for 1 h at 120,000 x g and 4 °C. The supernatant containing solubilised proteins was collected.

solubilisation buffer	Tris-HCl pH 8.0	50 mM
	KCl	100 mM

2.8.5 Anion Exchange Chromatography

Protein purification was performed by anion exchange chromatography. The positively charged matrix diethylaminoethyl-sepharose (DEAE) interacts with negative charges occurring on surfaces of proteins. This interaction is interrupted by the presence of salts leading to the elution of respective proteins. To obtain best binding properties the supernatant of solubilised proteins (2.8.4) was diluted tenfold with DEAE buffer. The sample was applied on a DEAE-sepharose FF gravity flow column with a bed volume (C_V) of 1 ml equilibrated with the same buffer. Three washing steps with 1 C_V of buffer were followed by the elution of the proteins. Elution was carried out in steps of 3 C_V with DEAE buffer additionally containing 100 mM NaCl, 150 mM NaCl, 200 mM NaCl and 500 mM NaCl, respectively. Obtained fractions were separated by SDS-PAGE. The gel was not stained afterwards. Lanes of fractions yielding high PPO activity were excised and used for the determination of the peptide content (section 2.9.4)

DEAE buffer	HEPES pH 7.5	50 mM

2.9 Recombinant Production, Purification and characterisation of Escherichia coli *HemG*

2.9.1 Cultivation of *Escherischia coli* Cells for the Production of HemG

For aerobic recombinant production of HemG in *E. coli*, LB (6 x 500 ml) containing ampicillin was inoculated with 5 ml of a preculture of *E. coli* BL21 (λDE3) carrying pETDuet-1-*hemG* in 1 l Erlenmeyer flasks. Cultures were grown aerobically at 37 °C and 200 rpm to an OD_{578nm} of approx. 0.6. Recombinant expression of *hemG* was induced by the addition of IPTG to a final concentration of 100 µM. Incubation was continued for 4 h at 25 °C and 200 rpm. Afterwards, cells were harvested (section 2.4.5).

2.9.2 Cultivation of *Bacillus megaterium* Cells for the Production of HemG

Five 100 ml cultures of recombinant *B. megaterium* WH323 carrying pC-His1622*hemG* were grown aerobically in LB to recombinantly produce HemG-His_{6x} as described (section 2.4.2). Protein production was induced by the addition of 0.5 % (w/v) xylose at an OD_{578nm} of approx. 0.4. Cultures were incubated at 250 rpm and 37 °C for six hours. Afterwards, cells were harvested (section 2.4.5).

2.9.3 Affinity-Purification of Recombinant HemG under Anaerobic Conditions

Cells cultivated and harvested according to 2.4.2, 2.4.5, 2.9.1 and 2.9.2 and were suspended in 20 ml of lysis buffer and disrupted (section 2.4.6). After cell disruption, the sample was stirred at 4 °C for 1 hour and centrifuged at 100,000 x g and 4 °C for 1 hour. The supernatant was filtered (filter pore width of 0.2 µm) and loaded onto a gravity flow column containing 1 ml of Ni-NTA Superflow (Qiagen) resin equilibrated with washing buffer. The column was washed with 6 C_V of washing buffer. Proteins bound to the resin were eluted with 5 C_V of elution buffer. The resulting fractions were stored at -20 °C.

lysis buffer	HEPES pH 7.5	50 mM
	NaCl	300 mM
	glycerol	20 % (v/v)
	Thesit®	2 % (v/v)
washing buffer	HEPES pH 7.5	50 mM
	NaCl	300 mM
	glycerol	20 % (v/v)
	imidazole	10 mM
elution buffer	HEPES pH 7.5	50 mM
	NaCl	300 mM
	glycerol	20 % (v/v)
	imidazole	500 mM

2.9.4 Mass-Spectrometry

Chromatographically purified fractions of sections 2.8.5 and 2.9.3 were analysed for the protein content by LC-MS/MS. This work was done by Dr. Dörthe Becher at the department of microbiology from the University of Greifswald, Germany.

2.9.5 Gel Permeation Chromatography of HemG

For gel permeation experiments, a Superdex 200 HR 10/30 column (GE Healthcare, Munich, Germany) was equilibrated with GPC buffer and calibrated with marker proteins of relative molecular weights: Cytochrome C from bovine heart with M_r of 12,400, carbonic anhydrase with M_r of ~29,000, bovine serum albumin with M_r of ~66,000 and alcohol dehydrogenase from yeast with M_r of ~150,000. Then 200 µg of purified HemG (2 mg/ml) which had been recombinantly produced

in *B. megaterium* and purified by affinity chromatography (2.9.3) were loaded onto and eluted with GPC buffer at a flow rate of 0.5 ml/ min.

GPC buffer	HEPES pH 7.5	50 mM
	NaCl	300 mM
	glycerol	20 % (v/v)
	Thesit®	2 % (v/v)

2.9.6 Cofactor Determination by High Performance Liquid Chromatography (HPLC)

After analysis of purified HemG (2.9.3) by UV-Vis spectroscopy (section 2.6.8), the protein was precipitated by the addition of 5 % (v/v) perchloric acid and centrifuged at 10,000 x g at RT for 10 min. The supernatant was analysed using a HPLC-system 1500 series (Jasco, Groß Umstadt, Germany) and an ODS Hypersil 250 x 4.6 mm column (Techlab, Erkerode, Germany). Isocratic separation was performed at a flow rate of 0.5 ml/min at 30 °C. Flavins were detected by fluorescence measurements using an excitation wavelength of 430 nm and an emission wavelength of 525 nm. Photometric diode array analysis from 200 to 650 nm wavelength was performed simultaneously. Flavin-adenin-dinucleotide (FAD) and flavin-mononucleotide (FMN, Fluka) were used as standards.

mobile phase	acetonitrile		water		triflouric acid		phosphoric acid (75 %)
ratio	14	:	84	:	1.5	:	0.09

2.10 Production and Purification of recombinant Escherichia coli *Fumarate Reductase*

Recombinant production and purification of *E. coli* fumarate reductase (FRD) was performed according to a published protocol (Luna-Chavez *et al*., 2000) with several modifications. For the production, the plasmid pH3 encoding the wildtype FRD ($frdA^+B^+C^+D^+$) was used in the *E. coli* strain DW35 ($frdA^-B^-C^-D^-$). Cultivation under anaerobic conditions led to an overproduction of recombinant FRD (Blaut *et al*., 1989).

2.10.1 Cultivation of Cells

A 50 ml overnight culture of *E. coli* DW35 pH3 was grown at 37 °C and 200 rpm in LB containing 100 µg/ml ampicillin. 6 ml of this culture was added to 100 ml of LB (100 µg/ml ampicillin) in an anaerobic bottle. The cells were grown anaerobically for approximately 8 h at 37 °C and 100 rpm. From this culture, 5 x 1 l of glycerol-fumarate-medium (35 µg/ml amp) in 1 l anaerobic flasks were inoculated with each 1 ml. Cells were grown anaerobically at 37 °C and 100 rpm overnight (~13 h)

and harvested (section 2.4.5). To separate the bacterial cells from precipitated medium components, the cell sediment was washed trice with 50 mM HEPES (pH 7.5).

2.10.2 Preparation of Membrane Fractions and Solubilisation of Fumarate Reductase

Sedimented cells (2.10.1) were suspended aerobically in 20 ml of FRD buffer and disrupted twice (section 2.4.6). Cell debris was removed by centrifugation for 15 min at 20,000 x g and 4 °C. The cell-free supernatant was carefully removed. The membranes were sedimented in an additional centrifugation step for 1 h at 120,000 x g and 4 °C. The sedimented fractions were kept at -20 °C until use.

Membrane proteins were solubilised by suspending the membrane fraction in buffer S and stirring at 4 °C for 1 h. Subsequent centrifugation for 1 h at 120,000 x g and 4 °C followed by the filtration of the supernatant was performed to prepare fractions containing the recombinant fumarate reductase for purification.

FRD buffer	Tris-HCl pH 6.8	100 mM
	EDTA	100 µM
Buffer S	HEPES pH 7.5	20 mM
	EDTA	100 µM
	Thesit®	2 % (v/v)

2.10.3 Purification of Fumarate Reductase by "Fast Performance Liquid Chromatography" (FPLC)

Purification of solubilised fumarate reductase was performed by "Fast Performance Liquid Chromatography" (FPLC) using an ÄKTA™-Purifier and a DEAE-Sepharose FF column.

The column (XK 16/20) with a C_V of 25 ml was equilibrated with 5 C_V of buffer A. After loading the supernatant (flow rate 2 ml/min), the column was washed with 2 C_V of buffer A to remove unbound proteins. By the addition of 10 % of buffer B (2 C_V), loosely bound proteins were eluted. A gradient from 10 % to a final concentration of 25 % of buffer B was applied for 3 C_V. Remaining proteins were eluted with 2 C_v of 100 % of buffer B. The fractions were collected in 5 ml aliquots. Fractions containing FRD were identified by SDS-PAGE (2.6.4), pooled and concentrated by ultrafiltration (2.6.2). The obtained FRD solution was diluted twofold with 80 % glycerol, flushed with molecular nitrogen and stored at –20 °C.

buffer A	HEPES pH 7.5	20 mM
	EDTA	100 µM
	Thesit®	0.05 % (v/v)

buffer B	HEPES pH 7.5	20 mM
	EDTA	100 µM
	Thesit®	0.05 % (v/v)
	NaCl	1 M

2.10.4 Determination of Fumarate Reductase-Activity

E. coli FRD activity was assayed under strictly anaerobic conditions according to a protocol published earlier (Cecchini *et al*., 1986). Fumarate-dependent oxidation of reduced benzyl viologen was assayed by the decrease of absorption at 550 nm during a time period of 10 min. The standard assay mixture had a total volume of 1 ml. For the reduction of benzyl viologen, 20 µl of sodium dithionite were added to 980 µl of reaction-buffer. Absorption was measured directly after the addition of 7 µg of protein solution.

reaction-buffer	Tris-HCl pH 8.0	50 mM
	EDTA	100 µM
	sodium fumarate	20 mM
	benzyl viologen	250 µM
stock solution sodium dithionite	sodium dithionite	10 mM

2.11 Production and Purification of recombinant Escherichia coli *Cytochrome* bo *Oxidase*

To obtain isolated recombinant *E. coli* cytochrome *bo* oxidase (Cyo), the *E. coli* plasmid strain GO105 pJRHisA was utilised which is able to recombinantly produce the 4 subunits of Cyo (CyoA, B, C and D). In this strain, the sequence for CyoB is fused to a sequence encoding for a His_{6x}-tag for purification. The published protocol (Rumbley *et al*., 1997) was used with minor modifications.

2.11.1 Recombinant Production of Cyo

Fifty ml of LB supplemented with tetracycline and ampicillin were inoculated from a glycerol-stock with GO105 pJRHisA and grown overnight at 37 °C and 250 rpm. 2 x 500 ml of LB containing the same antibiotics were inoculated with 5 ml of the preculture each and incubated at 37 °C and 200 rpm. When the culture reached an $OD_{578nm,}$ of 0.6 the cells were harvested (section 2.4.5).

2.11.2 Preparation of Membrane Fractions and Solubilisation of Cyo

Sedimented bacterial cells (2.11.1) were suspended in 10 ml of Cyo Buffer and disrupted trice (section 2.4.6). Cell debris was removed by centrifugation at 20,000 x g and 4 °C for 20 min. The supernatant was subjected to a centrifugation step at 100,000 x g and 4 °C for 1 h and the supernatant was discarded. The sedimented membrane fraction was suspended in 10 ml of buffer C, stirred for 1 h at 4 °C and centrifuged again at 100,000 x g and 4 °C for 1 h. The obtained supernatant was filtered (pore width 0.2 µm) and used for further purification.

Cyo buffer	Tris-HCl pH 8	50 mM
	$MgSO_4$	5 mM
	benzonase	2 µl
	Complete mini; protease inhibitor cocktail	1 tablet
buffer C	Tris-HCl pH 8	50 mM
	Triton® X-100	1 % (v/v)
	N-octylglucoside	1.25 % (v/v)

2.11.3 Purification of Cyo

Due to the His_{6x}-tag fused to subunit CyoB, an affinity chromatography purification was pursued. The protein solution obtained in section 2.11.2 was loaded onto a gravity column wiht a C_v of 1 ml Ni-NTA Superflow resin (Qiagen, Hilden, Germany). The resin was equilibrated with buffer D. After loading, it was washed with 4 C_V of buffer D. Proteins bound to the resin were eluted with 4 times 0.5 C_V of buffer E. Fractions were analysed by SDS-PAGE (section 2.6.4). Fractions were stored at 4 °C and -20 °C, respectively.

buffer D	Tris-HCl pH 8	50 mM
	Triton® X-100	0.1 % (v/v)
	NaCl	250 mM
buffer E	Tris-HCl pH 8	50 mM
	Triton® X-100	0.1 % (v/v)
	NaCl	250 mM
	imidazole	300 mM

2.12 Production and Purification of recombinant Escherichia coli *Cytochrome* bd *Oxidase*

The *E. coli* plasmid strain GO105 pTK1 was utilised to obtain recombinant *E. coli* cytochrome *bd* oxidase (Cyd). The plasmid encodes for both subunits of Cyd. Published instructions were slightly modified (Kaysser *et al*., 1995).

2.12.1 Recombinant Production of Cyd

A glycerol-stock was used to inoculate 50 ml of LB supplemented with tetracycline and ampicillin. The cells were grown overnight at 37 ℃ and 250 rpm. 2 x 500 ml LB containing antibiotics were inoculated with 5 ml of preculture each and incubated at 37 ℃ and 200 rpm. After 24 h, the cells were harvested (section 2.4.5).

2.12.2 Preparation of Membrane Fractions and Solubilisation of Cyd

Sedimented bacterial cells (2.12.1) were suspended in 10 ml of Cyd Buffer and disrupted trice (section 2.4.6). Centrifugation at 20,000 x g and 4 ℃ for 20 min removed cell debris. The obtained supernatant was again centrifuged at 100,000 x g and 4 ℃ for 1 h. While the supernatant was discarded, the sedimented membrane fraction was suspended in 10 ml of buffer F, stirred for 1 h at 4 ℃ and centrifuged again at 100,000 x g and 4 ℃ f or 1 h. The supernatant was filtered (pore width 0.2 µm) and used for further purification.

Cyd buffer	Tris-HCl pH 8	50 mM
	EDTA	15 mM
	Complete mini; protease inhibitor cocktail	1 tablet
buffer F	Tris-HCl pH 6.8	75 mM
	EDTA	5 mM
	KCl	150 mM
	CHAPS	10 mM

2.12.3 Purification of Cyd

For the purification of the untagged Cyd, anion exchange chromatography on an ÄKTA^{TM}-purifier system was performed.

At a flowrate of 1 ml/min, the supernatant obtained in section 2.12.2 was loaded onto a DEAE Fast Flow HR 5/5 column with a C_v of 1 ml resin (GE Healthcare, Munich, Germany) which was equilibrated with buffer G. After loading, the resin was washed with 5 C_V of buffer G. Proteins

bound to the resin were eluted with a gradient of 0 - 100 % of buffer H in a total of 20 C_V. Aliquots of all collected 1.5 ml fractions were analysed by SDS-PAGE (section 2.6.4). Relevant fractions were stored at 4 °C and -20 °C, respectively.

buffer G	Tris-HCl pH 6.8	75 mM
	EDTA	5 mM
	KCl	150 mM
	CHAPS	3 mM
buffer H	Tris-HCl pH 6.8	75 mM
	EDTA	5 mM
	KCl	500 mM
	CHAPS	3 mM

2.13 Production, Isolation and Characterisation of Chlorobaculum tepidum *oxygen-independent Mg-protoporphyrin IX monomethyl ester oxidative Cyclase BchE*

To obtain recombinant oxygen-independent Mg-protoporphyrin IX monomethyl ester oxidative cyclase (BchE) from *C. tepidum*, *E. coli* BL21 (λDE3) was transformed with pGEX-6P-1 *bchE* and pGEX6-P-1 *bchE* His_{4x}. These constructs encode for N-terminal fusion proteins of a glutathione-S-transferase (GST) tag with the target protein which allows the purification by affinity chromatography.

2.13.1 Recombinant Production of BchE

Fifty ml of LB supplemented with ampicillin were inoculated with recombinant *E. coli* BL21 (λDE3) pGEX6-P-1 *bchE* or *E. coli* BL21 (λDE3) pGEX6-P-1 *bchE* His_{4x} (2.1.3) from a glycerol stock. The preculture was grown aerobically overnight at 37 °C and 200 rpm. 1 ml of the preculture was used to inoculate a 100 ml main culture of LB containing ampicillin which was incubated at 37 °C and 200 rpm. After reaching an OD_{578nm} of 0.6 - 1, recombinant protein production was induced by the addition of 500 µM of IPTG. Cells were grown to an OD_{578nm} of 3 and harvested (2.4.5).

2.13.2 Isolation of tagged BchE Cyclase

Sedimented bacterial cells were suspended in 25 ml of BchE buffer and disrupted trice (2.4.6). The cell lysate was subjected to centrifugation at 120,000 x g and 4 °C for 40 min. The resulting supernatant was filtered (pore width 0.2 µm) and loaded onto a gravity column with a C_v of 250 µl glutathione sepharose 4 Fast Flow (GE Healthcare, Munich, Germany) equilibrated with buffer K.

After loading, the resin was washed with 6 C_V of buffer K. Proteins bound to the resin were eluted with 6 C_V of buffer L. All fractions were stored at 4 °C.

BchE buffer	HEPES pH 7.5	20 mM
	NaCl	500 mM
	Triton® X-100	0.01 % (v/v)
	glycerol	20 % (v/v)
PBS:	NaCl	137 mM
	KCl	27 mM
	Na_2HPO_4 x 7 H_2O	100 mM
	KH_2PO_4	20 mM
buffer K	1x PBS	
	glycerol	20 % (v/v)
buffer L	Tris-HCl pH 8	50 mM
	glutathione	10 mM
	glycerol	20 % (v/v)

2.13.3 PreScission™ Protease Cleavage and second Chromatography

PreScission™ Protease (GE Healthcare, Munich, Germany) specifically cleaves at a certain recognition sequence between the GST protein and the target protein. Four units of PreScission™ Protease which was also fused to a GST-tag were added to the pooled protein solution (protein concentration 500 µg/ml). The cleavage reaction was stirred overnight at 4 °C.
During cleavage, the protein solution was dialysed against 500 ml of buffer K (section 2.13.2) to remove the glutathione. In a second affinity chromatography step on glutathione sepharose, the cleaved GST-tag, uncleaved fusion protein and the PreScission™ were removed. 250 µl of glutathione sepharose 4 Fast Flow were equilibrated with buffer K and the protein solution was loaded. The flow-through containing the target protein BchE was collected and stored at 4 °C. All fractions were analysed by SDS-PAGE (section 2.6.4).

2.13.4 Determination of Iron Content

The iron content of recombinant purified BchE was determined colourimetrically with *o*-phenanthroline (Lovenberg *et al.*, 1963). Hundred µl of each protein solution were mixed with 10 µl of HCl (37 %) and 390 µl H_2O. Samples were incubated at 80 °C for 10 min to den ature proteins and subsequently cooled on ice for 5 min. Subsequently, 100 µl of a 1 M hydroxylammonium chloride solution, 500 µl of an *o*-phenanthroline monohydrate solution (0.3 % (w/v) in 70 % (v/v) ethanol) and 500 µl H_2O were added to each sample. Samples were mixed and incubated at RT for

30 min. After precipitation of the proteins by centrifugation at 7,000 x g for 10 min, the absorption of the supernatant at 512 nm was measured. The iron content of the samples was determined via a calibration curve obtained from a series of dilutions of an iron standard (Merck, Darmstadt, Germany).

2.13.5 Chemical Reconstitution of Iron-Sulphur Clusters

To accomplish an optimal incorporation of FeS clusters, an anaerobic chemical reconstitution was attempted in accordance to published instructions (Okada and Hase, 2005). For this purpose, 100 µl of protein solution were mixed with DTT in 50-fold molaric excess and incubated for 10 min. Buffer M was added to a final volume of 300 µl. $FeCl_3$ and Na_2S were added in 10-fold molaric excess and the assay was incubated for 4 h at 17 °C. Afterwards, the assay was dialysed against 500 ml buffer M and subsequently, UV-Vis spectra (section 2.6.8) were recorded.

buffer M	Tris-HCl pH 8	50 mM
	glycerol	20 % (v/v)

2.13.6 Cyclase Activity assays

In order to analyse the activity of oxygen-independent Mg-protoporphyrin IX monomethyl ester oxidative cyclase, several different approaches were pursued. The cyclase activity test described earlier was used (Gough *et al*., 2000).

For *in vivo* assays, 200 µl of *R. capsulatus* DSM938 cells (OD_{578nm} of 1, kindly provided by Katharina Herbst) were anaerobically supplemented with 8 µM of Mg protoporphyrin IX monomethyl ester (MgPME, dissolved in DMSO) and 10 mM of nicotinic acid. The assay was incubated for 1h at 17 °C in the dark and centrifuged for 10 min at 10,000 x g and RT. The sediment was suspended in stopping solution and centrifuged again. The supernatant was then analysed in the luminescence spectrometer and by HPLC.

To determine the influence of additional components on the activity of oxygen-independent Mg-protoporphyrin IX monomethyl ester oxidative cyclase, 15 µM of Vitamin B_{12} or 5 µg of purified BchE from *C. tepidum* were added to the assay. In control reactions, *R. capsulatus* cells were omitted.

For *in vitro* experiments in a final volume of 200 µl, the assay contained 100 mM of Tris-HCl pH 7.5, 30 mM of $MgCl_2$, 10 mM of nicotinic acid, 500 µM of S-adenosyl-methionine, 150 µM of Vitamin B_{12}, 8 µM of MgPME, 10 µg of purified BchE from *C. tepidum* and 0.3 % (v/v) of Triton® X-100. The assay was anaerobically incubated at 37 °C and 450 rpm for 2 h. Then, 20 µl were transferred to 400 µl of stopping solution and centrifuged at 20,000 x g at 4 °C for 5 min. The supernatant was analysed via HPLC.

In control reactions, $MgCl_2$, nicotinic acid, SAM, Vitamin B_{12}, MgPME, the BchE preparation or Triton® X-100 were omitted. Additional controls were supplemented with 8 µM of protochorophyllide without the addition of enzyme or MgPME.

stopping solution	acetone		H_20		32 % Ammonia solution
ratio	80	:	20	:	1

Settings of the Luminescence Spectrometer

Excitation Wavelength 440 nm
Emission Scan Range 500 - 700 nm
Scan Speed 200 nm/min
Slit Width for Excitation 5 nm
Slit Width for Emission 5 nm

2.13.7 HPLC-Analysis of Cyclase Activity Test Products

For the identification of tetrapyrroles, the reaction products were separated by a 1500 series Jasco HPLC sytem. A published separation protocol (Jensen *et al*., 1999) was used.
An Ultrasphere ODS (5 µm, 250 x 4.6 mm) C_{18}-reversed phase column (Techlab, Erkerode, Germany) was run at 1 ml/min and 30 °C. 20 µl or 50 µl of sample were injected. As eluent A 0.005 % (v/v) of triethylamine in H_20 was used. Eluent B consisted of 100 % of acetonitrile. To achieve optimal separation, an elaborate gradient program was developed:
During a period of 25 min, a gradient from 25 to 40 % of eluent B was applied. Within 2 min, a gradient to 100 % of eluent B followed by 8 min of continuous 100 % of eluent B was used to elute all retarded compounds. Another gradient was used to return to 25 % of eluent B within 2 min. 25 % of eluent B were maintained for 8 min to reequilibrate the column.
Since the tetrapyrroles have different fluorescence characteristics, the fluorescence detector was set at an excitation wavelength of 440 nm and an emission wavelength of 635 nm for the first 14 minutes. After this time period, settings were changed to 420/595 nm. Due to this change, both substrate and product could be securely detected within one sample injection.

3 Results and Discussion

3.1 Chromatographic purification of oxygen-independent PPO from Escherichia coli

The identification of the oxygen - independent PPO of *E. coli* was one of the central goals of this thesis. A classical chromatography strategy was applied to enrich PPO activity under anaerobic conditions. Therefore, the established activity test developed by Dr. Daniela Breckau was employed (2005). *E. coli* cells were grown and the cells were lysed. For the determination of the anaerobic PPO activity, an anaerobic cell-free extract was prepared. In addition to the cell-free extract, the assay contained the substrate proto´gen prepared by the chemical reduction of proto. Furthermore, fumarate was applied as electron acceptor.

PPO activity results in the conversion of the colourless proto´gen into the coloured and fluorescent proto. The fluorescence emission peaks were detected online with the luminescence spectrometer at 633 nm wavelength when an excitation wavelength of 409 nm is used (fig. 11).

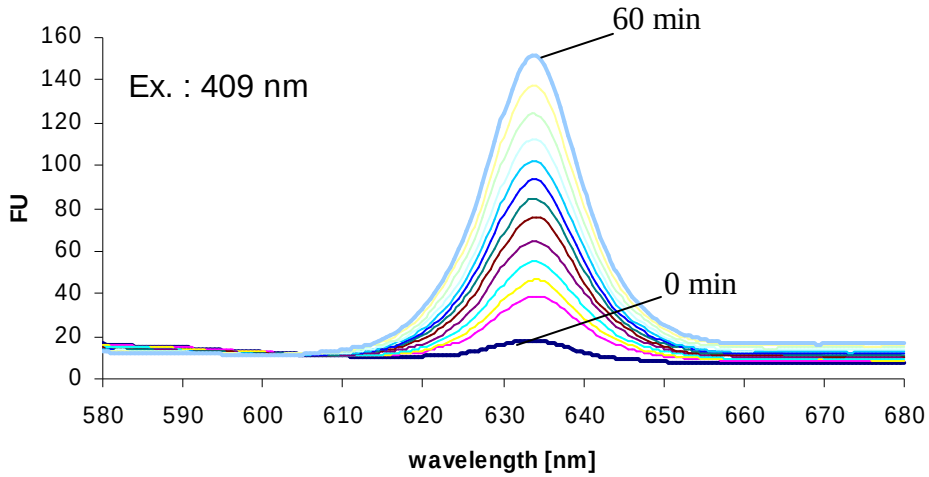

Fig. 11: Fluorescence detection of proto formation in cell-free *E. coli* extracts.
50 mM TRIS-HCl pH 7.5, 1 mM EDTA, 5 mM glutathione, 0.3 % Triton® X-100, 100 mM NaCl, 10 µM proto and 10 mM fumarate were mixed with 100 µl of a cell-free *E. coli* extract in a total volume of 250 µl and incubated at RT. Fluorescence spectra (exitation wavelength 409 nm) were recorded every 5 minutes. FU: fluorescence units

The assay contains residual amounts of proto (t=0). This is due to incomplete chemical reduction of proto during the preparation of the substrate proto´gen. Fluorescence values at t = 0 were subtracted from all values obtained thereafter. In most activity tests displayed in this thesis, the obtained fluorescence values are indicated as bars. Product

concentrations were determined with the help of the calibration curve (fig. 10). The protein content of samples was determined by Bio-Rad Protein Assay (Bio-Rad, Munich, Germany) and specific PPO activities were calculated where appropiate.

With this PPO activity test, enrichment of *E. coli* PPO activity was started by separating cytosolic proteins from the membrane fraction. A previously developed protocol for the separation of membrane and cytosolic fraction was used. A strong enrichment of PPO activity was observed in the membrane fraction after using differential centrifugation in combination with a three step sucrose gradient. The membrane fraction was enriched in brownish band on top of the 60 % (w/v) sucrose solution.

While the cell extract had a specific PPO activity of 23 pmol h^{-1} mg^{-1} protein, the membrane fraction obtained by the described separation protocol possessed a significantly higher specific PPO activity. A specific PPO activity of 114 pmol h^{-1} mg^{-1} protein was observed in fractions prepared using the three-step sucrose gradient (20, 40 and 60 % sucrose).

To further purifiy the PPO of *E. coli*, the yet unknown protein had to be extracted from the membrane fraction. This can be facilitated by the addition of detergent. In previous experiments it was shown that Triton® X-100, Tween® 80 and Thesit® are capable of solubilising PPO activitity from the membrane fraction (Breckau, 2005). These detergents are mixtures of molecules with differing lengths, hampering subsequent LC-MS/MS analysis required for the identification of the protein.

Therefore, four additional non-ionic detergents were tested, at a concentration of 0.5 % (w/v), for their ability to release PPO from *E. coli* membranes (fig. 12). The compounds (undecyl-β-D-maltoside, Digitonin, Cymal 6, and dimethyldodecyl-phosphinoxid) are of homogenous composition and should therefore allow for an LC-MS/MS analysis. In control experiments either Triton® X-100 or no detergent at all was used in order to evaluate the efficiency of extraction by the detergents.

PPO activity was observed after the extraction with all detergents tested. Interestingly, in control experiments where the membrane fraction was stirred in buffer without detergent, a high specific PPO activity was detected after extraction as well. The absence of detergent in these fractions was a good prerequisite for their further use in LC-MS/MS analysis and chromatographic purification steps.

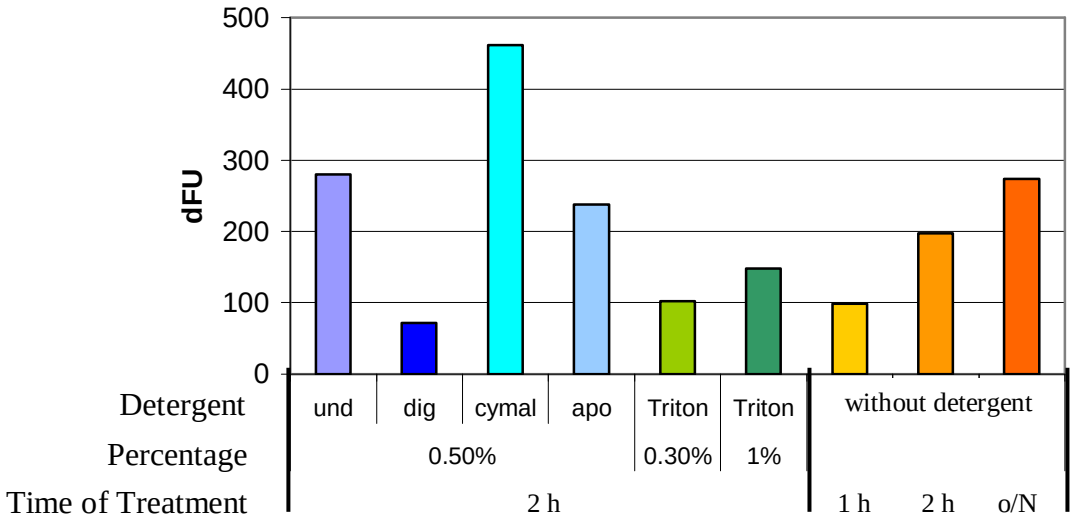

Fig. 12: Oxygen-independent PPO activity after solubilisation from cytosolic membranes.
The PPO activity assay was performed as described (2.7.3) with fumarate. Extractions were performed for 2 h or as indicated. Used detergents were: Und = undecyl-β-D-maltoside, Dig = Digitonin, Cymal = Cymal 6, apo = dimethyldodecyl-phosphinoxid, Triton = Triton® X-100, o/N = overnight. dFU = fluorescence units with t = 0 min subtracted from t = 60 min.

After extraction of PPO activity without detergent, an anion exchange chromatography on DEAE sepharose was performed. The positively charged matrix interacts with negatively charged regions occurring on surfaces of proteins. The stepwise increase of salt concentrations leads to the interruption of these interactions and the elution of respective proteins. The protein fractions obtained were analysed by SDS-PAGE (fig. 13 A) and tested for PPO activity (fig. 13 B).

A:

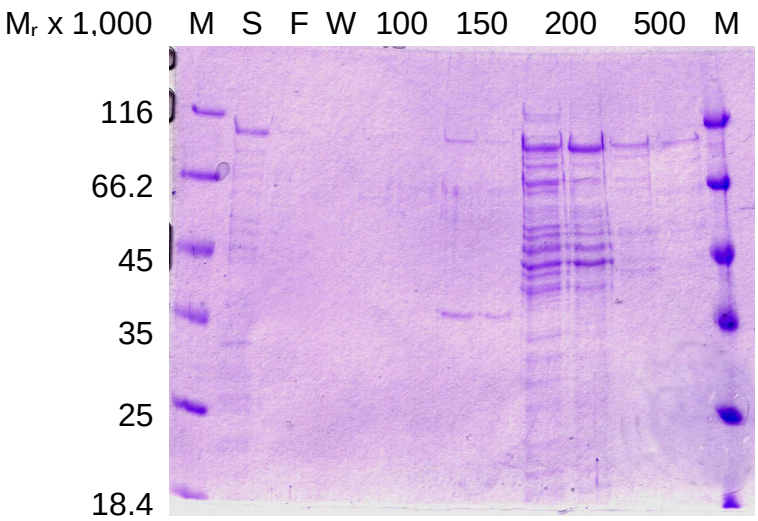

B:

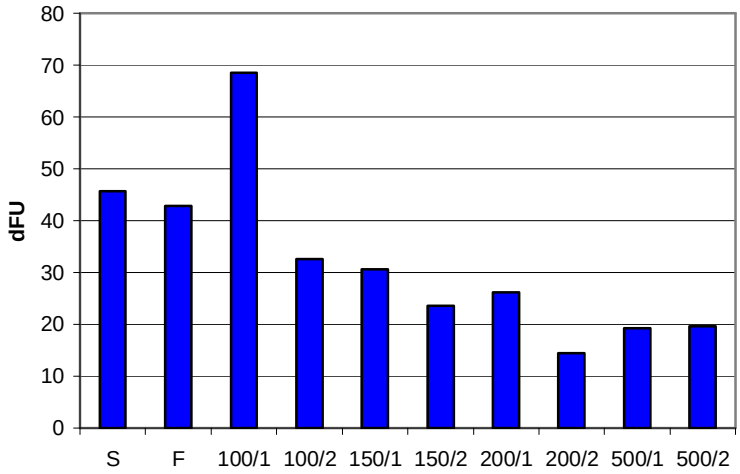

Fig. 13 A: Polyacrylamide gel (12 %) of the proteins obtained after the anion exchange chromatography of the solubilised membrane fraction proteins on DEAE sepharose FF.
Protein fractions of the chromatography were separated by SDS-PAGE, afterwards the gel was stained with Coomassie Brilliant Blue. M: Molecular weight marker with relative molecular masses of marker proteins are noted at the left. S: solubilised protein sample before chromatography. F: flow through. W: pooled washing steps. 100-500: mM concentrations of NaCl in the fractions after chromatography.
B: PPO activities after DEAE sepharose chromatographic purification.
The PPO activity assay was performed as described (2.7.3) with TTC as electron acceptor. S: solubilised protein sample before chromatography. F: flow through. 100/x-500/x: mM concentrations of NaCl in elution fraction x after chromatography. dFU: fluorescence units with t = 0 min subtracted from t = 60 min.

The SDS-PAGE analysis revealed that most proteins bound to the DEAE material eluted at a salt concentrations above 150 mM. In fractions containing ≤ 150 mM NaCl, only few proteins were detectable after staining the SDS-PAGE gel with Coomassie Blue. However, when tested for PPO activity, the highest activities were observed in fraction one eluted with 100 mM NaCl. Significant PPO activity was also detected in the flow through fraction. This indicates weak binding of the PPO to the chromatography resin. Additionally, PPO activity was observed in all other elution fractions as well. These

fractions displayed less than half of the PPO activity when compared to the 100 mM fraction. These results might indicate that the PPO extracted from membranes without detergent shows no distinct chromatographic behaviour for the employed resin.

Nevertheless, the majority of PPO activity could be separated from contaminating proteins during this purification step. A 1.5 fold enrichment of PPO activity was observed when the solubilised and the 100 mM fractions are compared. Twenty µl of the 100 mM fraction were applied to an SDS-PAGE and respective lanes were excised. After tryptic digestion, the peptide content (see appendix 1) was determined by Dr. Dörte Becher via LC-MS/MS analysis (Institut für Mikrobiologie Greifswald, Germany). In this analysis, the peptides of a sample are separated by high perfomance liquid chromatography (HPLC) and the molecular masses subsequently determined by mass spectrometry.

Peptide fragments of up to 60 proteins per sample were identified in this analysis. Many ribosomal proteins, elongation factor EF-Tu, and few hypothetical proteins were among the proteins identified. None of these hypothetical proteins was present in all samples. When analysed for their size, the genome context of the corresponding genes or the distribution in anaerobic or facultative organisms, all hypothetical proteins had to be excluded as candidates for the PPO of *E. coli*. However, in all analysed fractions, peptides derived from HemG were found. HemG was the protein for which the most peptides were detected in almost all samples.

This result supports the proposed participation of HemG in the enzymatic conversion of proto´gen to proto described by Sasarman *et al*. (1993). An additonal protein, assumed to be necessary for PPO activity (Panek and O´Brian, 2002), was not found in these experiments. Due to these findings it was unclear whether HemG is capable of catalysing the PPO reaction alone. To further investigate characteristics of the protein HemG, the protein was recombinantly overproduced and purified.

3.2 Production and purification of recombinant Escherichia coli *HemG*

E. coli hemG was cloned into the expression vector pET Duet-1 (Novagen, Madison, USA) for the recombinant production in *E. coli.* The vector encodes the fusion protein of HemG with an N-terminal polyhistidine-tag (Schröder, 2006). The plasmid mediates resistance to ampicillin.

3.2.1 Overproduction of recombinant HemG in *Escherichia coli*

The vector pET Duet-1 *hemG* was transformed (section 2.7.5) into *E. coli* BL21 (λDE3). The recombinant cells were cultivated and HemG production was induced by the addition of 100 µM IPTG. The production was monitored by taking samples from the culture at defined time points and analysing them by SDS-PAGE.

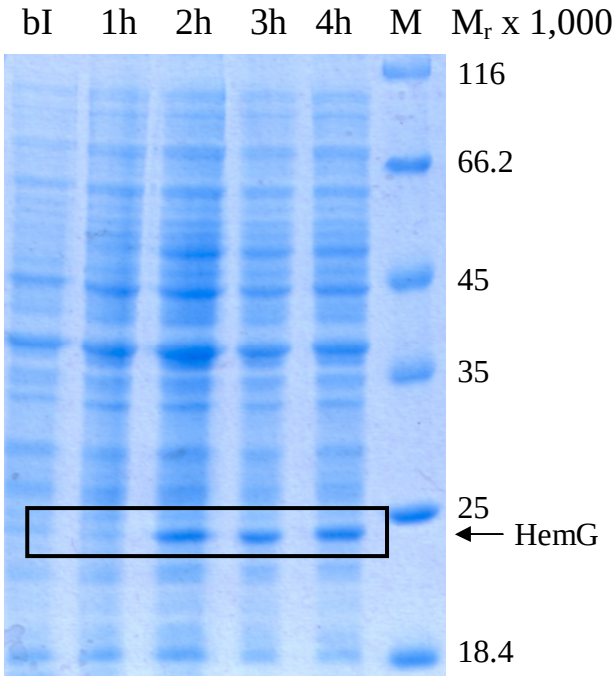

Figure 14: Recombinant protein production of *E. coli* HemG in *E. coli*.
Cultures of *E. coli* BL21 (λDE3) pET Duet-1 *hemG* were grown at 37°C. Recombinant gene expression was induced with 100 µM IPTG. Samples of the cultivation were taken at indicated time points and proteins were prepared for SDS-PAGE analysis by lysing the cells by boiling for 5 min in SDS loading dye. The figure shows a polyacrylamide gel (12 % (w/v)) of all proteins after separation and staining with Coomassie Brilliant Blue. **bI:** Sample before induction of gene expression by IPTG. **1h, 2h, 3h, 4h:** sample taken 1 h, 2 h, 3 h and 4 h after induction. **M:** Protein Molecular Weight Marker. The relative molecular masses (M_r x 1,000) of the marker proteins are given.

Figure 14 shows the recombinant overproduction of HemG. The calculated molecular mass of the N-terminal fusion protein (22,127 Da) is in good agreement with the observed relative molecular mass of ~ 23,000.

It was investigated which effect recombinant overproduction of HemG would have on the PPO activity of cell-free extracts. Cells with induced protein production were grown to optical densities at 578 nm 0.6, 0.9 and 1.4, respectively. Subsequently, they were harvested and disrupted. Then, the standard activity assay was performed. The observed activities were compared to PPO activties of *E. coli* cells harbouring the geneless expression vector.

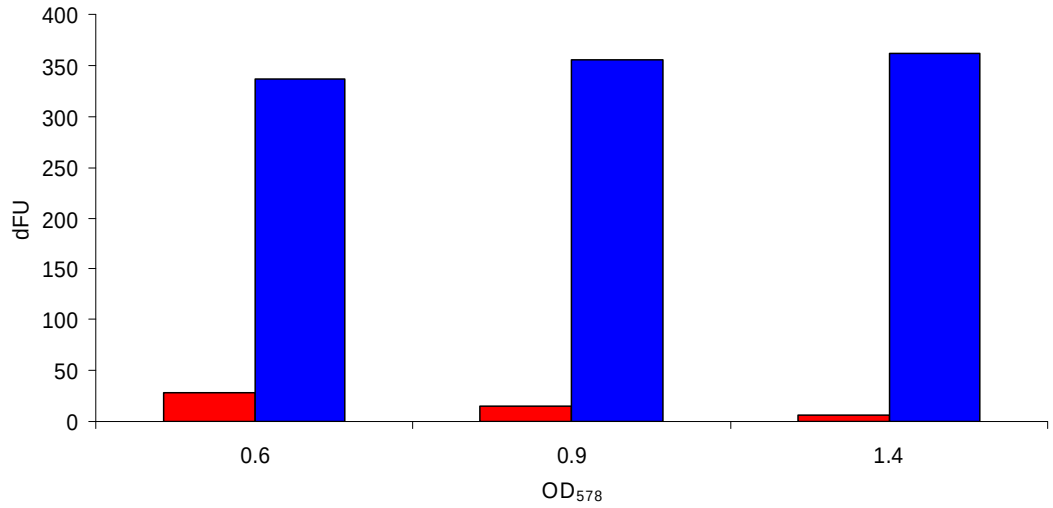

Fig. 15: PPO-activities of *E. coli* BL21 (λDE3) after overproduction of homologous HemG.
PPO-activities of cell lysates of BL21 (λDE3) containing pETDuet-1 (red) were compared to lysates of BL21 (λDE3) transformed with pETDuet-1 *hemG* (blue) overproducing HemG. Recombinant gene expression was induced with 100 µM IPTG. Both strains were grown to an OD_{578nm} of 0.6, 0.9, and 1.4, respectively. The cells were harvested, lysed and the PPO-activities were recorded for 60 min. TTC was used as electron acceptor. dFU: fluorescence units with t = 0 min subtracted from t = 60 min.

In any growth phase, PPO activity was found to be more than 12 times higher in the strain overproducing HemG. From these results it was concluded that HemG is essential for PPO activity. Either HemG is an essential part of a PPO-catalytic complex where HemG concentrations are limiting for the overall PPO activity. Another option is that HemG is solely capable to facilitate the PPO reaction in *E. coli*.

3.2.2 Purification of HemG from *Escherichia coli* Host Cells

HemG was purified by affinity chromatography to Ni-NTA. Six histidines are located within the tag fused to the N-terminus of HemG. Thereby, this tag possesses an affinity towards nickel atoms. The metal is immobilized on an inert resin and can thus be used for purification of His_{6x}-tagged fusion proteins. Cell-free extract of *E. coli* recombinantly overproducing HemG (section 3.2.1) was loaded onto the gravity column and stringent washing was applied. Proteins retained on the column were eluted by the addition of

imidazole. Obtained fractions were analysed by SDS-PAGE (fig. 16 A) and tested for their ability to convert proto´gen into proto (fig. 16 B).

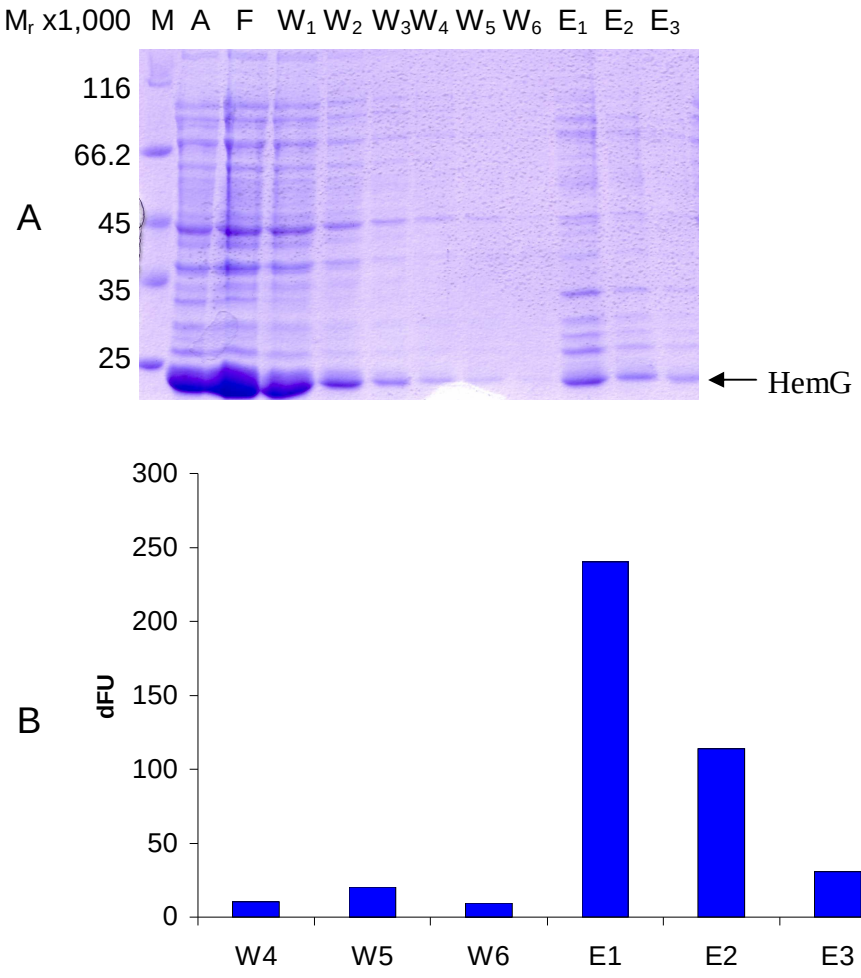

Fig 16 A: Affinity chromatography of *E. coli* HemG using Ni-NTA Superflow.
Fivehundred ml cultures of BL21 (λDE3) pETDuet-1 *hemG* were grown and recombinant gene expression was induced with 100 µM IPTG. Cells were harvested and disrupted anaerobically. The cell-free extract was applied to 1 ml Ni-NTA Superflow resin. The column was washed with 6 C_V and bound protein was eluted with 500 mM imidazole. The picture shows a polyacrylamide gel (12 % (w/v)) of proteins after and staining with Coomassie Brilliant Blue. M: Protein Molecular Weight Marker. The relative molecular masses of the marker proteins are given. A: Cell-free extract applied to the column. F: flow through. W_{1-6}: Washing steps. E_{1-3}: Elution steps.
B: PPO-activities of fractions from the purification of HemG by affinity chromatography.
PPO-activities were obtained as described in section 2.7.3. 100 µl of the given purification fractions with TTC as electron acceptor were used and the proto formation after 60 min depicted. W4-6: Washing steps 4-6 of the chromatography. E1-3: Elution steps 1-3 of the chromatography. dFU: fluorescence units with t = 0 min subtracted from t = 60 min.

As can be observed in the SDS-PAGE analysis of the chromatography (fig. 16 A), HemG can be found in the applied sample, but also in the flow through of the column and the washing steps. This indicates that a considerable amount of HemG is not retained on the column. It was speculated that the His_{6x}-tag is not readily accessible to bind to the nickel atoms of the resin but might be concealed by amino acid residues of the HemG protein.

Nevertheless, HemG was found in the elution fractions (E1 - 3). Apparently, the His_{6x}-tag of HemG has been properly bound to the affinity matrix in a subset of protein molecules. When the mentioned fractions where analysed for PPO activity (fig. 16 B), significantly higher activities where found in the elution fractions compared to the washing steps. The observed PPO activity correlates with the observed HemG protein amount in the SDS-PAGE gel. Since the elution fractions still contain several contaminating host proteins, it was not clear wether the HemG protein is capable of catalysing the PPO reaction by itself. In the case that a putative multi-subunit PPO exists in *E. coli* , the affinity of HemG to this PPO complex would have to be strong enough that the PPO complex remains intact upon purification.

In order to find proteins that possibly interact with HemG, the elution fractions obtained were analysed for their protein content by LC-MS/MS. Again, ribosomal proteins and the elongation factor EF-Tu were found in the samples (appendix 2). Interestingly, fumarate reductase and cytochrome *bd* oxidase subunits were found with many peptides. Fumarate reductase and cytochrome *bd* oxidase are part of the respiratory system of *E. coli.* Fumarate reductase has been postulated by Breckau (2005) and Jacobs and Jacobs (1975) to be involved in the electron transfer to fumarate.

To finally determine if HemG is the *E. coli* PPO, a protein production strategy had to be established in a host devoid of such anaerobic PPO system. In our group, the genome project "*Bacillus megaterium*" was started in 2006. The newly available genome sequence of this organism revealed a homolog of the *hemY* gene, but no orthologous gene sequence for *hemG*. Over the years our lab has gained solid experience with this protein production system (Biedendieck 2007), making *B. megaterium* a prime candidate for this strategy.

3.2.3 Cloning of *hemG* into *Bacillus megaterium* Expression Vectors

Two different *hemG* DNA sequences were used for cloning into *B. megaterium* expression vectors: the original *E. coli hemG* sequence which was obtained by PCR from the *E. coli* expression vector pETDuet-1 *hemG*. However, it is known that protein production in *B. megaterium* is sensitive to the codon usage of the target gene (Yang *et al*., 2007). The correlation of the codon occurence within the target gene and the preferred codons of the host is indicated as the “codon adaptation index” (CAI). This value can range from 0 (no similarity) to 1 (identical codon usage). It was found that recombinant genes with a CAI below 0.3 are not expressed in significant amounts in *B. megaterium*. The original *E .coli hemG* DNA sequence showed a CAI of 0.25. The DNA sequence of *hemG* was optimised with regard to its codon usage for the protein production in *B. megaterium* with the program JCAT (www.jcat.de). The new CAI was 0.99. The artificial *hemG* gene was generated by GeneArt (Regensburg, Germany) encoding for the original amino acid sequence of HemG. Both sequences were inserted into expression vectors by the *Sph*I and *Bgl*II restriction sites. The constructs will lead to recombinant HemG fused to an N- or C-terminal His_{6x}-tag. Protoplasts of *B. megaterium* WH323 were transformed with the resulting constructs as described in section 2.5.9.

3.2.4 Overproduction of *Escherichia coli* HemG in *Bacillus megaterium*

Recombinant *B. megaterium* cells either harbouring the original *E. coli hemG* or the artifical *hemG* were grown in 100 ml cultures. Recombinant protein production was induced by the addition of 0.5 % (w/v) of xylose. Proteins of samples taken from the cultures 1, 2, and 3 h after induction were analysed by SDS-PAGE (fig. 17). The occurrence of a protein with a size corresponding to the calculated size (M_r = 24,500) of HemG was observed in strains carrying the artificial gene, but not in cells harbouring the original *E. coli hemG*. It was concluded that HemG cannot be efficiently produced using the latter constructs. As mentioned in 3.3.3, this might be due to the low CAI of the original *hemG* gene for the host *B. megaterium*.

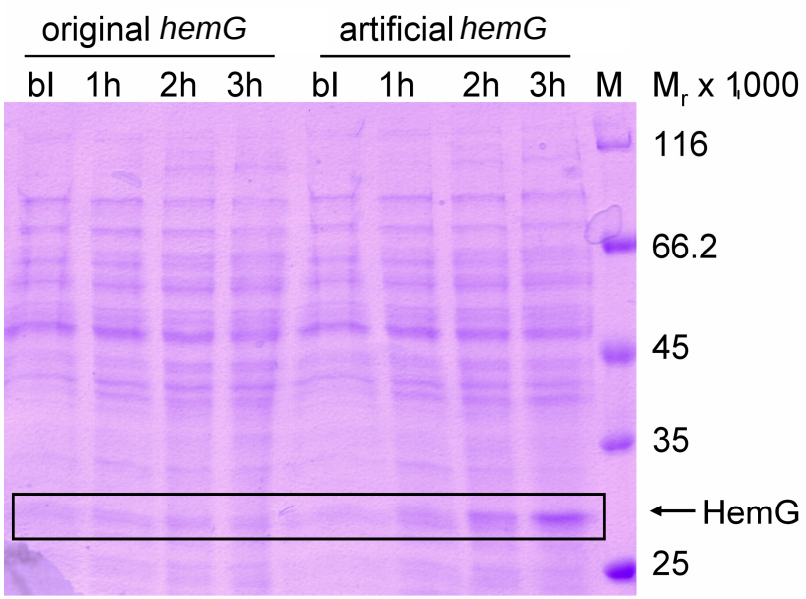

Fig. 17: Production of recombinant *E. coli* HemG in *B. megaterium*.
Proteins of 1 ml samples of 100 ml cultures of recombinant *B. megaterium* were analysed by SDS-PAGE. The picture shows a 12 % polyacrylamide gel of prepared proteins after separation and staining with Coomassie Brilliant Blue. **bI:** Sample before induction of gene expression by 0.5 % (w/v) xylose. **1h, 2h, 3h:** sample taken 1 h, 2 h and 3 h after induction. **M:** Protein Molecular Weight Marker. The relative molecular masses (M_r x 1,000) of the marker proteins are given.

3.3 Verification of PPO activity for Escherichia coli *HemG*

After production of HemG, the recombinant *Bacillus* cells were harvested and disrupted to analyse the lysates for anaerobic PPO activity with TTC as electron accceptor. In addition to the constructs described, a strain containing a vector without target gene was tested as a negative control. For this control, O_2-independent PPO activity was not detectable (fig. 18). This is consistent with the genetic backround of *B. megaterium* (3.2.2) with no orthologous *hemG* sequence. The strain containing the vector with the original *hemG* DNA sequence showed no anaerobic formation of proto. However, in the strain overproducing HemG from the artificial codon usage optimised gene, a strong and clearly detectable formation of proto could be observed .

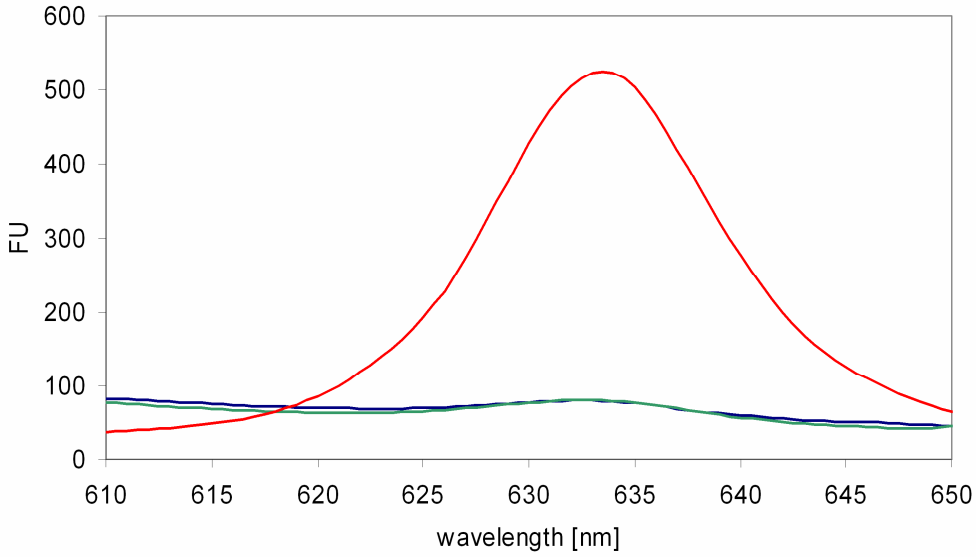

Fig. 18: Anaerobic PPO activity in *B. megaterium* strains harbouring no, the original or the artificial codon usage optimised *hemG* genes.
Standard PPO activity tests were performed with 100 µl of cell lysate and TTC. green: *B. megaterium* transformed with pN-His1622 (control). blue: *B. megaterium* transformed with pN-His1622 *hemG* (original). red: *B. megaterium* transformed with pN-His1622 *hemG* (artificial). FU: fluorescence units

The results indicate that the HemG protein is capable of the conversion of proto´gen to proto in cellular extracts of *B. megaterium*. Therefore, HemG is concluded to be the PPO of *E. coli*. Although it has been speculated for many years about the participation of HemG in this reaction (Panek and O'Brian, 2002; Sasarman *et al*., 1993), this is the first time such a biochemical evidence is provided.

The prescence of HemG is not limited to *E. coli*, it can be found in all Enterobacteriaceae such as *Salmonella*, *Yersinia* and *Vibrio* species. It is also found in anoxygenic phototrophs such as *Rhodobacter sphaeroides*. It has been reported that *R. sphaeroides* couples the oxidation of proto´gen to the electron transport chain (Jacobs and Jacobs, 1981), thus presumably producing functional HemG. All these organisms have a demand for tetrapyrroles under oxygen-restricted conditions.

3.4 Purification of recombinantly produced Escherichia coli *PPO*

After demonstrating that HemG is the PPO of *E. coli*, the enzyme was to be biochemically characterised. For this purpose, HemG was purified after overproduction in *B. megaterium* using the artificial codon optimised *hemG* sequence.

3.4.1 Purification of recombinant HemG by Affinity Chromatography

The construct pC-His1622 *hemG* (codon optimised) encoding for a C-terminal fusion protein of HemG and a His_{6x} tag was utilised for all further purifications. Figure 19 displays the affinity purification via Ni-chelating resin and the stability of HemG in solution over time.

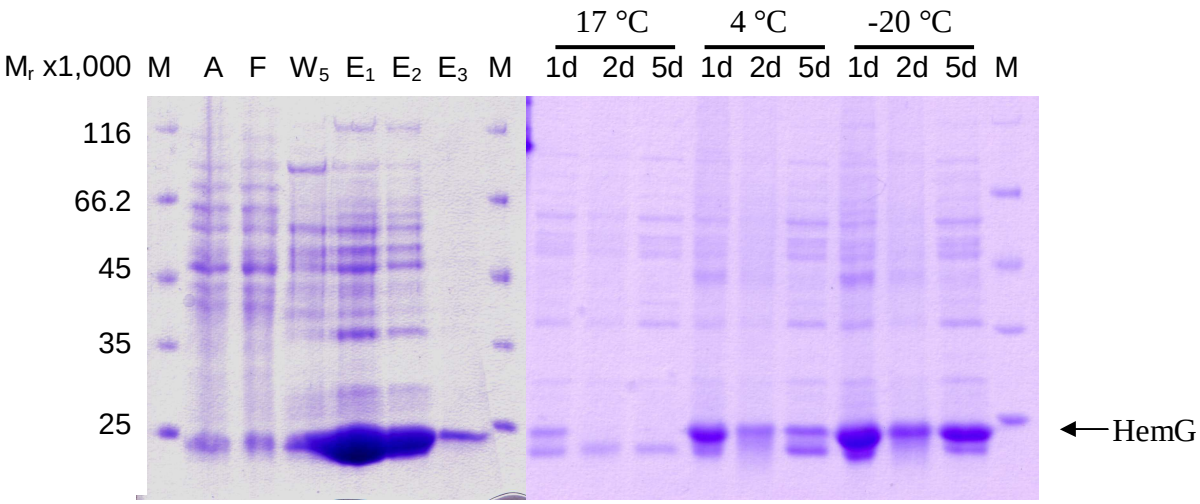

Fig. 19: Affinity purification of HemG-His after production in *B. megaterium*
B. megaterium cells transformed with pC-His1622 *hemG* (codon optimised) of a 400 ml culture were used for the purification. The figure shows a 12 % polyacrylamide gel of proteins after separation and staining with Coomassie Brilliant Blue. M: Protein Molecular Weight Marker. The relative molecular masses of the marker proteins are given. A: Sample applied to the purification. F: flow through. W_5: Washing step 5. E_{1-3}: Elution steps. 1d, 2d, 5d : HemG 1, 2 and 5 days anaerobically incubated at the temperatures given.

With this protocol, high amounts of HemG were purified. The obtained elution fractions were yellow in colour and showed a very high PPO activity. However, purified HemG was unstable and prone to degradation. After 5 days at 17 °C, full length HemG was no longer visible in SDS gels stained with Coomassie Brilliant Blue. A decrease in HemG content in the fractions was also noted when the protein was stored at 4 °C. Therefore, it was stored at -20 °C. Here, only a slight reduction of HemG was ob served. As can be deduced from figure 19, HemG was not purified to homogeneity by this purification step. Therefore, a subsequent gel permeation chromatography was performed.

3.4.2 Gel Permeation Chromatography

Gel permeation chromatography (GPC) separates proteins by their native state size. Big proteins get eluted first, while small proteins are retarded longer. A column was applied which is suitable for proteins with a M_r of 10,000 to 600,000. First attempts were unsuccessful due to the elution of HemG in the void volume (7.7 ml), which indicates a M_r of the protein above 600,000. Since HemG has a calculated M_r of 24,500 for a single peptide, the protein seemed to form large aggregates in solution (fig. 20). After the addition of the detergent Thesit®, HemG could be eluted within the separating range of the column (14.37 ml).

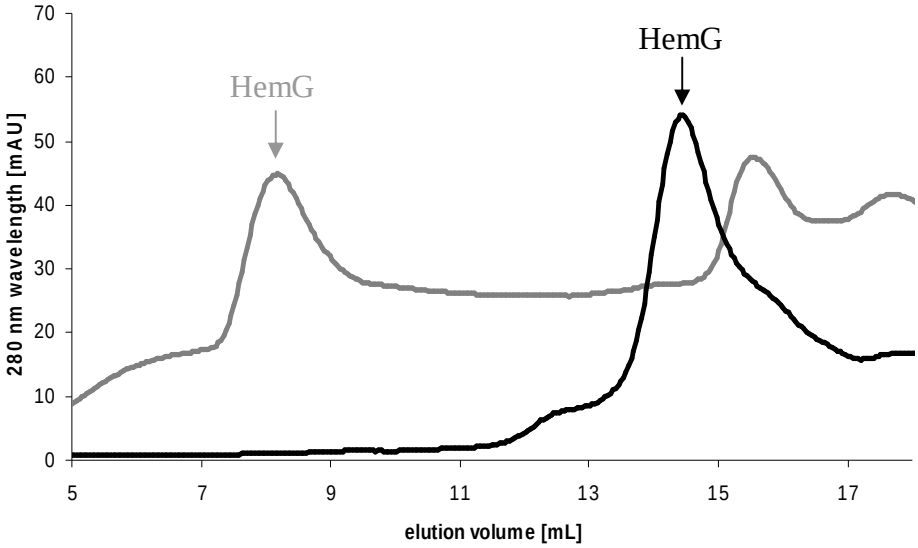

Fig. 20: Gel permeation chromatography of HemG
Hundred µl of HemG solution (2 mg/ml) were loaded on a Superdex 200 HR 10/30 column and eluted with buffers containing no detergent (grey) or 2 % Thesit® (black), with the absorption at 280 nm wavelength being recorded. Without detergent, high molecular weight complexes (Mr > 600,000) of HemG were eluted in the void volume of the column (V_0 = 7.7 ml). After the addition of 2 % Thesit®, HemG was eluted in the separating range of the column (14.37 ml).

It seems possible that HemG possesses hydrophobic regions which are responsible for the association to the membrane. Consequently, due to these regions HemG is prone to aggregation if not masked by detergent molecules. HemG was isolated from *B. megaterium* host proteins by this second purification step as judged by SDS-PAGE (fig. 21).

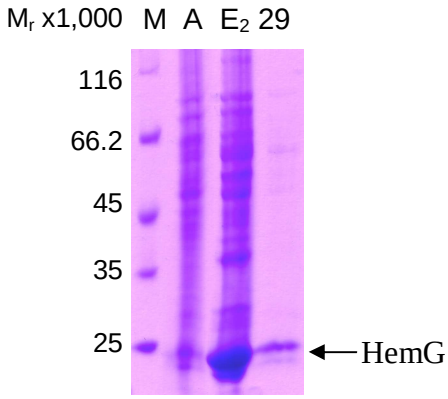

Fig. 21: Summary of purification steps performed to isolate HemG
The picture shows a 12 % polyacrylamide gel of proteins after separation and staining with Coomassie Brilliant Blue. M: Protein Molecular Weight Marker. The relative molecular masses of the marker proteins are given. A: *B. megaterium* cell extract. E_2: Elution fraction 2 of affinity chromatography. 29: fraction 29 of GPC.

3.5 Electron Transfer from HemG in vitro

The O_2-dependent PPO, HemY, directly transfers electrons evolving from the reaction onto molecular oxygen. In this study, it was to be determined which electron acceptors are utilised by HemG. Since HemG could be successfully isolated, investigations concerning direct and terminal electron acceptors were performed.

3.5.1 Direct Electron Acceptors for the HemG catalysed Reaction

To investigate which compounds are capable of directly taking up electrons from HemG, activity tests containing HemG and the substrate, proto´gen, together with several chemicals were performed. Fumarate, nitrate, oxygen, and TTC, but also menaquinone (MQ) and ubiquinone (Q_1) were shown to be electron acceptors of the PPO reaction if HemG purified from *E. coli* was used (fig. 22). The utilisation of quinones (MQ an Q_1) fits well with earlier proposals (Jacobs and Jacobs, 1976). The applied HemG-fraction was contaminated with proteins of the *E. coli* host, among them subunits from fumarate reductase (section 3.3.1). It was assumed that activities observed with fumarate, nitrate and oxygen derive from the corresponding, co-purified terminal oxidases of *E. coli*.
HemG purified from *B. megaterium* was devoid of PPO activity with fumarate and nitrate, but capable of oxidising proto´gen with oxygen, MQ, Q_1 and TTC. It is tempting to assume that these molecules are indeed direct electron acceptors. However, it should be noted that the *B. megaterium* genome possesses open reading frames (ORF_5403 and ORF_6607) with high homologies to *cydA* and *cydB* of *Bacillus subtilis,* which encode cytochrome *bd* oxidase subunits. It might be possible that minor amounts of cytochrome

oxidase of *B. megaterium* adhere to *E. coli* HemG during the purification process. This would explain the reproducible utilisation of oxygen as electron acceptor. If HemG uses oxygen directly or the respiratory chains of *B. megaterium* are used cannot be elucidated with these experiments. Therefore, only MQ, Q_1 and TTC were assigned with certainty as direct electron acceptors of HemG.

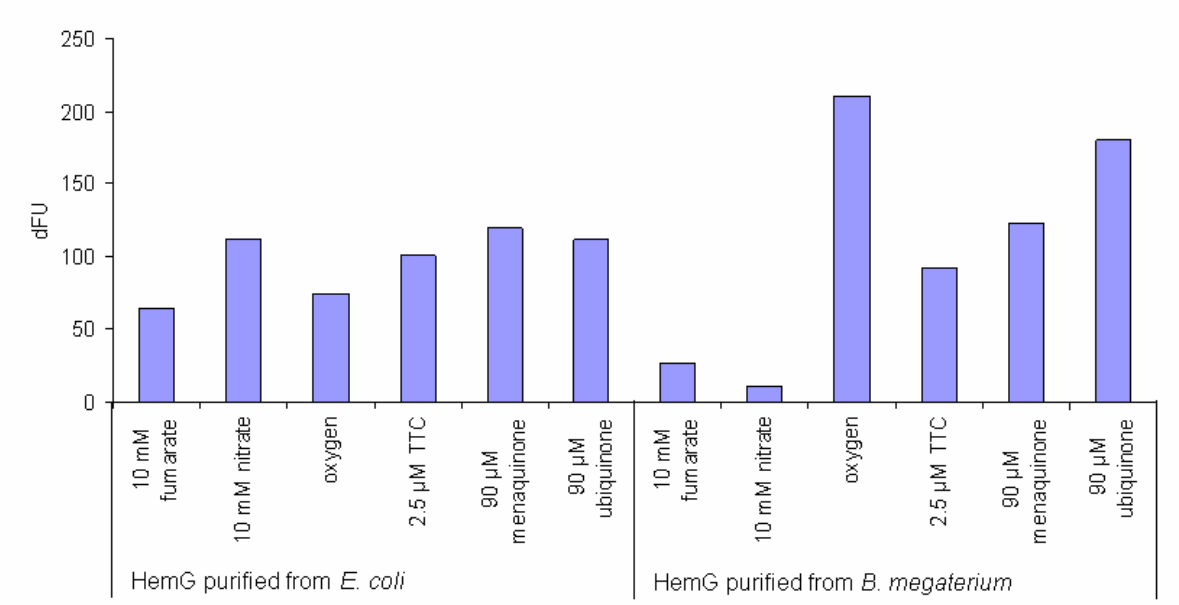

Fig 22: Electron acceptors for the PPO reaction catalysed by *E. coli* HemG
The PPO activity assay was set up and started as outlined in 2.7.3. 30 pmol of purified HemG prepared from *E. coli* or *B. megaterium* were applied. The electron acceptors were added in the concentrations given. dFU: fluorescence units with t = 0 min subtracted from t = 60 min.

3.5.2 Production and Purification of Terminal Oxidases

Next, the role of the terminal oxidases for the PPO reaction was investigated. To accomplish this, four *E. coli* terminal oxidases had to be purified and subsequently applied to an *in vitro* activity assay.

Fumarate Reductase

Fumarate reductase (FRD) was purified by FPLC as described by Luna-Chavez *et al*. (2000). DW35 pH3 cells overproducing FRD where cultivated in glycerol-fumarate-medium and harvested. After cell disruption, membrane fractions were prepared and FRD extracted with the help of the detergent Thesit®. The solubilised proteins were subjected to an anion exchange chromatography on DEAE sepharose. Analysis of these fractions by SDS PAGE visualised all subunits (FrdABCD) of the fumarate reductase (fig. 23).

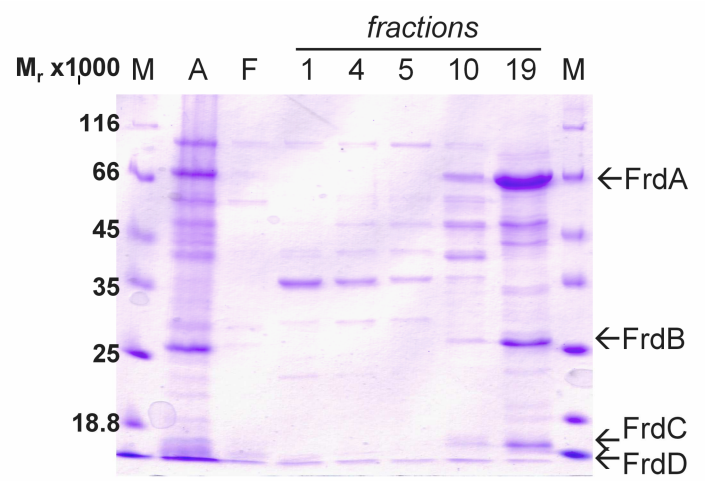

Fig. 23: FPLC purification of *E. coli* fumarate reductase
The pictures shows a 12 % polyacrylamide gel of proteins after separation and staining with Coomassie Brilliant Blue. M: Protein Molecular Weight Marker. The relative molecular masses of the marker proteins are given. A: *E. coli* DW35 pH3 cell extract. F: flow through.

After FPLC purification, obtained fractions were brown in colour, indicating the presence of a Fe-S-cluster described for subunit B (Luna-Chavez *et al*., 2000). The fractions where tested for the ability to reduce fumarate. In the assay, reduced benzyl viologen acts as electron donor. The molecule is coloured in this fully reduced state, but loses this property when oxidised. Applied to the assay, the purified fractions exhibited high fumarate reductase activity observable in the decrease of absorption (fig. 24).

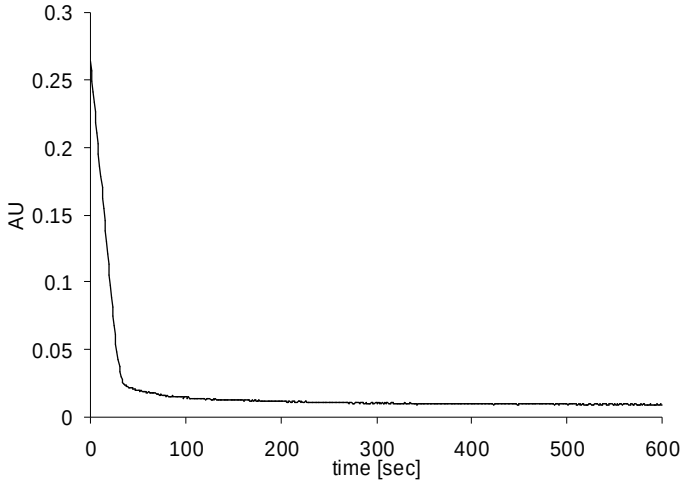

Fig 24: *E. coli* fumarate reductase activity test
The activity of fumarate reductase was assayed anaerobically as described before (Cecchini et al., 1986). First, benzyl viologen (250 µM) is reduced by Na-dithionite (10 mM). Then, purified fumarate reductase (7 µg) is added and the photometric detection started. Reduced benzyl viologen is oxidised by fumarate reductase. Electrons abstracted from benzyl viologen are transferred to fumarate (20 mM). During the reaction, absorption at 550 nm wavelength decreases, which was monitored for 10 min. AU: Absorbtion units.

Cytochrome Oxidases

Cytochrome *bo* and *bd* oxidase (Cyo and Cyd, respectively) were purified as described (Rumbley *et al.*, 1997; Kaysser *et al.*, 1995). *E. coli* cells overproducing one or the other oxidase where grown and harvested aerobically. Membrane fractions were prepared and the enzymes extracted either by the detergents Triton® X100 and N-octylglucoside or by the detergent CHAPS. Since subunit II of Cyo (CyoB) was fused to a His_{6x}-tag, an affinity purification of the Cyo complex was performed on Ni-NTA Superflow. Cyd had to be obtained by anion exchange chromatography to DEAE sepharose.The fractions of the purifications were analysed via SDS-PAGE (fig. 25). In this analysis, three of four subunits of cytochrome *bo* oxidase (CyoABCD) and both subunits of cytochrome *bd* oxidase (CydAB) were visible.

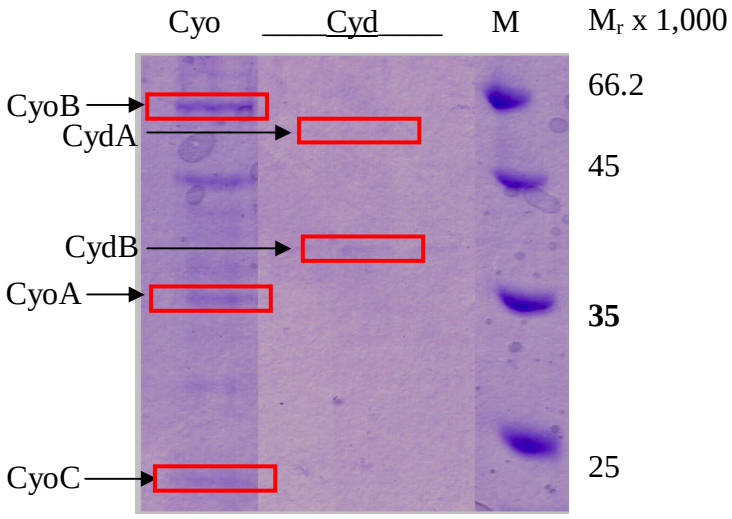

Fig. 25: Purification of Cytochrome *bo* and *bd* Oxidase
The picture shows a 12 % polyacrylamide gel of the proteins after separation and staining with Coomassie Brilliant Blue. Cyo: Cytochrome *bo* oxidase elution fraction 3. Cyd: cytochrome *bd* oxidase fraction 7 - 9. M: Protein Molecular Weight Marker. The relative molecular masses of the marker proteins are given. Observed proteins with relative molecular weights corresponding to Cyo or Cyd subunits are marked at the left.

Nitrate Reductase

Nitrate reductase NarGHI was kindly provided by Rodrigo Arias, CNRS, Marseille, France. The newly established protocol for the purification of Nar included the preparation of membranes and the extraction of the enzyme with the help of the detergent DDM. Currently it is under review to be published.

3.5.3 Application of the Terminal Oxidases in PPO *in vitro* Assays

The obtained *E. coli* terminal oxidases were each tested for the ability to take up electrons from quinones and transferring these electrons onto the terminal electron acceptor. Each terminal oxidase and the corresponding terminal electron acceptor were added to HemG purified from *B. megaterium.*

MQ was applied to assays containing fumarate reductase and nitrate reductase, while the assays with cytochrome oxidases were each supplemented with the ubiquinone Q_1. Since it was shown that quinones act as electron acceptors for the PPO reaction (3.5.1) when present in surplus (90 µM), the concentration of the quinones was lowered (1.8 µM). Hence, only minor proto formation should be observed when the electron flow terminates at the reduced quinones. In order to allow for significant proto formation, the quinones need to enter a cycle of being reduced by HemG and being oxidised by the terminal oxidases. In this type of assay, the quinones would act as electron "shuttles", as described for the natural respiratory system.

Since all the applied terminal oxidases have been reported to possess associated quinones and prosthetic groups, they were deemed capable of acting as electron acceptors as well. Thus they were applied in equimolar concentrations to HemG.

It was expected that proto formation should only occur when the terminal oxidases are functional in the PPO reaction. The reaction was started by the addition of proto´gen and the formation of proto was determined after one hour by fluorescence spectrometry (fig. 26).

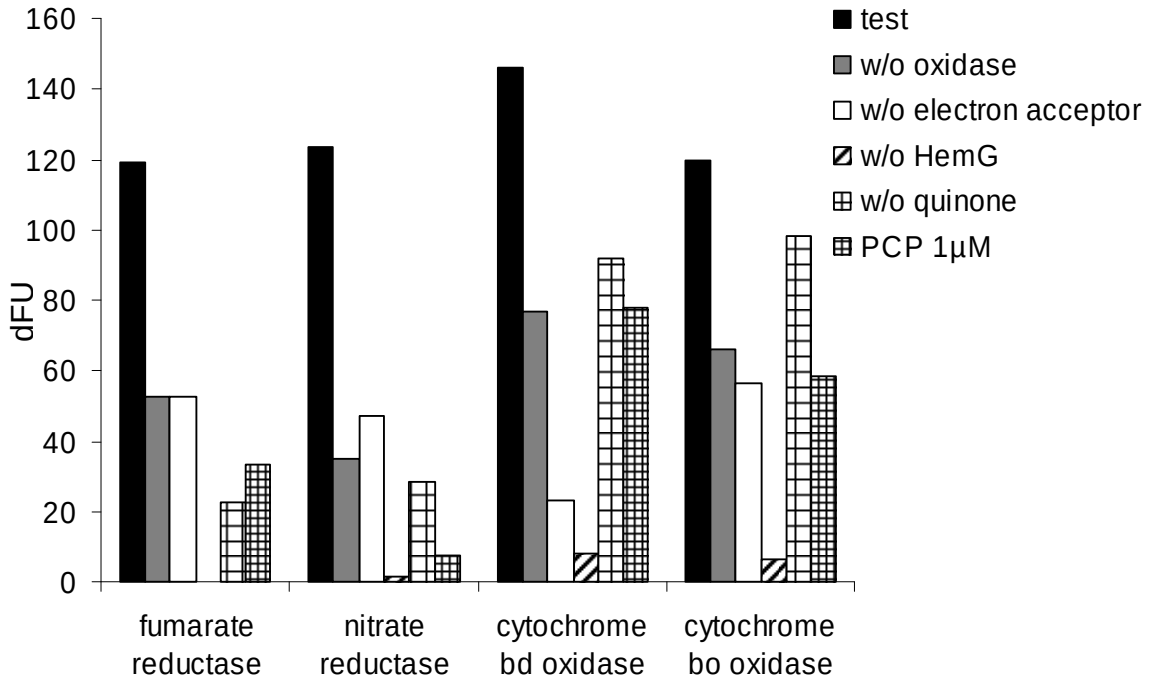

Fig. 26: Terminal oxidases tested for the participation in the *E. coli* PPO reaction catalised by HemG. The assay outlined in section 2.7.3 was performed with 30 pmol of HemG and 30 pmol of the specified oxidase. The corresponding terminal electron acceptor (10 mM fumarate, nitrate or for cytochrome oxidases: air) and 1.8 µM of menaquinone or ubiquinone, respectively, were added. 10 µM proto´gen was applied to start the assay and the formation of proto was recorded after 60 min. dFU: fluorescence units with t = 0 min subtracted from t = 60 min. w/o : without.

All terminal oxidases tested assisted HemG in the electron dissipation from proto´gen towards terminal electron acceptors (fig. 26). Variation in total activities was attributed to the quality of the preparation and kinetic properties of the terminal oxidases. Controls missing the terminal electron acceptor revealed significantly decreased PPO activity. If the assay was devoid of HemG, no activity was detectable. This indicated that neither terminal oxidase nor terminal electron acceptors oxidise proto´gen by themselves.

Under these conditions, the utilisation of oxygen by HemG fractions purified from *B. megaterium* (3.6.1) was insignificant. As mentioned above, good aerobic proto formation is only observed in the presence of Cyo and Cyd, respectively.

Interestingly, the overall PPO reaction seems to be sensitive to inhibition by pentochlorophenol (PCP). While assays containing Cyo and Cyd were moderately affected (52 and 47 %), tests with fumarate reductase and nitrate reductase were severely reduced in proto formation (73 % and 94 %, respectively). PCP is a compound known to efficiently occupy the quinone binding sites of some terminal oxidases (Bertero *et al*., 2005). Further, omitting quinones from the assay only partially reduces the PPO activity in some cases. For example, in the control experiment containing the terminal oxidase Cyo without the addition of quinone Q_1, still 81 % of proto was formed. As mentioned before, terminal oxidases have quinones associated to the membrane-spanning subunits. These

quinones seem to adhere to the oxidases during purification. For instance, the solved crystal structure of fumarate reductase purified by the same protocol displays menaquinone in subunits D and C (Iverson *et al*., 1999).

Taken together, the results indicate the utilisation of the qinones associated to terminal oxidases. For the transfer of electrons to these quinones a physical interaction of HemG and the oxidases seems to be necessary. The prescence of fumarate reductase and cytochrome *bd* oxidase subunits in HemG purifications from *E. coli* (section 3.2.1) and observed activities with corresponding terminal electron acceptors (section 3.5.1) confirm this proposal.

3.6 In vivo studies of Escherichia coli *mutants*

To confirm the results of the *in vitro* experiments, additional *in vivo* experiments were performed. Cell lysates of *E. coli* mutants deficient in terminal oxidases were to be investigated for their PPO activity. First, the strains were grown under conditions allowing for efficient cell growth of the mutants. Afterwards, the cultures were shifted to growth conditions which allow for a strong phenotype expression. *E. coli* DW35, deficient in the fumarate reductase, was first grown to an $OD_{578\ nm}$ of 2 under *aerobic* conditions. Then, this mutant was incubated *anaerobically* in medium supplemented with fumarate. JCB4023, deficient in functional nitrate reductase, was treated accordingly. Mutants of the cytochrome oxidases (DS253, FB20172 and FB 20228) where first grown anaerobically and then shifted to aerobic growth. The capability to form proto was compared to *E. coli* BL21 (λDE3), the wildtype strain, grown under the same conditions (fig. 27).

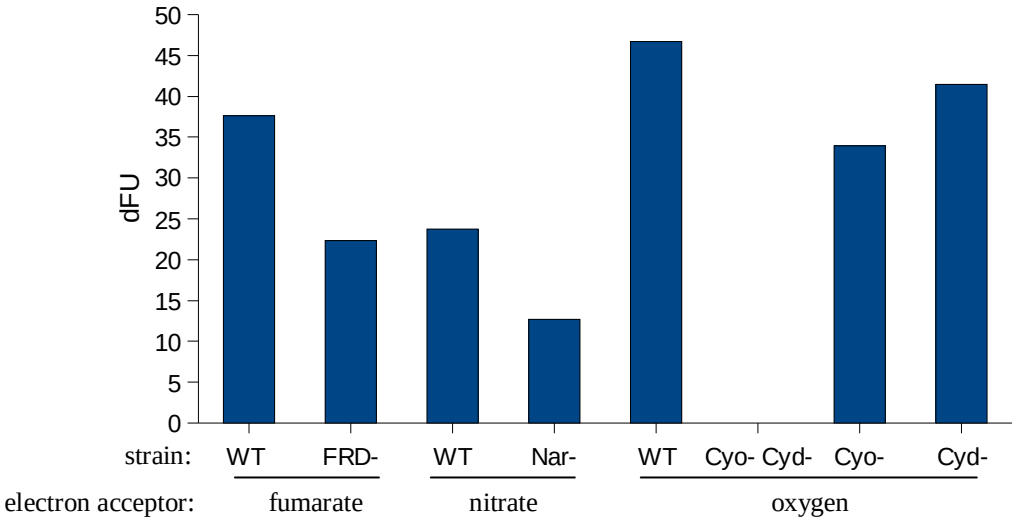

Fig 27: PPO activities in *E. coli* mutants deficient in components of the respiratory chains.
The activity assay were performed with cell-free extract of the respective strain containing 100 µg whole protein. 10 mM fumarate and 10 mM nitrate were used as electron acceptors in anaerobic assays. To test wether O_2 could be utilised as electron acceptor, aerobic assays were performed. To start the reaction, 10 µM proto´gen was applied and the assays incubated in the dark for 60 min at RT. The product formation was monitored by luminescence spectrometry. The excitation and emission wavelength were set at 409 nm and 633 nm, respectively. dFU: fluorescence units with t = 0 min subtracted from t = 60 min

With these experiments, the results of the *in vitro* experiments could be confirmed. All mutants deficient in terminal oxidases were reduced in PPO activity when tested with the corresponding terminal electron acceptor. However, only in the case of the Cyo/Cyd double mutant, PPO activty was completely abolished. Mutants deficient in either Cyo or Cyd retained 73 % and 88 % of wildtype activity. It was speculated that the PPO electron flow towards oxygen remains largely intact as long as one cytochrome oxidase is present in the cell.

The mutants deficient in fumarate reductase or nitrate reductase are capable of performing PPO activity to some extent (59 % and 53 % of wildtype activity, respectively) as well. It is possible that the remaining terminal oxidases (e.g. in DW35: Cyo, Cyd and nitrate reductase) take up electrons and transfer them to residual amounts of terminal electron acceptors (e.g. in DW35: O_2 and nitrate). This PPO activity seems to be independent of the electron acceptor added in the experiment.

The observation that mutants deficient in components of the electron transfer chains downstream of HemG are still able to perform the PPO reaction unambigiously underlines the redundancy of these respiratory chains in *E. coli*. The transfer of electrons into the respiratory chains allows *E. coli* to synthesize heme under a variety of environmental conditions.

3.7 Characterisation of Escherichia coli *HemG*

Besides the elucidation of electron “disposal” from the reaction, HemG was biochemically investigated.

3.7.1 Size of native enzyme

The purification principle of GPC is the separation of proteins by their native size. Therefore, this method can also be utilised to analyse the oligomeric state of HemG. A calibration curve with the elution volumes of marker proteins (cytochrome c from bovine heart: 18.27 ml; carbonic anhydrase: 17.29 ml; bovine serum albumin: 15.37 ml; alcohol dehydrogenase from yeast: 14.77 ml) was prepared. Then, the native molecular weight was estimated from the elution volume of HemG (14.44 ml; fig. 28).

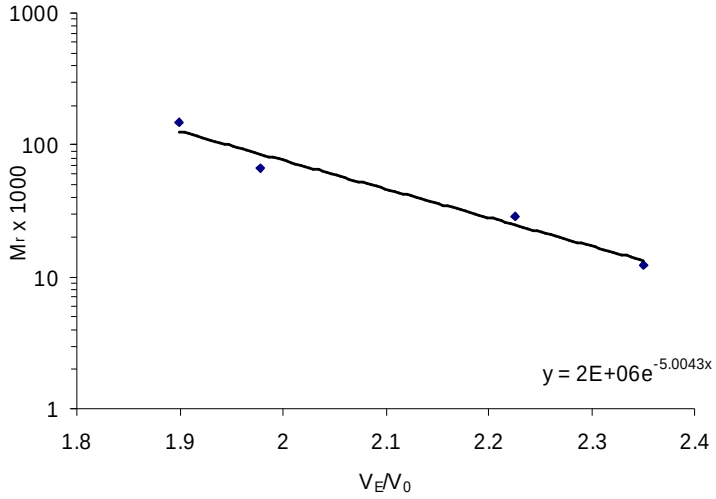

Fig. 28: GPC calibration curve with marker proteins
Marker proteins were loaded onto a Superdex 200 HR 10/30 column (GE Healthcare) and eluted with 50 mM of HEPES pH 7.5, 300 mM of NaCl, 20 % (v/v) of glycerol and 2 % of Thesit® (v/v) at a flow rate of 0.5 ml/min. The column was equilibrated with marker proteins of known relative molecular weight (M_r): Cytochrome c from bovine heart with 12,400, carbonic anhydrase with ~29,000, bovine serum albumin with ~66,200 and alcohol dehydrogenase from yeast with ~150,000 relative molecular mass. HemG eluted at a volume of 14.44 ml, which corresponded to a relative molecular weight of ~150,000.

With the help of the calibration curve, a M_r of 150,000 for the native HemG was calculated. Since a monomer of HemG-His_{6x}-tag fusion protein has a calculated mass of 24,500, a hexameric composition of *E. coli* PPO was implicated. For HemY a formation of a homodimer in several organisms is described (Corradi *et al*., 2006; Koch *et al*., 2004), with each monomer possessing an active site. It remains to be elucidated if each HemG monomer is coordinating one substrate molecule or if hexameric HemG is able to bind one proto´gen molecule.

3.7.2 Identification of the HemG Cofactor

As mentioned in section 3.5.1, purified HemG appears yellow in colour. UV-Vis spectra from the protein (fig. 29) showed peaks at 366 and 433 nm wavelength typical for flavin cofactors such as FMN and FAD (Craig *et al*., 2001; Kleiner *et al*., 1999). Interestingly, the UV-Vis spectrum featured an additional peak at a wavelength of 412 nm which could derive from a bound tetrapyrrole (Dailey and Dailey, 1996). The HemG protein was precipitated by the addition of trichloric acid (TCA) to find out if the putative flavin is covalently or noncovalently bound to HemG. The molecule responsible for the flavin spectrum remained in the supernatant after precipitation. This indicated a noncovalent binding of the compound.

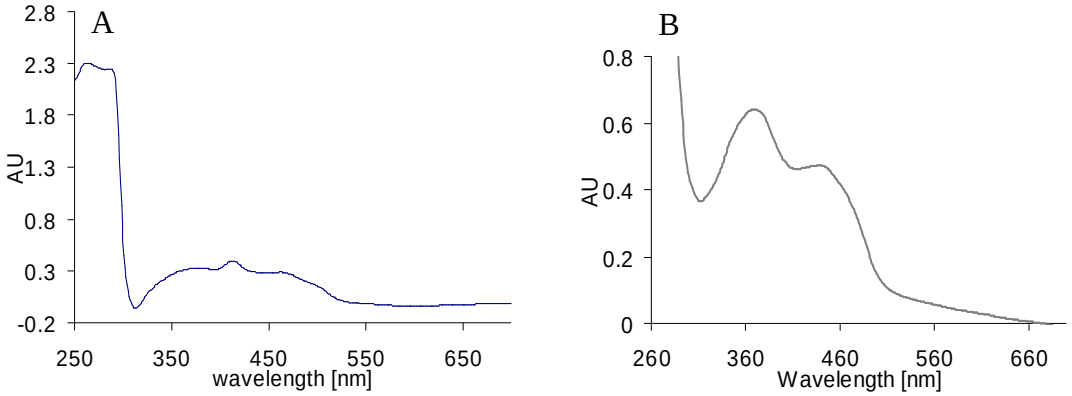

Figure 29: Spectral analysis of HemG for cofactor characterisation
A UV-Vis spectrum of purified HemG with elution buffer as background was recorded (A). Protein was precipitated by trichloric acid and the supernatant was analysed again (B). The spectra indicate the presence of a flavin cofactor, with characteristic peaks at 366 and 433 nm for the investigated supernatant.

To determine which flavin was utilised as cofactor by HemG, HPLC analysis was performed. Here, molecules are separated due to their hydrophobicity and elute from the column at specific retention times. Authentic standards of FAD and FMN had retention times of 7.5 and 10.1 minutes, respectively (fig. 30).

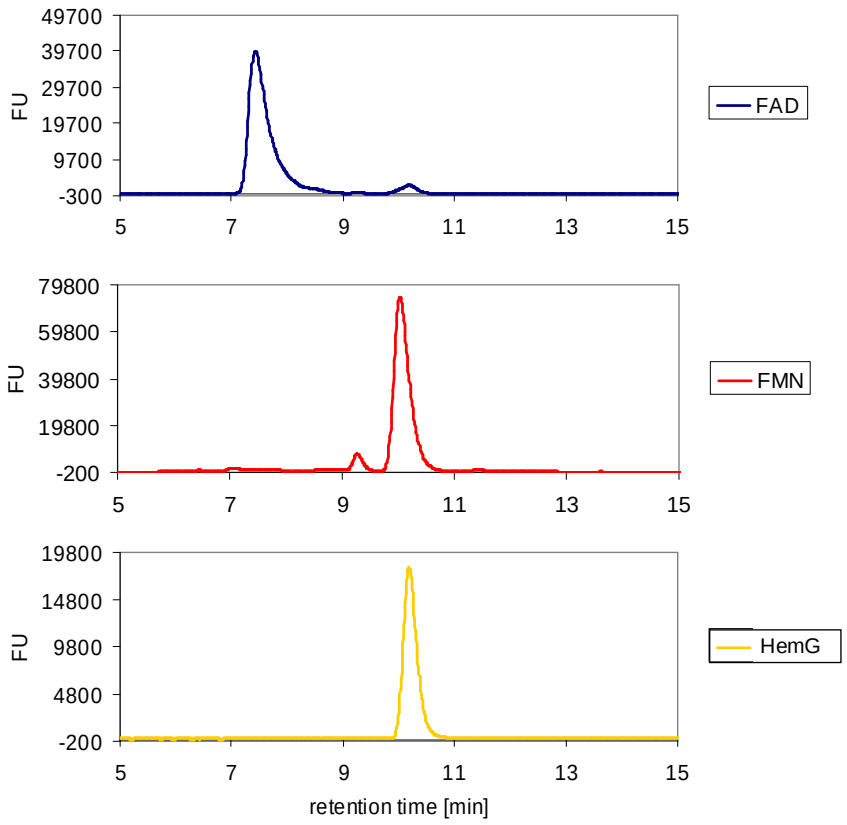

Figure 30: HPLC analysis of the FMN cofactor of HemG
HemG was precipitated by the addition of 5 % (v/v) of perchloric acid and a following centrifugation at 10,000 x g. Fifty µl of the obtained supernatant were injected on an ODS Hypersil 250 x 4.6 mm column. Flavins were detected by fluorescence measurements (Ex.: 430 nm; Em.: 525 nm). Authentic standards of FAD and FMN showed retention times of 7.5 and 10.1 minutes, respectively. The flavin bound to HemG eluted at the retention time of FMN. FU: Fluorescence units.

The flavin of HemG was found to have the identical retention time as determined for the FMN standard. This revealed that FMN was a cofactor noncovalently bound to HemG. In most investigations of HemY, a noncovalently bound FAD was found associated to the enzyme (Koch *et al*., 2004). FMN can reversibly take up two electrons and two protons, leading to $FMNH_2$. Therefore, it is involved in electron transfer reactions (Goni *et al*., 2008; Kim *et al*., 2007).

3.7.3 Kinetic Parameters of HemG

Kinetic data were obtained for the wildtype PPO of *E. coli*. To investigate the affinity to its substrate proto´gen, the Michaelis Menten constant K_M was determined for HemG. The maximal velocity V_{max} was determined as well. This was achieved by measuring the initial constant velocity of protoporphyrin IX formation from protoporphyrinogen IX over a substrate range from 2.3 to 92 µM of proto'gen. Interestingly, the use of amalgam-reduced substrate resulted in a lag phase of up to 120 sec before reaching maximum turnover rates. Additionally, the velocity of the reaction decreased with substrate concentrations

above 3 µM (fig. 31 A). This phenomenon was ascribed to the potential toxicity of trace amounts of amalgam in the substrate solution. By using substrate reduced by molecular hydrogen and palladium (Phillips, 2007), a Michaelis Menten kinetic was observed (fig. 31 B). Hence, only the kinetic data obtained from latter assays was used to calculate K_M and V_{max}.

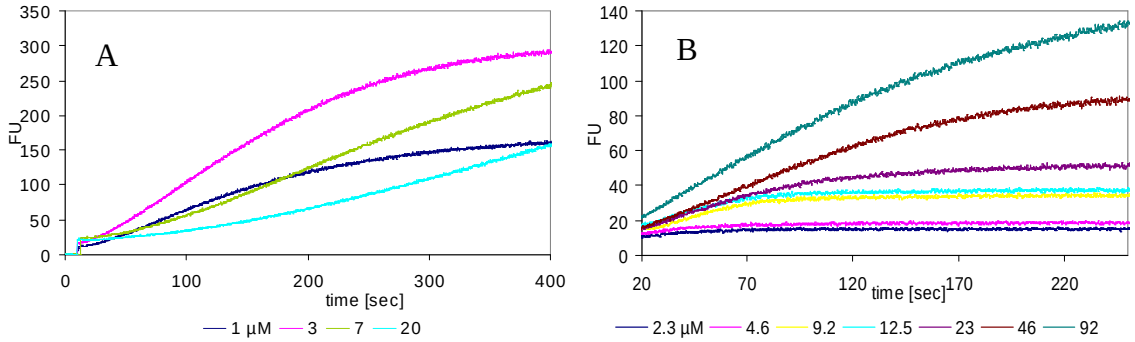

Fig. 31: Kinetics of the proto formation by *E. coli* PPO
The formation of proto was monitored with the luminescence spectrometer with the excitation and emission wavelength set at 409 and 633 nm, respectively. 400 nM HemG and 180 µM menaquinone as electron acceptor were applied. A: Amalgam-reduced substrate applied in the concentrations given. B: Utilised substrate was reduced by molecular hydrogen and palladium (Phillips, 2007). Data generated with the latter assays was used for the calculation of K_M and V_{max}. FU: fluorescence units.

The ratio of substrate concentration/velocity against the substrate concentrations was plotted in a Hanes-Woolf-diagram and linear regression was applied (fig. 32). K_M values were calculated to be 17.3 µM. The affinity towards the substrate was 15 times lower when compared to tobacco HemY (K_M of 1.17 µM). On the other hand, the calculated maximal velocity V_{max} of HemG of 16 µM min^{-1} mg^{-1} is 4-fold higher than that of tobacco HemY with 4.27 µM min^{-1} mg^{-1}.

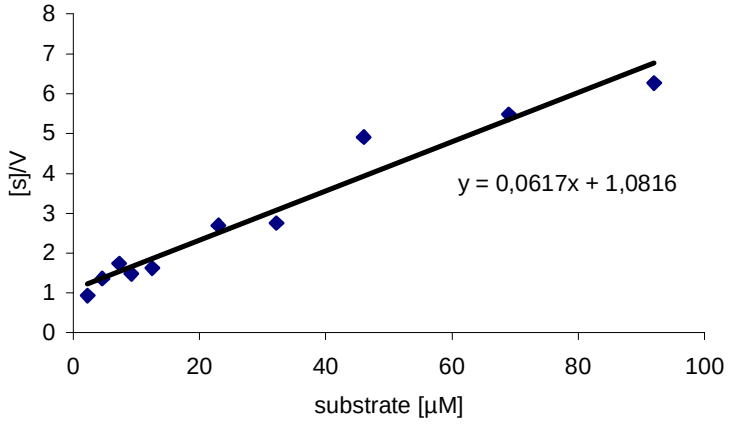

Fig. 32: Hanes-Woolf-plot of initial velocities of the PPO reaction with hydrogen-reduced substrate
The initial velocity of proto formation was determined over a broad range of proto´gen concentrations using the outlined PPO assay and saturating concentrations for the residual substrates (fig. 31). Proto formation followed Michaelis-Menten kinetics. The apparent K_m for proto´gen was 17.3 µM, V_{max} was determined to be 16 μM min^{-1} mg^{-1}. [S]/V: substrate concentration to velocity ratio.

Interestingly, mutants of tobacco HemY had turnover rates above the wildtype enzyme, indicating that wildtype HemY could have higher turnover rates (Heinemann *et al*., 2007).
A high PPO activity would lead to the accumulation of proto which cannot be instantly converted by the following enzyme, ferrochelatase. Proto is a molecule that can act as a photosensitiser by generating singlet oxygen in the prescence of light. Singlet oxygen causes lipid peroxidation and cell death (Lermontova and Grimm, 2006). Consequently, one might expect that only minimal amounts of proto exist within the cell.
On the other hand, slowing down or stopping PPO activity, e.g. by inhibitors (sections 1.4.1 and 3.7.4), leads to the nonenzymatical accumulation of proto (Lermontova and Grimm, 2006). It is generated from proto´gen due to a spontaneous reaction with molecular oxygen.
These findings indicate that accumulation of both substrate or product may harm the organism in which they occur. A balance of PPO activity between coproporphyrinogen III oxidase (HemN or HemF) and ferrochelatase activities might be essential to prevent cell damage.

3.7.4 Inhibitors of HemG

There are known inhibitors for HemY, some of which are used as herbicides. Of these herbicides, acifluorfen is the best investigated (Corradi *et al*., 2006). Inhibitory properties for bilirubin, a linear tetrapyrrole, have been reported as well (Ferreira *et al*., 1988). To investigate if acifluorfen or bilirubin function as an inhibitor of HemG-catalysis as well, these compounds were applied to the PPO activity assay.

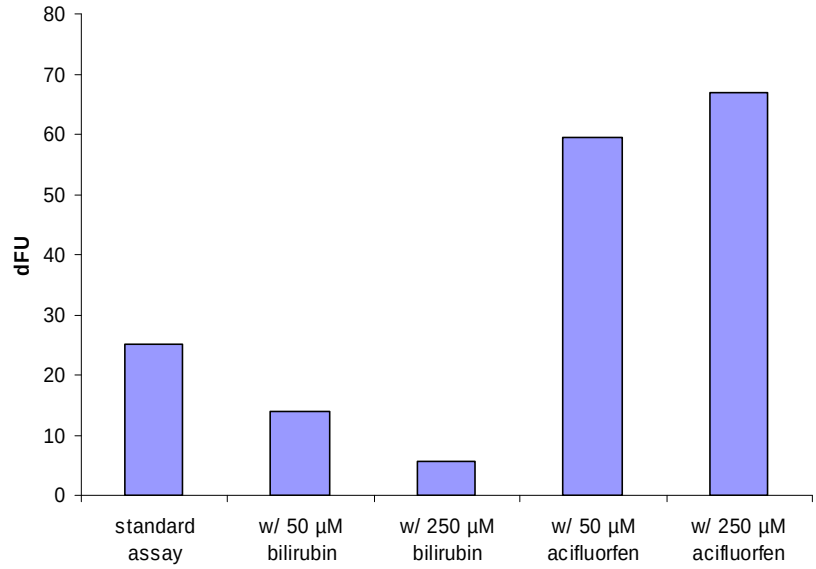

Fig. 33: PPO assay with the potential inhibitors bilirubin and acifluorfen
The PPO assay with 100 nM of HemG, 90 µM of menaquinone as electron acceptor and 10 µM of proto´gen was performed as described in section 2.7.3. The inhibitors were applied in the given concentrations. dFU: fluorescence units with t = 0 min subtracted from t = 60 min.

The obtained data clearly indicate that HemG, in contrast to HemY, is not inhibited by acifluorfen. In fact, a reproducible enhancement of the PPO activity was observed. It is uncertain why acifluorfen has this stimulating effect. Bilirubin has the same influence on HemG as described for HemY (Ferreira *et al*., 1988). At a concentration of 50 and 250 µM bilirubin PPO activity showed a reduction of 45 % and 77 % in the assays. As a tetrapyrrole, it might better mimic the substrate than acifluorfen, a diphenyl ether. It may therefore efficiently block the substrate binding pocket of HemG. Taken together, these results might point towards a different architecture of the active site of HemG in comparison to that of HemY.

3.8 Model of the Escherichia coli *PPO and the Electron Flux to Electron Acceptors*

From these results a model for the electron flow of the PPO reaction in *E. coli* was assembled (fig. 34). HemG enzymatically converts proto´gen to proto, probably via hydride transfer to FMN. From this flavin, the electrons are transferred to quinones. These can be floating freely in the membrane or might be directly associated to terminal oxidases. Six electrons need to be abstracted from proto´gen, but one quinone can only accept two electrons. The quarternary structure of HemG offers the possibility that multiple quinone molecules are oxidised simultaneously. Electron uptake from terminal oxidases recycles the quinones. Under anaerobic conditions, electrons are dissipated to the terminal electron acceptors fumarate and nitrate by the respective reductases. When oxygen is present, it is used as electron acceptor via cytochrome oxidases. This renders the *E. coli* PPO system, with HemG in its center, dependent on oxygen under these conditions. Therefore it is proposed to term the *E. coli* PPO as "electron transfer chain coupled PPO".

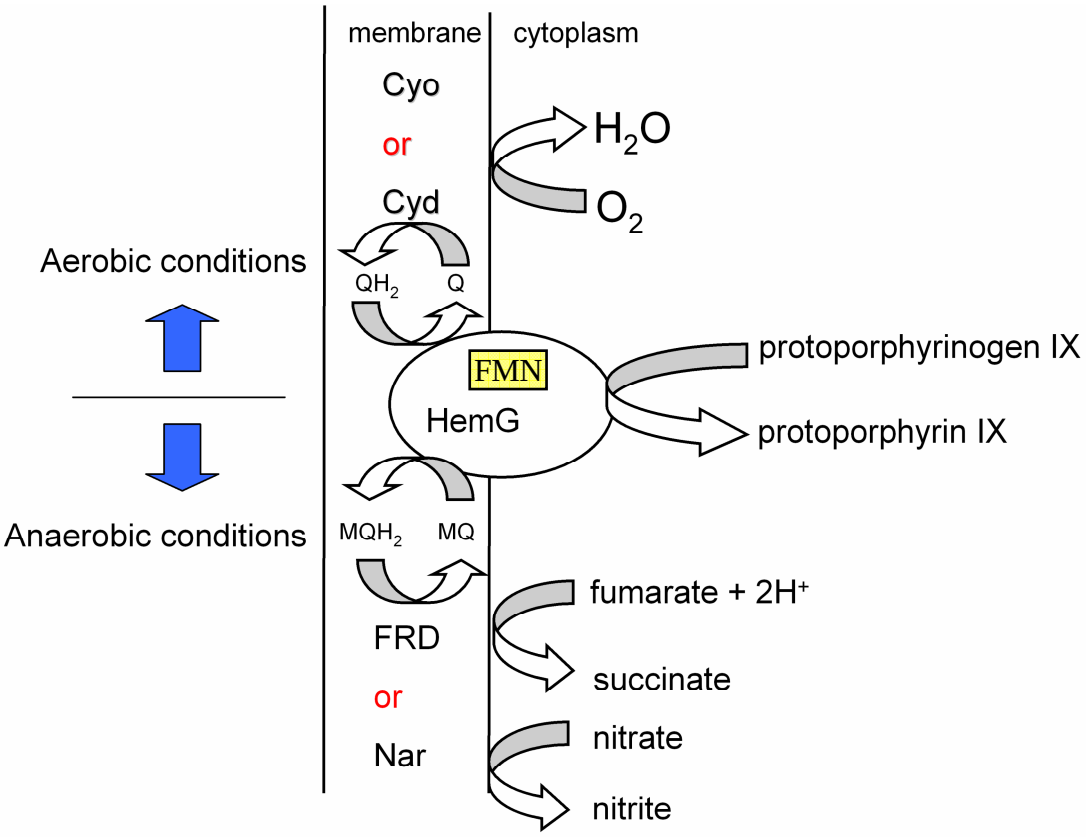

Fig. 34: Model of *E. coli* PPO and the electron flux

As a consequence, a proton motive force can be generated at the terminal oxidases during the conversion of proto´gen to proto in organisms possessing the HemG-class of PPO´s. Fumarate reductase does not move protons from the cytoplamic to the periplasmic side of the membrane in *E. coli.* However, emerging succinate can used in the citric acid cycle, therefore directly coupling the anabolic cofactor biosynthesis (heme biosynthesis) to the catabolism. This is an energetic advantage compared to the HemY-class of PPO´s. In the HemY-mediated reaction, the reducing power is simply lost by transferring electrons directly to oxygen. Additionally, the evolving hydrogen peroxide needs to be detoxified (Koch *et al*., 2004).

The fact that *E. coli* utilises nitrate reductase and cytochrome oxidases for the synthesis of heme is noteworthy since these enzymes require heme as cofactor (Lanciano *et al*., 2007; Zhang *et al*., 2004). For the *E. coli* system it becomes apparent that at least one of the quinol oxidoreductases has to function, even if no heme is available, to ensure heme biosynthesis. In *E. coli*, fumarate reductase does not possess heme as cofactor (Iverson *et al*., 2002).

Interestingly, fumarate reductase of *Wolinella succinogenes* does require heme as cofactor (Madej *et al*., 2006). The sequenced genome of this bacterium encodes genes for heme-dependent cytochrome oxidases, but not for a respiratory nitrate reductase. *W. succinogenes* also possesses a gene annotated as *hemG* with a amino acid sequence identity to *E. coli hemG* of 20.3 %, but no *hemY*. Thus, *W. succinogenes* is presumably dependent on the respiratory chains to form heme as well. The question arises how *W. succinogenes* facilitates this in the absence of heme.

This paradox situation possibly comprises a bottleneck for many organisms possessing HemG. Together with the relative complexity of the whole PPO system, this could be why it is not ubiquitously present in all organisms synthesizing tetrapyrroles. To date, two PPOs are known: HemG and HemY. It can be assumed that the HemG-class of PPOs has evolved earlier than the HemY-class. Tetrapyrrole biosynthesis has evolved before the oxygen-rich atmosphere. Hence proto formation had to develop in the absence of oxygen as an electron acceptor, which is possible with HemG. It seems reasonable that further mechanisms of the conversion of proto´gen to proto, e.g. in *P. aeruginosa*, exist in nature. *Pseudomonas aeruginosa* does not possess a gene homologous to *hemG* and is insensitive to deletorious mutations of the gene annotated as *hemY* (Max Schobert, personal communication). It is apparent that *P. aeruginosa* is capable of synthesizing heme, possessing various heme-dependent enzymes (Michel *et al*., 2007; Rinaldo *et al*., 2007). It remains to be determined how *P. aeruginosa* facilitates the PPO reaction.

Only few investigated anabolic enzymatic systems make use of the respiratory chains. DsbA, an enzyme for disulfide bond formation in the periplasma of procaryots, has been

reported (Bader *et al*., 1999). Here, the electrons emerging from the oxidative covalent bonding of two cysteine residues of proteins are transferred to quinones and to terminal oxidases via DsbB. A dihydroorotate dehydrogenase involved in pyrimidine synthesis has been described to use fumarate, quinones and oxygen as electron acceptors (Norager *et al*., 2002).

Taken together, the results obtained provide a first insight into the PPO reaction of *E. coli* and probably many other facultative and anaerobic organisms. The energy conserving properties and the ability to use a wide variety of electron acceptors are truly fascinating. It is certain that further interesting aspects of this enzymatic system will be discovered in future research.

3.9 The Oxygen-Independent Mg-Protoporphyrin Monomethyl Ester Oxidative Cyclase (BchE)

The tetrapyrrole chlorophyll is the central pigment of photosynthesis. Starting from 5-aminolevulinic acid, heme and (bacterio-) chlorophyll are synthesized via the same biosynthesis pathway to produce proto. Two enzymes compete for proto as a substrate: Ferrochelatase inserts ferrous iron into proto to perpetuate heme biosynthesis. Proto is fed into the (bacterio-) chlorophyll biosynthesis branch by Mg-chelatase, which inserts magnesuim into the macrocycle. Further enzymatic steps result in the formation of (bacterio-) chlorophyll.

The second project of this study was the investigation of an enzymatic step in the (bacterio-) chlorophyll biosynthesis branch: the addition of a fifth ring to the tetrapyrrole, catalysed by the O_2-independent cyclase. The *bchE* gene-product was proposed to facilitate this reaction in anoxygenic phototrophs. To investigate this protein, the *bchE* gene of *C. tepidum* was cloned into the expression vector pGEX-6P-1 (GE Healthcare, Munich, Germany) for the recombinant overproduction in *E. coli*. This vector construct encoded an N-terminal fusion protein of glutathione-S-transferase (GST)-tag and BchE.

3.9.1 Cloning of *Chlorobaculum tepidum bchE* into pGEX-6p-1

A PCR reaction containing the primers listed in section 2.2.3 amplified *bchE* from *C. tepidum* cells. The obtained fragment was cut with the endonucleases *Eco*RI and *Sal*I and ligated into the vector pGEX-6P-1 cut with the same endonucleases. For recombinant protein production, *E. coli* BL21 (λDE3) cells were transformed with the obtained constructs.

3.9.2 Recombinant production of O_2-independent Cyclase

E. coli BL21 (λDE3) harbouring pGEX-6P-1 *bchE* were cultivated as described in section 2.13.1. The recombinant protein production was initiated by the addition of 500 µM IPTG. Samples were taken during protein production and analysed via SDS-PAGE (fig. 35). A protein band with a M_r of ~90,000 emerging after induction corresponded to the calculated size of GST-BchE (M_r 90,602).

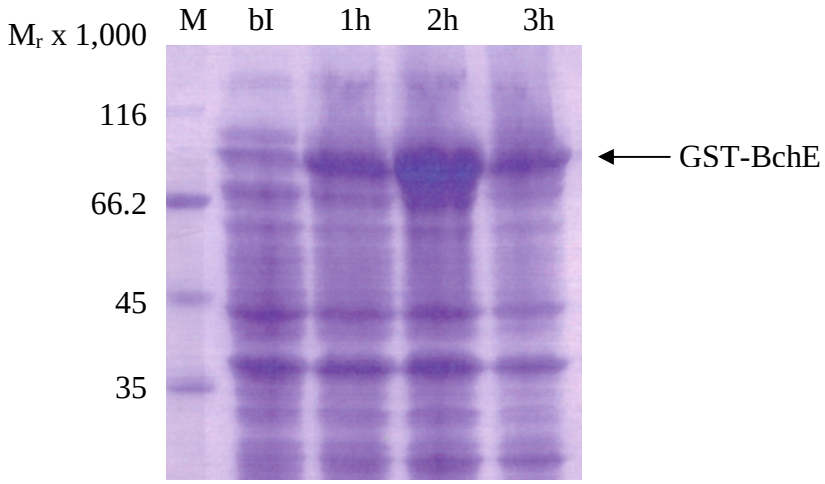

Fig. 35: Recombinant production of *C. tepidum* BchE in *E. coli* BL21 (λDE3)
The picture shows a 12 % polyacrylamide gel of proteins after separation and staining with Coomassie Brilliant Blue. *E. coli* BL21 (λDE3) harbouring pGEX-6P-1 *bchE* was cultivated as described in section 2.13.1. The recombinant protein production was initiated by the addition of 500 µM IPTG. Lane **M**: Protein Molecular Weight Marker. The relative molecular masses of the marker proteins are given. **bI**: Whole cell sample before induction of gene expression by IPTG. **1h, 2h, 3h:** sample taken 1 h, 2 h and 3 h after induction.

3.9.3 Purification of O_2-independent Cyclase

Cultures of *E. coli* cells recombinantly overproducing GST-BchE were harvested and cells were disrupted by French® Press. After centrifugation at 120,000 x g, GST-BchE was anaerobically purified from the supernatant via glutathione sepharose affinity chromatography (2.13.2). Analysis of this purification by SDS-PAGE revealed that the majority of GST-BchE was found in the sediment after ultracentrifugation (fig. 36). This indicated a high amount of insoluble GST-BchE protein. However, besides contaminating host proteins, a fraction of GST-BchE was purified as a soluble protein. Two protein bands with molecular masses similar to GST-BchE were visible in the SDS-PAGE gel. Upon storage at 4 °C degradation of the “upper band” was observed. Concurrently the intensity of the “lower band” increased (lane 17d). These results indicate that BchE is proteolytically degraded during storage.

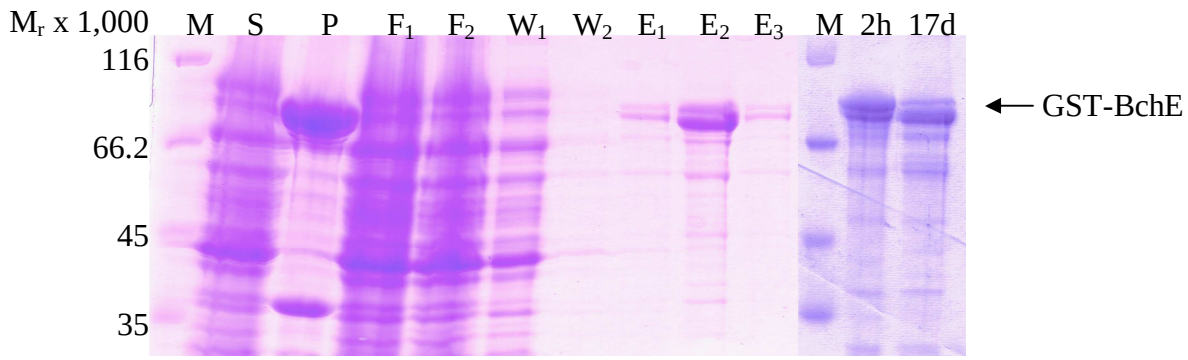

Fig. 36: Affinitiy purification of *C. tepidum* BchE fused to GST-tag
The picture shows a 12 % polyacrylamide gel of proteins after separation and staining with Coomassie Brilliant Blue. Lane **M**: Protein Molecular Weight Marker. The relative molecular masses of the marker proteins are given. **S**: Soluble fraction after ultracentrifugation. **P**: sediment after ultracentrifugation **F_{1+2}**: flow through. **W_{1+2}**: Washing steps. **E_{1-3}**: Elution fractions. **2h**: sample of E_2 after 2 hours. **17d**: sample of E_2 17 days at 4 °C.

In a subsequent western blot both bands were detected with an antibody directed against the GST-tag (fig. 37). It was concluded that both protein bands contain GST-BchE, with the lower band being a stable product of C-terminal degradation.

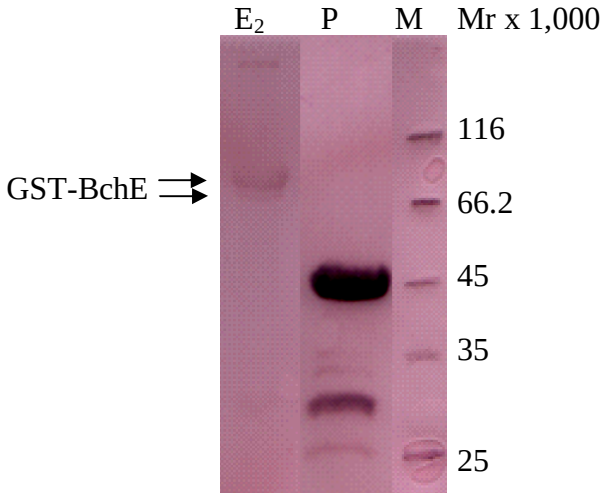

Fig. 37: Immunodetection of GST-BchE
Picture of a PVDF membrane after blotting and detection of GST fusion proteins by Anti-GST antibodies. A 12 % SDS-Page gel was run with samples of the elution fraction 2 of the affinity purification (**E_2**, see above) and hemeoxygenase (BphO) from *Pseudomonas aeroginosa* as positive control (**P**). Proteins were transferred by semidry blotting and detected by Anti-GST antibody. A second antibody directed against the Anti-GST antibody and conjugated to alkaline phosphatase was applied. Staining with NBT and BCIP was carried out until bands were visible. Lane **M**: Protein Molecular Weight Marker. The relative molecular masses of the marker proteins are given.

3.9.4 Modification of the Construct to Prevent Degradation

For the purification of the full-length fusion protein, a new vector was cloned leading to a gene product which possesses an additional His_{4x}-tag located on the C-terminus. After the

successful cloning and transformation, the recombinant protein was produced and purified as above. SDS-PAGE analysis showed only one band with a relative molecular weight of GST-BchE (90,000; fig. 38). This indicated that the C-terminal end of BchE was protected from degradation due to the His_{4x}-tag.

Fehler!

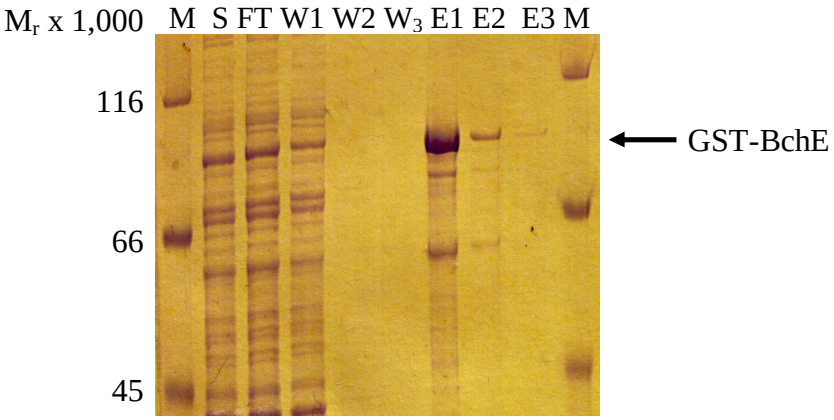

Fig. 38: Affintiy purification of GST-BchEHis_{4x}
The picture shows a 12 % polyacrylamide gel of proteins after separation and staining with Coomassie Brilliant Blue. Lane **M**: Protein Molecular Weight Marker. The relative molecular masses of the marker proteins are given. **S**: Soluble fraction after ultracentrifugation. **FT**: flow through. **W_{1-3}**: Washing steps. **E_{1-3}**: Elution fractions.

3.9.5 Biophysical and Biochemical Characterisation of O_2-Independent Cyclase

The fusion protein was subsequently analysed by UV-Vis spectrometry. The spectrum revealed a peak at 420 nm wavelength characteristic for [4Fe-4S] clusters (fig 39). Such a spectrum was already observed for BchE from *Rubrivivax gelatinosus* (Ouchane *et al.*, 2004).

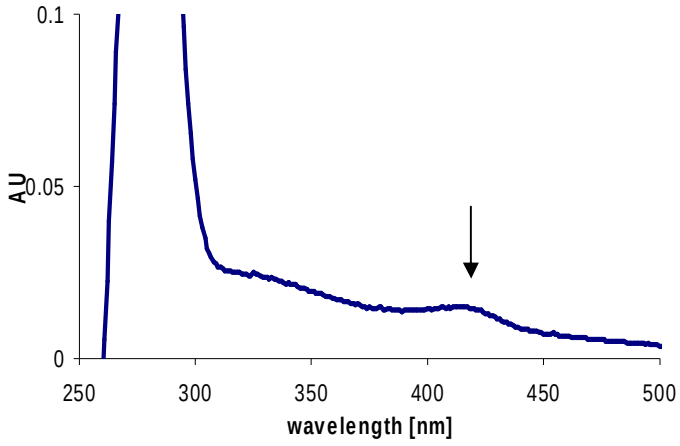

Fig. 39: Spectral analysis of GST-BchE
A UV-Vis spectrum of purified GST-BchE against elution buffer was recorded. The absorption peak at 420 nm is marked with an arrow.

The iron content was determined colourimetrically with *o*-phenanthroline after acidic denaturation of the protein (Lovenberg *et al*., 1963) to be 2.6 moles iron per mole fusion protein. Together with the bioinformatic predictions of a sequence motif characteristic for proteins containing an [4Fe-4S] cluster it was concluded that BchE from *C. tepidum* contains an Fe-S cluster. Since UV/Vis spectroscopic analysis do not allow for the identification of the specific Fe-S cluster type, further studies habe to be performed to give precise evidence.

3.9.6 Activity assay of the O_2-Independent Cyclase

For many years the analysis of the cyclase enzyme was hampered since no reproducible acitivty assay is available. In the present investigations a cyclase assay according to the description of Gough *et al*. (2000) was employed. Fluorescence properties and separation behaviour during HPLC analysis were used to detect the tetrapyrrole compounds (fig. 40). While Mg-protoporphyrin monomethyl ester was commercially available (Frontier Scientific, Logan, USA), protochlorophyllide prepared from a biological source (Suzuki and Bauer, 1995) was kindly provided by Johannes Walther.

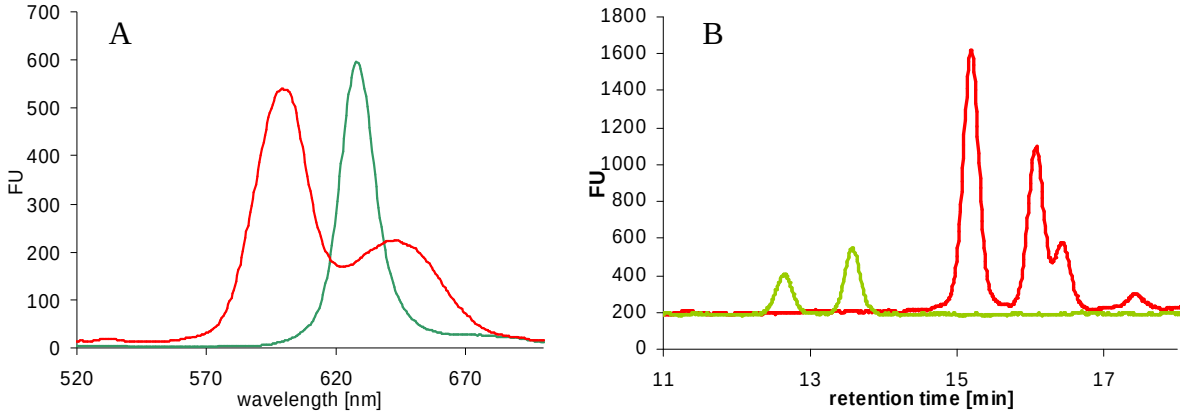

Fig. 40: Detection of Mg-protoporphyrin IX monomethyl ester and protochlorophyllide
Each compound was dissolved in stopping solution (200 µM, see section 2.13.6) and analysed by luminescence spectrometry (A) and HPLC (B) on an Ultrasphere ODS (5 µm, 250 x 4.6 mm) C_{18}-reversed phase column. As eluent A, 25 % acetonitrile (v/v) and 0.005 % (v/v) of triethylamine in H_20 was used. Eluent B consisted of 100 % of acetonitrile. During a period of 25 min, a gradient from 25 to 40 % of acetonitrile was applied. Mg-protoporphyrin IX monomethyl ester (MgPME) was excited at 420 nm. The emission of light by MgPME was detected by an emission scan at the luminescence spectrometer or at 595 nm wavelength in the HPLC analysis (red curves). Protochlorophyllide (green) was excited at 440 nm and detected at 635 nm wavelength.

Mg-protoporphyrin IX monomethyl ester (MgPME) showed a characteristic double peak emission spectrum. In figure 40A, the MgPME spectrum seems to overlap with the single emission peak of protochlorophyllide. However, due to the different excitation properties, the substrate and product can be clearly distinguished. In the HPLC analysis, both compounds did not result in a single peak. It has been described that protochlorophyllide

occurs as mono- and divinylvariant in *Rhodobacter capsulatus* (Suzuki and Bauer, 1995). The observed peaks might derive from these to molecules. Nevertheless, the established methods allowed the analysis of the tetrapyrrole compounds of the cyclase reaction.

First assays were performed according to the protocol established by Gough *et al*. (2000). *R. capsulatus* cells were grown and employed to the assay together with substrate and nicotinic acid. After 60 min, the assay was stopped by the addition of a acetone/water/ammonia mix. Initial analysis of the cyclase assay was performed by fluorescence spectrometry. An emission peak with a maximum of 635 nm wavelength, a property for protochlorophyllide, was detectable (fig. 41).

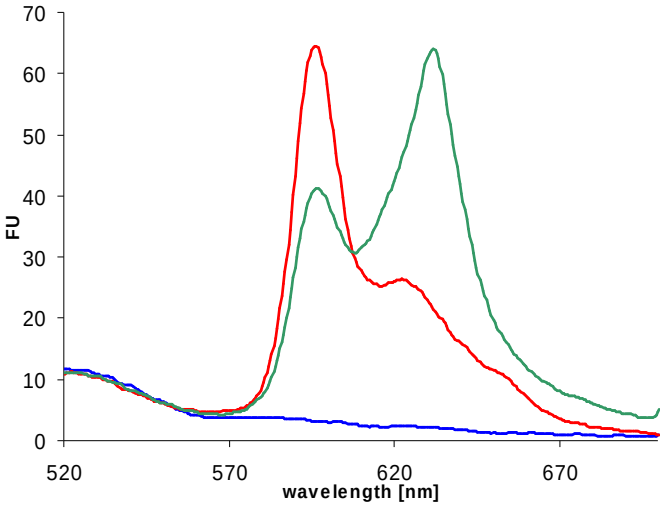

Fig. 41: Cyclase activity assay with *R. capsulatus* cells
The assay was performed as outlined in 2.13.6. The assays contained the components given for each spectrum below. After 60 min, the assay was stopped by the addition of a acetone/water/ammonia mix Initial analysis was performed by luminescence spectrometry. Excitation wavelength was set at 440 nm. Blue: Control without substrate. Red: Control without nicotinic acid. Green: Assay containing *R. capsulatus* cells, substrate (MgPME) and nicotinic acid. FU: fluorescence units.

From this analysis it was assumed that this assay was capable of monitoring O_2-independent product formation. However, when the samples where analysed by HPLC, only peaks derived from the substrate with retention times of 15-19 min, but no protochlorophyllide peaks with retention times of 12.5 - 14min where detectable (fig. 42).

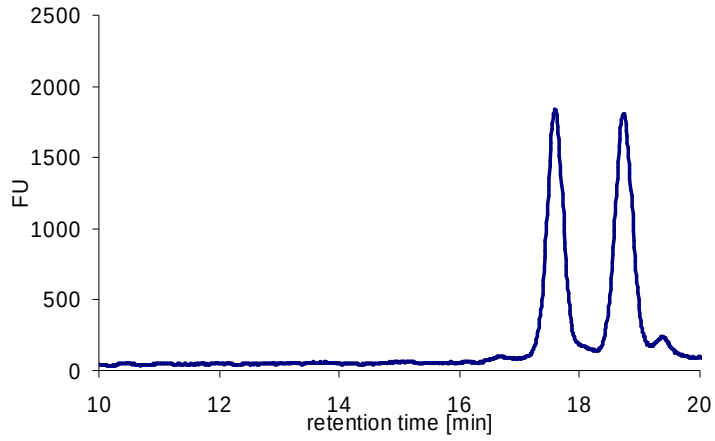

Fig. 42: HPLC analysis from cyclase assay performed with *R. capsulatus* cells.
The assay containing *R. capsulatus* cells, substrate (MgPME) and nicotinic acid was stopped and the supernatant after centrifugation was analysed by HPLC on a C_{18} Ultrasphere ODS (5 µm, 250 x 4.6 mm) reversed phase column. The column was equilibrated in 25 % (v/v) acetonitrile and 0.005 % (v/v) of triethylamine in H_20. A gradient from from 25 to 40 % acetonitrile was applied. The fluorescence detector was set at an excitation wavelength of 440 nm and 635 nm for emission wavelength for the first 14 minutes. After this time period, settings were changed to 420/595 nm. FU: fluorescence units.

In order to analyse these results in detail, further control reactions were performed. Interestingly. a control reaction without *R. capsulatus* cells was not described in the publication of Gough *et al*. (2000). In this control experiment, a peak at 635 nm wavelength was observed when analysed by fluorescence spectrometry (fig. 43). Apparently, nicotinic acid alone can alter the fluorescence properties of Mg-protoporphyrin monomethyl ester towards an emission maximum at 635 nm very similar to protochlorophyllide. Due to fluorescence properties of the employed assay conditions, this particular approach to investigate the enzymatic activity of the O_2-independent cyclase was abandoned. The published approach (Gough *et al*., 2000) was found to be unable to display BchE activity.

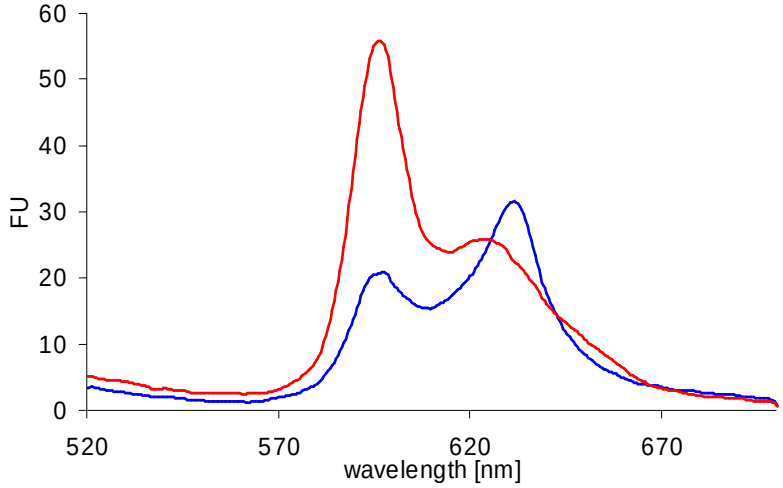

Fig. 43: Fluorescence spectra of Mg-protoporphyrin IX monomethyl ester with (blue) and without nicotinic acid (red)
After 60 min, the assay was stopped by the addition of a acetone/water/ammonia mix and centrifuged. The resulting supernatant was excited at 440 nm wavelength during luminescence spectrometry analysis. FU: fluorescence units.

In all further experiments, recombinantly produced BchE was applied as cell extract or purified, either truncated from the GST-tag or as GST-fusion protein. In control experiments, several ingredients were tested such as Vitamin B_{12}, Triton® X-100 and S-adenosyl-methionine (section 2.13.6). In all assays, only substrate was detectable when analysed by HPLC (fig. 44).

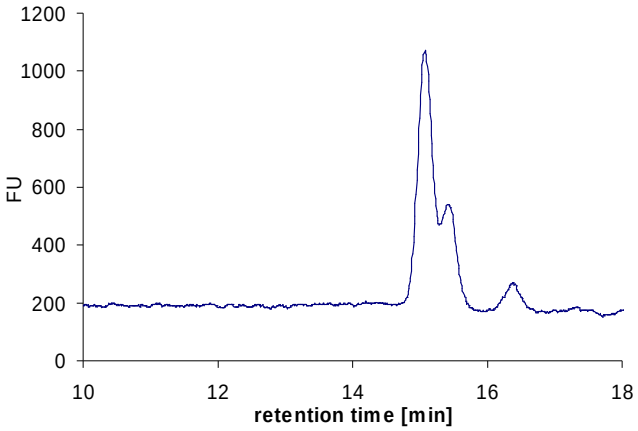

Fig. 44: Exemplatory HPLC analyis of *in vitro* cyclase activity test
HPLC analysis of the cylase assay was performed as described above. FU: fluorescence units. Only the substrate of the cyclase reaction could be detected.

From thes results it was speculated that the protein possibly requires special conditions not found in the assays performed. An alternative explanation would be the involvement of additional protein subunits in the cyclase reaction. Another possibility why BchE was unable to carry out the cyclisation of MgPME is that it cannot be properly folded by the *E. coli* protein synthesis machinery.

Summary

The penultimate step of heme biosynthesis – the conversion of protoporphyrinogen IX (proto´gen) into protoporphyrin IX (proto) – is catalysed by protoporphyrinogen IX oxidases (PPOs). While the O_2-dependent enzyme system of eukaryotes and Gram positive bacteria is well investigated, little was known about the O_2-independent PPO found in facultative and anaerobic organisms.

In this work, the yet unknown O_2-independent PPO of *E. coli* was identified. To achieve this, PPO activity was localised in the membranes of *E. coli* from which it was extracted. Further, the PPO activity was purified by classic chromatography from wildtype *E. coli* cells. In LC-MS/MS analysis of the purified fractions, the protein HemG was repeatedly found. HemG was recombinantly produced in *E. coli* which drastically increased PPO activity of the corresponding cell lysates. Subsequently, *B. megaterium* was used to recombinantly produce HemG. Afterwards, cell lysates of the host, formerly devoid of detectable O_2-independent PPO activity, were capable of anaerobic formation of proto. These results establish HemG as the O_2-independent PPO of *E. coli*.

Once identified, the O_2-independent PPO was chromatographically purified and biochemically characterised. A FMN cofactor was identified by HPLC analysis. Gel permeation chromatography experiments indicated a hexameric oligomerisation state of native HemG. Kinetic data was obtained, yielding a K_m value of 17.3 µM and a maximal velocity rate of 16 µM min^{-1} mg^{-1} HemG.

Besides the PPO itself, the proposed electron transfer properties towards the respiratory chains were investigated. First, menaquinone and ubiqinone were shown to be able to take up electrons from HemG. Then, the purified terminal oxidases fumarate reductase, nitrate reductase and cytochrome *bo* and *bd* oxidase were applied to PPO activity assays. Electrons were found to be transferred from the quinones to the terminal electron acceptors fumarate, nitrate and oxygen via the corresponding terminal oxidase. *In vivo* investigations using *E. coli* mutants devoid of one or two terminal oxidases confirm the *in vitro* findings. Since under certain environmental conditions oxygen is an indirect electron acceptor of the PPO reaction in *E. coli*, it is suggested to use the term “electron transport chain coupled” PPO system.

An additional aim was to study the O_2-independent conversion from magnesium protoporphyrin IX monomethyl ester to protochlorophyllide during (bacterio-)chlorophyll biosynthesis. The protein BchE, proposed in the literature to be capable of the reaction, was recombinantly produced, purified and analysed. The possible prescence of a Fe-S cluster was observed spectrometrically. The detection of the involved tetrapyrroles by HPLC and fluorimetry was established. An activity test in accordance to published results

was shown to be useless. Further attempts to observe O_2-independent cyclase activity with BchE alone proved to be unsuccessful. Consequently, the proposal of O_2-independent cyclase activity for BchE was proven wrong.

Outlook

As outlined above, the results of this work provided the identification and characterisation of the O_2-independent PPO. The following questions should be addressed in future experiments:

- Investigations on the physical interaction to the terminal oxidases. Interactions towards proceeding and following enzymes of the heme and chlorophyll pathways should be determined as well.
- Construction of a *E. coli* mutant deficient in HemG which is then transformed with a genomic library of *Pseudomonas aeruginosa*. The genome fragment encoding the yet unknown PPO of *P. aeruginosa* should rescue the mutant and enable growth.
- Obtain stuctural data of possibly hexameric HemG.

Concerning the O_2-independent cyclisation of Mg-protoporophyrin IX monomethyl ester resulting in protochlorophyllide, initial biochemical studies of BchE were performed. Further studies have to be carried out to determine its features more closely:

- Search for additional subunits of the O_2-independent cyclase
  - ▪ by mutagenesis studies of anoxygenic phototrophs
  - ▪ copurification with tagged BchE from a suitable host
- EPR spectroscopy to identify the FeS-cluster in the BchE protein
- Screening for conditions for the display of O_2-independent cyclase activity
- Overproduction of BchE in a anoxygenic phototroph to ensure proper folding of the protein.

References

Bader, M., Muse, W., Ballou, D. P., Gassner, C., and Bardwell, J. C. (1999). Oxidative protein folding is driven by the electron transport system. Cell *98*, 217-227.

Battersby, A. R. (2000). Tetrapyrroles: the pigments of life. Nat Prod Rep *17*, 507-526.

Beale, S. I., and Yeh, J. I. (1999). Deconstructing heme. Nat Struct Biol *6*, 903-905.

Bertero, M. G., Rothery, R. A., Boroumand, N., Palak, M., Blasco, F., Ginet, N., Weiner, J. H., and Strynadka, N. C. (2005). Structural and biochemical characterization of a quinol binding site of *Escherichia coli* nitrate reductase A. J Biol Chem *280*, 14836-14843.

Biel, A. J., and Marrs, B. L. (1983). Transcriptional regulation of several genes for bacteriochlorophyll biosynthesis in *Rhodopseudomonas capsulata* in response to oxygen. J Bacteriol *156*, 686-694.

Blaut, M., Whittaker, K., Valdovinos, A., Ackrell, B. A., Gunsalus, R. P., and Cecchini, G. (1989). Fumarate reductase mutants of *Escherichia coli* that lack covalently bound flavin. J Biol Chem *264*, 13599-13604.

Bollivar, D. W., and Beale, S. I. (1996). The Chlorophyll Biosynthetic Enzyme Mg-Protoporphyrin IX Monomethyl Ester (Oxidative) Cyclase (Characterization and Partial Purification from *Chlamydomonas reinhardtii* and *Synechocystis sp.* PCC 6803). Plant Physiol *112*, 105-114.

Bollivar, D. W., Suzuki, J. Y., Beatty, J. T., Dobrowolski, J. M., and Bauer, C. E. (1994). Directed mutational analysis of bacteriochlorophyll a biosynthesis in *Rhodobacter capsulatus*. J Mol Biol *237*, 622-640.

Bradford, M. M. (1976). A rapid and sensitive method for the quantitation of microgram quantities of protein utilizing the principle of protein-dye binding. Anal Biochem *72*, 248-254.

Breckau, D. (2005) Die Bildung von Protoporphyrin IX in *Escherichia coli*, PhD, Technische Universität Carolo-Wilhelmina zu Braunschweig, Braunschweig.

Camadro, J. M., Matringe, M., Scalla, R., and Labbe, P. (1991). Kinetic studies on protoporphyrinogen oxidase inhibition by diphenyl ether herbicides. Biochem J *277 (Pt 1)*, 17-21.

Camadro, J. M., Thome, F., Brouillet, N., and Labbe, P. (1994). Purification and properties of protoporphyrinogen oxidase from the yeast *Saccharomyces cerevisiae*. Mitochondrial location and evidence for a precursor form of the protein. J Biol Chem *269*, 32085-32091.

Cecchini, G., Ackrell, B. A., Deshler, J. O., and Gunsalus, R. P. (1986). Reconstitution of quinone reduction and characterization of *Escherichia coli* fumarate reductase activity. J Biol Chem *261*, 1808-1814.

Cecchini, G., Maklashina, E., Yankovskaya, V., Iverson, T. M., and Iwata, S. (2003). Variation in proton donor/acceptor pathways in succinate:quinone oxidoreductases. FEBS Lett *545*, 31-38.

Chang, C. K. (1994). Haem d_1 and other haem cofactors from bacteria. Ciba Found Symp *180*, 228-238; discussion 238-246.

Chereskin, B. M., Wong, Y. S., and Castelfranco, P. A. (1982). In Vitro Synthesis of the Chlorophyll Isocyclic Ring : Transformation of Magnesium-Protoporphyrin IX and Magnesium-Protoporphyrin IX Monomethyl Ester into Magnesium-2,4-Divinyl Pheoporphyrin A(5). Plant Physiol *70*, 987-993.

Corradi, H. R., Corrigall, A. V., Boix, E., Mohan, C. G., Sturrock, E. D., Meissner, P. N., and Acharya, K. R. (2006). Crystal structure of protoporphyrinogen oxidase from *Myxococcus xanthus* and its complex with the inhibitor acifluorfen. J Biol Chem *281*, 38625-38633.

Craig, D. H., Barna, T., Moody, P. C., Bruce, N. C., Chapman, S. K., Munro, A. W., and Scrutton, N. S. (2001). Effects of environment on flavin reactivity in morphinone reductase: analysis of enzymes displaying differential charge near the N-1 atom and C-2 carbonyl region of the active-site flavin. Biochem J *359*, 315-323.

Dailey, H. A. (2002). Terminal steps of haem biosynthesis. Biochem Soc Trans *30*, 590-595.

Dailey, H. A., and Dailey, T. A. (1996). Protoporphyrinogen oxidase of *Myxococcus xanthus*. Expression, purification, and characterization of the cloned enzyme. J Biol Chem *271*, 8714-8718.

Dailey, T. A., and Dailey, H. A. (1998). Identification of an FAD superfamily containing protoporphyrinogen oxidases, monoamine oxidases, and phytoene desaturase. Expression and characterization of phytoene desaturase of *Myxococcus xanthus*. J Biol Chem *273*, 13658-13662.

Dailey, T. A., Meissner, P., and Dailey, H. A. (1994). Expression of a cloned protoporphyrinogen oxidase. J Biol Chem *269*, 813-815.

Darwin, A. J., Li, J., and Stewart, V. (1996). Analysis of nitrate regulatory protein NarL-binding sites in the *fdn*G and *nar*G operon control regions of *Escherichia coli* K-12. Mol Microbiol *20*, 621-632.

Ferreira, G. C., Andrew, T. L., Karr, S. W., and Dailey, H. A. (1988). Organization of the terminal two enzymes of the heme biosynthetic pathway. Orientation of protoporphyrinogen oxidase and evidence for a membrane complex. J Biol Chem *263*, 3835-3839.

Frankenberg, N., Moser, J., and Jahn, D. (2003). Bacterial heme biosynthesis and its biotechnological application. Appl Microbiol Biotechnol *63*, 115-127.

Friedmann, H. C., Klein, A., and Thauer, R. K. (1990). Structure and function of the nickel porphinoid, coenzyme F430 and of its enzyme, methyl coenzyme M reductase. FEMS Microbiol Rev *7*, 339-348.

Giordani, R., and Buc, J. (2004). Evidence for two different electron transfer pathways in the same enzyme, nitrate reductase A from *Escherichia coli*. Eur J Biochem *271*, 2400-2407.

Goni, G., Serrano, A., Frago, S., Hervas, M., Peregrina, J. R., Rosa, M. A., Gomez-Moreno, C., Navarro, J. A., and Medina, M. (2008). Flavodoxin-Mediated Electron Transfer from Photosystem I to Ferredoxin-NADP(+) Reductase in *Anabaena*: Role of Flavodoxin Hydrophobic Residues in Protein-Protein Interactions. Biochemistry.

Gough, S. P., Petersen, B. O., and Duus, J. O. (2000). Anaerobic chlorophyll isocyclic ring formation in *Rhodobacter capsulatus* requires a cobalamin cofactor. Proc Natl Acad Sci U S A *97*, 6908-6913.

Hansson, M., and Hederstedt, L. (1994). *Bacillus subtilis* HemY is a peripheral membrane protein essential for protoheme IX synthesis which can oxidize coproporphyrinogen III and protoporphyrinogen IX. J Bacteriol *176*, 5962-5970.

Heinemann, I. U., Diekmann, N., Masoumi, A., Koch, M., Messerschmidt, A., Jahn, M., and Jahn, D. (2007). Functional definition of the tobacco protoporphyrinogen IX oxidase substrate-binding site. Biochem J *402*, 575-580.

Iverson, T. M., Luna-Chavez, C., Cecchini, G., and Rees, D. C. (1999). Structure of the *Escherichia coli* fumarate reductase respiratory complex. Science *284*, 1961-1966.

Iverson, T. M., Luna-Chavez, C., Croal, L. R., Cecchini, G., and Rees, D. C. (2002). Crystallographic studies of the *Escherichia coli* quinol-fumarate reductase with inhibitors bound to the quinol-binding site. J Biol Chem *277*, 16124-16130.

Jacobs, J. M., and Jacobs, N. J. (1984). Protoporphyrinogen oxidation, an enzymatic step in heme and chlorophyll synthesis: partial characterization of the reaction in plant organelles and comparison with mammalian and bacterial systems. Arch Biochem Biophys *229*, 312-319.

Jacobs, J. M., and Jacobs, N. J. (1987). Oxidation of protoporphyrinogen to protoporphyrin, a step in chlorophyll and haem biosynthesis. Purification and partial characterization of the enzyme from barley organelles. Biochem J *244*, 219-224.

Jacobs, N. J., and Jacobs, J. M. (1975). Fumarate as alternate electron acceptor for the late steps of anaerobic heme synthesis in *Escherichia coli*. Biochem Biophys Res Commun *65*, 435-441.

Jacobs, N. J., and Jacobs, J. M. (1976). Nitrate, fumarate, and oxygen as electron acceptors for a late step in microbial heme synthesis. Biochim Biophys Acta *449*, 1-9.

Jacobs, N. J., and Jacobs, J. M. (1978). Quinones as hydrogen carriers for a late step in anaerobic heme biosynthesis in *Escherichia coli*. Biochim Biophys Acta *544*, 540-546.

Jacobs, N. J., and Jacobs, J. M. (1981). Protoporphyrinogen oxidation in *Rhodopseudomonas spheroides*, a step in heme and bacteriochlorophyll synthesis. Arch Biochem Biophys *211*, 305-311.

Jahn, D., Hungerer, C., and Troup, B. (1996). [Unusual pathways and environmentally regulated genes of bacterial heme biosynthesis]. Naturwissenschaften *83*, 389-400.

Jensen, P. E., Gibson, L. C., Shephard, F., Smith, V., and Hunter, C. N. (1999). Introduction of a new branchpoint in tetrapyrrole biosynthesis in *Escherichia coli* by co-expression of genes encoding the chlorophyll-specific enzymes magnesium chelatase and magnesium protoporphyrin methyltransferase. FEBS Lett *455*, 349-354.

Jones, H. M., and Gunsalus, R. P. (1985). Transcription of the *Escherichia coli* fumarate reductase genes (*frd*ABCD) and their coordinate regulation by oxygen, nitrate, and fumarate. J Bacteriol *164*, 1100-1109.

Kaysser, T. M., Ghaim, J. B., Georgiou, C., and Gennis, R. B. (1995). Methionine-393 is an axial ligand of the heme b_{558} component of the cytochrome *bd* ubiquinol oxidase from *Escherichia coli*. Biochemistry *34*, 13491-13501.

Kleiner, O., Butenandt, J., Carell, T., and Batschauer, A. (1999). Class II DNA photolyase from *Arabidopsis thaliana* contains FAD as a cofactor. Eur J Biochem *264*, 161-167.

Klemm, D. J., and Barton, L. L. (1987). Purification and properties of protoporphyrinogen oxidase from an anaerobic bacterium, *Desulfovibrio gigas*. J Bacteriol *169*, 5209-5215.

Koch, M., Breithaupt, C., Kiefersauer, R., Freigang, J., Huber, R., and Messerschmidt, A. (2004). Crystal structure of protoporphyrinogen IX oxidase: a key enzyme in haem and chlorophyll biosynthesis. EMBO J *23*, 1720-1728.

Kusaba, A., Ansai, T., Akifusa, S., Nakahigashi, K., Taketani, S., Inokuchi, H., and Takehara, T. (2002). Cloning and expression of a *Porphyromonas gingivalis* gene for protoporphyrinogen oxidase by complementation of a *hem*G mutant of *Escherichia coli*. Oral Microbiol Immunol *17*, 290-295.

Laemmli, U. K. (1970). Cleavage of structural proteins during the assembly of the head of bacteriophage T4. Nature *227*, 680-685.

Lanciano, P., Magalon, A., Bertrand, P., Guigliarelli, B., and Grimaldi, S. (2007). High-stability semiquinone intermediate in nitrate reductase A (NarGHI) from *Escherichia coli* is located in a quinol oxidation site close to heme b_D. Biochemistry *46*, 5323-5329.

Lermontova, I., and Grimm, B. (2006). Reduced activity of plastid protoporphyrinogen oxidase causes attenuated photodynamic damage during high-light compared to low-light exposure. Plant J *48*, 499-510.

Lermontova, I., Kruse, E., Mock, H. P., and Grimm, B. (1997). Cloning and characterization of a plastidal and a mitochondrial isoform of tobacco protoporphyrinogen IX oxidase. Proc Natl Acad Sci U S A *94*, 8895-8900.

Lovenberg, W., Buchanan, B. B., and Rabinowitz, J. C. (1963). Studies on the Chemical Nature of Clostridial Ferredoxin. J Biol Chem *238*, 3899-3913.

Luna-Chavez, C., Iverson, T. M., Rees, D. C., and Cecchini, G. (2000). Overexpression, purification, and crystallization of the membrane-bound fumarate reductase from *Escherichia coli*. Protein Expr Purif *19*, 188-196.

Luo, J., and Lim, C. K. (1993). Order of uroporphyrinogen III decarboxylation on incubation of porphobilinogen and uroporphyrinogen III with erythrocyte uroporphyrinogen decarboxylase. Biochem J *289 (Pt 2)*, 529-532.

Madej, M. G., Nasiri, H. R., Hilgendorff, N. S., Schwalbe, H., and Lancaster, C. R. (2006). Evidence for transmembrane proton transfer in a dihaem-containing membrane protein complex. Embo J *25*, 4963-4970.

Maklashina, E., Hellwig, P., Rothery, R. A., Kotlyar, V., Sher, Y., Weiner, J. H., and Cecchini, G. (2006). Differences in protonation of ubiquinone and menaquinone in fumarate reductase from *Escherichia coli*. J Biol Chem *281*, 26655-26664.

McFarlane, M. J., Hunter, C. N., and Heyes, D. J. (2005). Kinetic characterisation of the light-driven protochlorophyllide oxidoreductase (POR) from *Thermosynechococcus elongatus*. Photochem Photobiol Sci *4*, 1055-1059.

Michel, L. V., Ye, T., Bowman, S. E., Levin, B. D., Hahn, M. A., Russell, B. S., Elliott, S. J., and Bren, K. L. (2007). Heme attachment motif mobility tunes cytochrome *c* redox potential. Biochemistry *46*, 11753-11760.

Nomata, J., Kitashima, M., Inoue, K., and Fujita, Y. (2006). Nitrogenase Fe protein-like Fe-S cluster is conserved in L-protein (BchL) of dark-operative protochlorophyllide reductase from *Rhodobacter capsulatus*. FEBS Lett *580*, 6151-6154.

Norager, S., Jensen, K. F., Bjornberg, O., and Larsen, S. (2002). *E. coli* dihydroorotate dehydrogenase reveals structural and functional distinctions between different classes of dihydroorotate dehydrogenases. Structure *10*, 1211-1223.

Okada, K., and Hase, T. (2005). Cyanobacterial non-mevalonate pathway: (E)-4-hydroxy-3-methylbut-2-enyl diphosphate synthase interacts with ferredoxin in *Thermosynechococcus elongatus* BP-1. J Biol Chem *280*, 20672-20679.

Ouchane, S., Steunou, A. S., Picaud, M., and Astier, C. (2004). Aerobic and anaerobic Mg-protoporphyrin monomethyl ester cyclases in purple bacteria: a strategy adopted to bypass the repressive oxygen control system. J Biol Chem *279*, 6385-6394.

Panek, H., and O'Brian, M. R. (2002). A whole genome view of prokaryotic haem biosynthesis. Microbiology *148*, 2273-2282.

Phillips, J. (2007), personal communication to M. Jahn, Institut für Mikrobiologie, Technische Universität Braunschweig, Germany.

Porra, R. J., Schafer, W., Katheder, I., and Scheer, H. (1995). The derivation of the oxygen atoms of the 13(1)-oxo and 3-acetyl groups of bacteriochlorophyll a from water in *Rhodobacter sphaeroides* cells adapting from respiratory to photosynthetic conditions: evidence for an anaerobic pathway for the formation of isocyclic ring E. FEBS Lett *371*, 21-24.

Potter, L. C., Millington, P., Griffiths, L., Thomas, G. H., and Cole, J. A. (1999). Competition between *Escherichia coli* strains expressing either a periplasmic or a membrane-bound nitrate reductase: does Nap confer a selective advantage during nitrate-limited growth? Biochem J *344 Pt 1*, 77-84.

Rich, P. R., Mischis, L. A., Purton, S., and Wiskich, J. T. (2001). The sites of interaction of triphenyltetrazolium chloride with mitochondrial respiratory chains. FEMS Microbiol Lett *202*, 181-187.

Riedmann, K. (2007) Produktion und Reinigung der Sauerstoff unabhängigen Protoporphyrinogen IX Oxidase aus *Escherichia coli*, diploma, Technische Universität Carolo-Wilhelmina zu Braunschweig, Braunschweig.

Righetti, P., Gianazza, E., Gelfi, C., and Chiari, M. (1990). Gel electrophoresis of proteins: a practical approach, 2nd edn: Oxford University Press).

Rinaldo, S., Brunori, M., and Cutruzzola, F. (2007). Nitrite controls the release of nitric oxide in *Pseudomonas aeruginosa* cd1 nitrite reductase. Biochem Biophys Res Commun *363*, 662-666.

Rudiger, W., Bohm, S., Helfrich, M., Schulz, S., and Schoch, S. (2005). Enzymes of the last steps of chlorophyll biosynthesis: modification of the substrate structure helps to understand the topology of the active centers. Biochemistry *44*, 10864-10872.

Rumbley, J. N., Furlong Nickels, E., and Gennis, R. B. (1997). One-step purification of histidine-tagged cytochrome *bo*3 from *Escherichia coli* and demonstration that associated quinone is not required for the structural integrity of the oxidase. Biochim Biophys Acta *1340*, 131-142.

Rygus, T., and Hillen, W. (1992). Catabolite repression of the xyl operon in *Bacillus megaterium*. J Bacteriol *174*, 3049-3055.

Rzeznicka, K., Walker, C. J., Westergren, T., Kannangara, C. G., von Wettstein, D., Merchant, S., Gough, S. P., and Hansson, M. (2005). Xantha-l encodes a membrane subunit of the aerobic Mg-protoporphyrin IX monomethyl ester cyclase involved in chlorophyll biosynthesis. Proc Natl Acad Sci U S A *102*, 5886-5891.

Sambrook, J., Fritsch, E. F., and &Maniatis, T. (1989). Molecular cloning: a laboratory manual, 2nd ed. (New York: Cold Spring Harbor Laboratory Press).

Sanger, F., Nicklen, S., and Coulson, A. R. (1977). DNA sequencing with chain-terminating inhibitors. Proc Natl Acad Sci U S A *74*, 5463-5467.

Sano, S., and Granick, S. (1961). Mitochondrial coproporphyrinogen oxidase and protoporphyrin formation. J Biol Chem *236*, 1173-1180.

Sasarman, A., Chartrand, P., Lavoie, M., Tardif, D., Proschek, R., and Lapointe, C. (1979). Mapping of a new hem gene in *Escherichia coli* K12. J Gen Microbiol *113*, 297-303.

Sasarman, A., Letowski, J., Czaika, G., Ramirez, V., Nead, M. A., Jacobs, J. M., and Morais, R. (1993). Nucleotide sequence of the *hem*G gene involved in the protoporphyrinogen oxidase activity of *Escherichia coli* K12. Can J Microbiol *39*, 1155-1161.

Schröder, S. (2006) Purification and Characterisation of the Oxygen-Independent Protoporphyrinogen IX Oxidase from *Escherichia coli*, diploma, Technische Universität Carolo-Wilhelmina zu Braunschweig, Braunschweig.

Scott, A. I., Kajiwara, M., and Santander, P. J. (1987). Biosynthesis of vitamin B_{12}: concerning the origin of the methine protons of the corrin nucleus. Proc Natl Acad Sci U S A *84*, 6616-6618.

Shepherd, M., and Hunter, C. N. (2004). Transient kinetics of the reaction catalysed by magnesium protoporphyrin IX methyltransferase. Biochem J *382*, 1009-1013.

Shibata, H., Suzuki, K., and Kobayashi, S. (2007). Menaquinone reduction by an HMT2-like sulfide dehydrogenase from *Bacillus stearothermophilus*. Can J Microbiol *53*, 1091-1100.

Siepker, L. J., Ford, M., de Kock, R., and Kramer, S. (1987). Purification of bovine protoporphyrinogen oxidase: immunological cross-reactivity and structural relationship to ferrochelatase. Biochim Biophys Acta *913*, 349-358.

Sofia, H. J., Chen, G., Hetzler, B. G., Reyes-Spindola, J. F., and Miller, N. E. (2001). Radical SAM, a novel protein superfamily linking unresolved steps in familiar biosynthetic pathways with radical mechanisms: functional characterization using new analysis and information visualization methods. Nucleic Acids Res *29*, 1097-1106.

Suzuki, J. Y., and Bauer, C. E. (1995). Altered monovinyl and divinyl protochlorophyllide pools in *bch*J mutants of *Rhodobacter capsulatus*. Possible monovinyl substrate discrimination of light-independent protochlorophyllide reductase. J Biol Chem *270*, 3732-3740.

Thauer, R. K., and Bonacker, L. G. (1994). Biosynthesis of coenzyme F_{430}, a nickel porphinoid involved in methanogenesis. Ciba Found Symp *180*, 210-222; discussion 222-217.

Unden, G., and Bongaerts, J. (1997). Alternative respiratory pathways of *Escherichia coli*: energetics and transcriptional regulation in response to electron acceptors. Biochim Biophys Acta *1320*, 217-234.

Viney, J., Davison, P. A., Hunter, C. N., and Reid, J. D. (2007). Direct measurement of metal-ion chelation in the active site of the AAA+ ATPase magnesium chelatase. Biochemistry *46*, 12788-12794.

Walker, C. J., Castelfranco, P. A., and Whyte, B. J. (1991). Synthesis of divinyl protochlorophyllide. Enzymological properties of the Mg-protoporphyrin IX monomethyl ester oxidative cyclase system. Biochem J *276 (Pt 3)*, 691-697.

Warren, M. J., Bolt, E., and Woodcock, S. C. (1994). 5-Aminolaevulinic acid synthase and uroporphyrinogen methylase: two key control enzymes of tetrapyrrole biosynthesis and modification. Ciba Found Symp *180*, 26-40; discussion 40-29.

Willows, R. D. (2003). Biosynthesis of chlorophylls from protoporphyrin IX. Nat Prod Rep *20*, 327-341.

Wu, C. K., Dailey, H. A., Rose, J. P., Burden, A., Sellers, V. M., and Wang, B. C. (2001). The 2.0 A structure of human ferrochelatase, the terminal enzyme of heme biosynthesis. Nat Struct Biol *8*, 156-160.

Yang, Y., Malten, M., Grote, A., Jahn, D., and Deckwer, W. D. (2007). Codon optimized Thermobifida fusca hydrolase secreted by *Bacillus megaterium*. Biotechnol Bioeng *96*, 780-794.

Zhang, J., Hellwig, P., Osborne, J. P., and Gennis, R. B. (2004). Arginine 391 in subunit I of the cytochrome *bd* quinol oxidase from *Escherichia coli* stabilizes the reduced form of the hemes and is essential for quinol oxidase activity. J Biol Chem *279*, 53980-53987.

Danksagung

Mein besonderer Dank gilt Prof. Dr. Dieter Jahn für die Vergabe der anspruchsvollen und spannenden Themen und für seine Förderung meiner wissenschaftlichen Laufbahn. Durch das von ihm kreierte Arbeitsumfeld war es mir möglich, unter optimalen Bedingungen zu forschen.

Prof. Dr. Michael Steinert danke ich für sein Interesse an meiner Arbeit und seine Bereitschaft, das Zweitgutachten dieser Dissertation zu übernehmen.

Prof. Dr. Ralf Mendel sei gedankt für die Übernahme des Vorsitzes der Prüfungskommission.

Ich danke Dr. Dörte Becher für die Analyse von Fraktionen der chromatografischen Reinigungen per LC-MS/MS.

Many thanks to Prof. Cecchini, Dr. Siegele, Prof. Blattner and Prof. Gennis for sending me *E. coli* mutants and to Rodrigo Arias for providing me purified nitrate reductase.

Ganz besonderer Dank gilt Dr. Jürgen Moser, für die hervorragende Betreuung, die sehr hilf- und lehrreichen Diskussionen und fortwährende Unterstützung und Motivierung.

Dank auch an Susanne Schröder, Katrin Riedmann und Katharina Herbst, die meine Arbeit während ihrer Diplomarbeiten unterstützt haben.

Ich möchte mich bei Corinna Lüer, Markus Bröcker, Stefanie Klein und Johannes Walther aus den Laboren 217/253, besonders aber bei Simone Virus und Denise Wätzlich für die tolle Atmosphäre und wichtige Diskussionen bedanken.

Beatrice Benkert, Ilka Heinemann und Rebekka Biedendieck möchte ich für die vielen kleinen Hilfen im Laboralltag und die entspannenden Kaffeepausen danken.

Ich danke allen Mitgliedern der AG Jahn für die freundliche Atmosphäre in der Arbeitsgruppe, die dafür gesorgt hat, dass das Arbeiten immer Spaß gemacht hat. Auch die schönen Unternehmungen und Feiern werden in meinem Gedächtnis bleiben.

Mein ganz besonderer Dank gilt meinen Eltern, meiner Familie und Freunden, vor allem aber meiner Frau Anca und meiner Tochter Elena, die mir viel Kraft gegeben und auch so manche Entbehrungen ertragen haben.

Appendices

Appendix 1: Peptides found in LC-MS/MS of fractions derived from the classic chromatography of PPO activity from *Escherichia coli*.

Sample 1 from November 7th 2005:

	Reference			MW
	Scan(s)	Peptide	MH+	Sp
1	gi|15804440|ref|NP_290480.1| protoporphyrinogen oxidase			21194,9
	900	R.TPQTNSYAR.K	1037,50105	864,5
	3053	R.EIAHLTDKPTLK.-	1365,77364	724,0
	3733	K.ELGIQADVANVHR.I	1421,74955	1055,9
	4083	R.IEEPQWENYDR.V	1478,65465	1695,4
	4089	R.YGHYHSAFQEFVK.K	1612,75430	2249,5
	4837	R.YGHYHSAFQEFVKK.H	1740,84927	2630,2
	4981	K.TLILFSTR.D	950,56694	826,2
	5034	R.EIASYLASELK.E	1223,65180	1203,5
	5702	R.LNSMPSAFYSVNLVAR.K	1768,90507	2234,6
	5814	K.EVVYTDWEQVANFAR.E	1826,87079	2688,9
	7526	R.KEVVYTDWEQVANFAR.E	1954,96575	1678,1
	7725	R.EIASYLASELKELGIQADVANVHR.I	2626,38351	3332,9
2	gi|16131220|ref|NP_417800.1| 30S ribosomal subunit protein S7			20020,0
	6812	R.LANELSDAAENK.G	1274,62229	1881,2
	7433	K.FVNILMVDGK.K	1135,61799	1150,9
	7459	R.VGGSTYQVPVEVRPVR.R	1742,95479	951,2
	7615	K.SELEAFEVALENVRPTVEVK.S	2259,18670	1283,5
	7655	K.STAESIVYSALETLAQR.S	1838,94943	2285,5
3	gi|133976|sp|P02358|RS6_ECOLI 30S ribosomal protein S6			15675,6
	2104	R.YTAAITGAEGK.I	1081,55242	1604,6
	7235	R.FNDAVIR.S	834,44683	750,8
	7473	K.HAVTEASPMVK.A	1169,59832	1724,2
	7799	K.AHYVLMNVEAPQEVIDELETTFR.F	2704,32869	1576,8
4	gi|15803764|ref|NP_289798.1| 30S ribosomal subunit protein S9			14857,1
	1886	K.GGGISGQAGAIR.H	1043,55923	1227,3
	7251	R.ALMEYDESLR.S	1226,57216	1058,4
	7286	R.SLEQYFGR.E	999,48942	984,7
	7999	R.QPLELVDMVEKLDLYITVK.G	2246,23523	1262,9

5	gi|16131180|ref|NP_417760.1| 50S ribosomal subunit protein L15			14981,3
	943	R.AAIEAAGGK.I	787,43084	1058,6
	2061	R.LNTLSPAEGSK.K	1116,58953	232,3
	2698	R.AAIEAAGGKIEE.-	1158,60009	960,1
	7309	K.VILAGEVTTPVTVR.G	1454,85771	1948,7
6	gi|15803823|ref|NP_289857.1| 30S ribosomal subunit protein S4			23469,9
	2683	K.AALELAEQR.E	1000,54219	702,7
	2909	R.RIYGVLER.Q	1005,58399	671,2
	3234	R.IYGVLER.Q	849,48288	496,1
	3373	R.LSDYGVQLR.E	1050,55784	1241,6
7	gi|15804576|ref|NP_290617.1| 50S ribosomal subunit protein L7/L12			12296,1
	6863	K.DLVESAPAALK.E	1113,61502	1324,1
	6940	K.ALEEAGAEVEVK.-	1244,63687	1730,1
	8247	K.DQIIEAVAAMSVMDVVELISAMEEK.F	2721,33952	1652,9
8	gi|15804792|ref|NP_290833.1| 50S ribosomal subunit protein L9			15769,9
	6868	R.DIADAVTAAGVEVAK.S	1429,75330	2936,9
	7244	K.LAEVLAAANAR.A	1098,62658	2183,5
	7272	K.INALETVTIASK.A	1259,72054	1804,7
9	gi|15803848|ref|NP_289882.1| 30S ribosomal subunit protein S10			11736,5
	7181	R.LIDQATAEIVETAK.R	1501,81081	2666,2
	7204	R.LVDIVEPTEK.T	1142,63033	932,5
	7977	R.LDLAAGVDVQISLG.-	1370,75257	685,2
10	gi|15803825|ref|NP_289859.1| 30S ribosomal subunit protein S13			13100,3
	7267	K.FVVEGDLR.R	934,49926	679,3
	7293	K.AILAAAGIAEDVK.I	1241,70998	2352,6
	7557	K.HAVIALTSIYGVGK.T	1428,82093	1283,0
11	gi|15799705|ref|NP_285717.1| 30S ribosomal subunit protein S20			9685,3
	6910	K.ANLTAQINK.L	972,54727	989,9
	7055	K.VYAAIEAGDK.A	1036,53095	838,2
	7237	K.AFNEMQPIVDR.Q	1319,64125	1273,9
12	gi|15803846|ref|NP_289880.1| 50S ribosomal subunit protein L4			22087,4
	8081	K.DMALEDVLIITGELDENLFLAAR.N	2561,31673	3904,2
	8134	K.LKDMALEDVLIITGELDENLFLAAR.N	2802,49576	2504,6
13	gi|15803845|ref|NP_289879.1| 50S ribosomal subunit protein L23			11200,0
	6449	K.EGQNLDFVGGAE.-	1235,55387	1399,5
	7937	K.LFEVEVEVVNTLVVK.G	1716,97821	2275,1

14	gi|15803830|ref|NP_289864.1| 30S ribosomal subunit protein S5			17604,3
	7291	R.VFMQPASEGTGIIAGGAMR.A	1892,93571	2200,9
	7540	R.AVLEVAGVHNVLAK.A	1419,83183	1962,3
15	gi|15803833|ref|NP_289867.1| 30S ribosomal subunit protein S8			14127,5
	1986	K.AVVESIQR.V	901,51016	917,8
	8182	K.VMAGLGIAVVSTSK.G	1332,75555	1684,6
16	gi|15803824|ref|NP_289858.1| 30S ribosomal subunit protein S11			13845,8
	7193	K.STPFAAQVAAER.C	1247,63788	544,1
	7494	R.KSTPFAAQVAAER.C	1375,73284	1782,3
17	gi|15834432|ref|NP_313205.1| 30S ribosomal subunit protein S18			8987,4
	7120	R.FTAEGVQEIDYK.D	1399,67399	2097,3
	7452	R.FTAEGVQEIDYKDIATLK.N	2041,04881	1364,5
18	gi|15803843|ref|NP_289877.1| 30S ribosomal subunit protein S19			10431,2
	7216	K.LGEFAPTR.T	890,47304	687,4
	7711	K.KGPFIDLHLLK.K	1280,77252	1165,5
19	gi|15803831|ref|NP_289865.1| 50S ribosomal subunit protein L18			12770,5
	1808	R.VQALADAAR.E	914,50541	770,4
	7070	K.LQELGATR.L	887,49451	719,7
20	gi|9911115|sp|P27307|YIJC_ECOLI Hypothetical transcriptional regulator yijC			
	7909	R.AFTEAQAEAMVTIVFSAGAEALDVGVEQR.R	3010,48263	2222,5
21	gi|15803712|ref|NP_289746.1| orf, hypothetical protein			
	8058	K.LTEMITAPVEALGFELVGIEFIR.G	2548,37312	2527,2
22	gi|15800345|ref|NP_286357.1| orf, hypothetical protein			
	7687	K.VMGQALPELVDQVVEVVQR.H	2109,13725	2482,5
23	gi|15804286|ref|NP_290325.1| heat shock protein			15746,1
	7680	R.KFQLAENIHVR.G	1354,75899	2138,1
24	gi|15799851|ref|NP_285863.1| 30S ribosomal subunit protein S2			
	6486	R.SQDLASQAEESFVEAE.-	1739,76063	2479,2
25	gi|15803822|ref|NP_289856.1|			36471,1
	7887	K.EGVQEDILEILLNLK.G	1725,96329	1840,1
26	gi|15801465|ref|NP_287482.1| DNA-binding protein HLP-II (HU, BH2, HD, NS)			15512,0
	2003	R.REEESAAAAEVEER.T	1575,72452	1569,5

27	gi|15803128|ref|NP_289159.1| 50S ribosomal subunit protein L19			
	7517	R.VFQTHSPVVDSISVK.R	1642,87990	1683,6
28	gi|15801863|ref|NP_287883.1| phage shock protein, putative inner membrane protein			
	988	R.SELSQSEQQR.L	1191,56002	1660,9
29	gi|15803836|ref|NP_289870.1| 50S ribosomal subunit protein L24			
	6761	R.DDEVIVLTGK.D	1088,58338	1597,0
30	gi|15832810|ref|NP_311583.1| RecA protein			
	1605	K.EGENVVGSETR.V	1176,54912	781,1
31	gi|15799710|ref|NP_285722.1| probable FKBX-type 16KD peptidyl-prolyl cis-trans isomerase			16052,9
	1212	K.LDDGTTAESTR.N	1165,53314	1432,9
32	gi|15803862|ref|NP_289896.1| FKBP-type peptidyl-prolyl cis-trans isomerase			20821,7
	4771	K.FNVEVVAIR.E	1046,59931	1500,9
33	gi|15833433|ref|NP_312206.1| 30S ribosomal subunit protein S3			
	4238	K.EFADNLDSDFK.V	1300,56919	866,1
34	gi|15802128|ref|NP_288150.1| 50S ribosomal subunit protein L20			
	7398	K.ILADIAVFDK.V	1104,62994	800,5
35	gi|15800773|ref|NP_286787.1| integration host factor (IHF), beta subunit			
	1364	K.TGDKVELEGK.Y	1075,56298	1080,0
36	gi|15804178|ref|NP_290217.1| 50S ribosomal subunit protein L28			
	7426	K.GIDTVLAELR.A	1086,61535	1336,7
37	gi|15804575|ref|NP_290616.1|			17682,4
	7190	K.QAIVAEVSEVAK.G	1243,68924	813,9
38	gi|15803726|ref|NP_289760.1| 50S ribosomal subunit protein L21			
	7407	K.IGVPFVDGGVIK.A	1200,69869	883,5
39	gi|15804102|ref|NP_290141.1| cold shock protein 7.4			7380,6
	6468	K.GPAAGNVTSL.-	886,46287	887,6
40	gi|16131057|ref|NP_417634.1| 30S ribosomal subunit protein S15			
	2559	R.YTQLIER.L	922,49926	735,1
41	gi|15799779|ref|NP_285791.1|			
	1406	R.NAADEDRDALR.A	1245,58182	513,4
42	gi|15803607|ref|NP_289640.1| 30S ribosomal subunit protein S21			
	2669	K.AGVLAEVR.R	814,47813	557,0

Sample 2 from November 7th 2005:

Reference			MW

	Scan(s)	Peptide	MH+	Sp
1	gi|15804440|ref|NP_290480.1| protoporphyrinogen IX oxidase			21194,9
	409	K.MSGGETDTRK.E	1081,49425	752,5
	1481	R.TPQTNSYAR.K	1037,50105	689,1
	2873	R.EIAHLTDKPTLK.-	1365,77364	833,6
	3329	R.YGHYHSAFQEFVKK.H	1740,84927	2408,5
	4759	K.FLMNSQWR.P	1081,52476	758,1
	4771	R.IEEPQWENYDR.V	1478,65465	1961,0
	5326	K.TLILFSTRDGQTR.E	1507,82272	283,2
	5330	K.ELGIQADVANVHR.I	1421,74955	907,9
	6182	R.YGHYHSAFQEFVK.K	1612,75430	2277,3
	7519	K.TLILFSTR.D	950,56694	860,9
	7858	K.EVVYTDWEQVANFAR.E	1826,87079	2529,6
	7897	R.KEVVYTDWEQVANFAR.E	1954,96575	2992,4
	7974	R.IEEPQWENYDRVVIGASIR.Y	2274,15132	1090,1
	8282	R.EIASYLASELK.E	1223,65180	1036,7
	8883	R.EIASYLASELKELGIQADVANVHR.I	2626,38351	3329,1
	8886	R.LNSMPSAFYSVNLVAR.K	1768,90507	2440,4
2	gi|15799851|ref|NP_285863.1|			26708,8
	975	K.AGVHFGHQTR.Y	1109,55990	867,3
	2381	R.NKVHIINLEK.T	1207,71573	1230,9
	2386	K.LENSLGGIK.D	930,52547	558,2
	2412	K.VHIINLEK.T	965,57784	675,8
	2989	R.LKDLETQSQDGTFDK.L	1724,83374	2658,9
	3423	K.DLETQSQDGTFDK.L	1483,65471	1899,5
	4935	R.ELEKLENSLGGIK.D	1429,78969	533,5
	6798	R.SQDLASQAEESFVEAE.-	1739,76063	2087,1
	7909	K.TVPMFNEALAELNK.I	1576,80396	754,0
	8234	R.WLGGMLTNWK.T	1205,61358	737,5
	9598	R.AVTLYLGAVAATVR.E	1404,82093	1772,6
3	gi|15833433|ref|NP_312206.1| 30S ribosomal subunit protein S3			25984,0
	1641	R.LGGAEIAR.T	786,44683	1102,7
	2370	R.PGIVIGK.K	683,44504	866,0
	4583	K.GEILGGMAAVEQPEKPAAQPK.K	2121,10087	1383,9
	5050	R.ADIDYNTSEAHTTYGVIGVK.V	2154,03495	1732,4
	5225	K.EFADNLDSDFK.V	1300,56919	776,4
	5518	K.LVADSITSQLER.R	1331,71652	1891,2
	6766	K.VVADIAGVPAQINIAEVR.K	1835,03852	852,4
	7874	R.KVVADIAGVPAQINIAEVR.K	1963,13349	1755,2
	8286	R.LGIVKPWNSTWFANTK.E	1861,99593	1692,6
4	gi|15803823|ref|NP_289857.1| 30S ribosomal subunit protein S4			23469,9
	2388	R.RIYGVLER.Q	1005,58399	833,1
	2808	K.AALELAEQR.E	1000,54219	1085,9
	3317	R.REGTDLFLK.S	1078,58914	666,3
	3723	R.LSDYGVQLR.E	1050,55784	1340,2
	6567	R.VVNIASYQVSPNDVVSIR.E	1960,04982	1740,1
	7439	K.GNTGENLLALLEGR.L	1456,77543	1972,8

	8540	R.LKGNTGENLLALLEGR.L	1697,95446	2372,2
	9467	R.SDLSADINEHLIVELYSK.-	2046,03898	1344,7
5	gi|15804574|ref|NP_290615.1| 50S ribosomal subunit protein L1			24730,5
	1301	R.GATVLPHGTGR.S	1065,57997	549,9
	2854	R.VAVFTQGANAEAAK.A	1376,71685	2304,3
	3224	K.VGTVTPNVAEAVK.N	1284,71579	660,0
	4621	R.VVGQLGQVLGPR.G	1222,72663	2018,6
	6824	K.AAGAELVGMEDLADQIK.K	1730,86293	1776,2
	7066	K.QYDINEAIALLK.E	1390,75766	335,9
	9050	K.FVESVDVAVNLGIDAR.K	1703,89628	1141,6
6	gi|16131220|ref|NP_417800.1|			19988,7
	2754	R.LANELSDAAENK.G	1274,62229	1883,9
	2914	R.LANELSDAAENKGTAVK.K	1730,89192	1959,9
	4046	R.VGGSTYQVPVEVRPVR.R	1742,95479	988,0
	5735	K.FVNILMVDGKK.S	1263,71296	1646,2
	6647	K.FVNILMVDGK.K	1135,61799	1206,6
	8493	K.SELEAFEVALENVRPTVEVK.S	2259,18670	2029,7
	8708	K.STAESIVYSALETLAQR.S	1838,94943	2647,1
7	gi|15803847|ref|NP_289881.1| 50S ribosomal subunit protein L3			22244,4
	790	K.MAGQMGNER.V	993,42406	1113,3
	1173	R.VTKPEAGHFAK.A	1184,64223	554,5
	4117	K.GAVPGATGSDLIVKPAVK.A	1679,96905	701,6
	4393	R.VTVQSLDVVR.V	1115,64190	1464,9
	7883	R.IFTEDGVSIPVTVIEVEANR.V	2188,14959	2950,7
	9029	R.LAEGEEFTVGQSISVELFADVK.K	2368,19185	2115,6
8	gi|15803765|ref|NP_289799.1| 50S ribosomal subunit protein L13			16019,4
	1331	K.TFTAKPETVK.R	1121,62010	736,9
	4411	K.RDWYVVDATGK.T	1309,65353	1232,1
	5169	K.QATFEEMIAR.R	1195,57758	372,6
	5668	R.DWYVVDATGK.T	1153,55242	1155,2
	6670	K.AEYTPHVDTGDYIIVLNADK.V	2234,09755	1985,2
9	gi|15803835|ref|NP_289869.1| 50S ribosomal subunit protein L5			20302,4
	6682	R.EQIIFPEIDYDKVDR.V	1879,94362	1215,5
	6689	K.LMTEFNYNSVMQVPR.V	1828,87205	2137,3
	6757	K.LLDNAAADLAAISGQK.P	1570,84351	2000,8
	6768	R.EQIIFPEIDYDK.V	1509,74715	876,6
	6931	K.LLDNAAADLAAISGQKPLITK.A	2123,20705	1113,9
10	gi|15803846|ref|NP_289880.1| 50S ribosomal subunit protein L4			22087,4
	2082	R.SGGVTFAAR.P	865,45264	810,9
	7488	R.DATGIDPVSLIAFDK.V	1561,81081	1674,8
	9229	K.DMALEDVLIITGELDENLFLAAR.N	2561,31673	3512,7
	9591	K.LKDMALEDVLIITGELDENLFLAAR.N	2802,49576	2360,2
11	gi|15803862|ref|NP_289896.1| FKBP-type peptidyl-prolyl cis-trans isomerase			20821,7
	6445	K.FNVEVVAIR.E	1046,59931	1530,0
	7576	K.DVFMGVDELQVGMR.F	1595,75563	2188,7

	8009	R.FLAETDQGPVPVEITAVEDDHVVVDGNHMLAGQNLK.F	3857,90144	1706,2
	9422	K.DLVVSLAYQVR.T	1262,71031	757,3
12	gi|15803830|ref|NP_289864.1| 30S ribosomal subunit protein S5			17604,3
	3566	K.AYGSTNPINVVR.A	1290,68008	1075,2
	3727	K.SVEEILGK.-	874,48802	626,5
	6466	R.VFMQPASEGTGIIAGGAMR.A	1892,93571	1806,7
13	gi|16128009|ref|NP_414556.1| DnaJ			
	2023	K.IPAGVDTGDR.I	1000,50580	799,3
	3678	K.EAYEVLTDSQK.R	1282,61614	1448,3
	6710	K.QLLQELQESFGGPTGEHNSPR.S	2324,12656	2230,8
14	gi|16130966|ref|NP_417542.1| hypothetical protein			
	2783	R.VNQSDISDAQIK.K	1317,66448	1526,5
	3267	R.DDSHGYELIK.A	1176,55314	813,2
	7490	R.LVILDILSR.D	1041,66666	888,2
15	gi|33347453|ref|NP_414968.2| putative polymerase/proteinase			
	4129	R.DNQIVTLTASR.D	1217,64844	1610,9
	8844	K.NIADAVNSVLTDTIADMSQDTSIHEFIK.Q	3048,48302	1267,7
16	gi|15803458|ref|NP_289491.1| putative transport protein			30858,7
	5511	K.QILTNIIQSEDR.I	1429,76453	783,9
	6464	R.LNELGASSINFVVR.V	1518,82747	2057,1
17	gi|15804522|ref|NP_290562.1| heat shock protein hslVU			
	5125	R.IAEAAWQVNESTENIGAR.R	1958,95664	961,7
	5448	K.PSDLIPELQGR.L	1224,65828	586,3
18	gi|16128190|ref|NP_414739.1| putative lipoprotein			
	5656	K.IVELEAPQLPR.S	1264,72596	918,1
	8565	K.LKDGVGLLPTVLDVVENPK.N	2006,15322	1739,2

19	gi|15832425|ref|NP_311198.1| NADH dehydrogenase I chain B			
	4402	R.LYDQMLEPK.W	1136,56562	1089,1
	5274	K.QEIVTDPLEQEVNK.N	1641,83301	1104,4
20	gi|15803871|ref|NP_289905.1|			23607,4
	5260	R.IAQTLLNLAK.Q	1084,67247	1104,7
	6663	K.VGNLAFLDVTGR.I	1261,68991	1398,4
21	gi|15799779|ref|NP_285791.1|			
	2222	K.GLGAGANPEVGR.N	1097,56980	1352,0
	5286	R.LDEFETVGNTIR.A	1393,69579	1774,6
22	gi|15803764|ref|NP_289798.1| 30S ribosomal subunit protein S9			
	1726	K.GGGISGQAGAIR.H	1043,55923	1290,8
	4593	R.ALMEYDESLR.S	1226,57216	990,7
23	gi|586658|sp|P37620|DCRB_ECOLI DcrB protein precursor			
	5078	K.MQQLDSIISAK.G	1233,65075	819,9
	6616	K.LSFSLPADMTDQSGK.L	1596,75740	729,7
24	gi|15834157|ref|NP_312930.1|			43268,3
	3479	K.ALEGDAEWEAK.I	1218,56371	1471,5
	5174	K.VGEEVEIVGIK.E	1171,65688	1863,3
25	gi|133976|sp|P02358|RS6_ECOLI 30S ribosomal protein S6			15675,6
	1535	K.HAVTEASPMVK.A	1169,59832	1176,1
	2138	R.YTAAITGAEGK.I	1081,55242	1694,1
26	gi|16128083|ref|NP_414632.1|			
	2159	R.VLVVGGSQGAR.I	1042,60037	1099,5
	6377	R.TDVLALPLPQQR.L	1350,77398	559,5
27	gi|15800320|ref|NP_286332.1| alkyl hydroperoxide reductase, C22 subunit			20730,4
	8895	R.ATFVVDPQGIIQAIEVTAEGIGR.D	2384,28200	1853,9
28	gi|15833970|ref|NP_312743.1| transcription termination factor Rho			46956,6
	9190	K.SGEDIFGDGVLEILQDGFGFLR.S	2384,17687	2888,7
29	gi|15803733|ref|NP_289767.1|			19546,1
	8911	K.SAMVLEDLIGQFLYGSK.G	1870,96191	2577,8
30	gi|16132234|ref|NP_416345.1| ProQ			
	5742	K.AGQNAMDATVLEITK.D	1561,78903	1987,8
31	gi|15799710|ref|NP_285722.1| probable FKBX-type 16KD peptidyl-prolyl cis-trans isomerase			16052,9
	8208	R.LGDASLSEGLEQHLLGLK.V	1880,01237	494,3
32	gi|16130591|ref|NP_417163.1|			
	9020	R.ALAINPDILLMDEAFSALDPLIR.T	2511,35272	1567,1
33	gi|15803119|ref|NP_289150.1| orf, hypothetical protein			
	5350	K.NADLPLAQAAIDR.F	1367,72775	1035,3
34	gi|16128998|ref|NP_415553.1| putative oxidoreductase component			
	8799	R.QPQDPLLVPLFTLIR.E	1750,02617	1267,6
35	gi|33347775|ref|NP_418098.2| putative			

	transcriptional regulator			
	9181	R.MFDSLIEFIEDSLITR.I	1928,96739	2803,1
36	gi|30064007|ref|NP_838178.1| hypothetical protein			
	5710	K.QLTAQAPVDPIVLGK.M	1549,89482	973,8
37	gi|15803822|ref|NP_289856.1| RNA polymerase, alpha subunit			
	8860	K.EGVQEDILEILLNLK.G	1725,96329	1541,1
38	gi|16131180|ref|NP_417760.1| 50S ribosomal subunit protein L15			
	5032	K.VEGGVVDLNTLK.A	1243,68924	1382,0
39	gi|15830966|ref|NP_309739.1| phosphoribosylpyrophosphate synthetase			
	4259	R.LYTSLGDAAVGR.F	1222,64263	1181,8
40	gi|15834295|ref|NP_313068.1|			
	5707	K.VILVGNLGQDPEVR.Y	1508,84312	995,0
41	gi|15803741|ref|NP_289775.1|			26766,1
	2265	R.DSMGQSLSGGER.R	1223,53209	1459,2
42	gi|15804335|ref|NP_290374.1| membrane-bound ATP synthase, F1 sector, delta-subunit			
	3366	R.AGDMVIDGSVR.G	1119,54628	1134,7
43	gi|15804523|ref|NP_290563.1| heat shock protein hslVU			
	4210	R.ALLENTELSAR.E	1216,65319	1846,5
44	gi|16130438|ref|NP_417008.1| hypothetical protein			
	6684	K.SDVTPALSEMMQMK.I	1567,71646	1260,4
45	gi|15804336|ref|NP_290375.1| membrane-bound ATP synthase, F0 sector, subunit b			
	3400	K.EIADGLASAER.A	1131,56404	1099,8
46	gi|16130861|ref|NP_417435.1| hypothetical protein			
	3075	K.NLSESNDYVPR.P	1293,60697	928,0
47	gi|16128183|ref|NP_414732.1| hypothetical protein			
	3441	K.ATVNVADLDR.N	1073,55856	1159,2
48	gi|15801211|ref|NP_287228.1| acyl carrier protein			8616,2
	3578	K.IIGEQLGVK.Q	956,57751	555,8
49	gi|15802999|ref|NP_289029.1|			26959,7
	3720	K.LAEAGIPTQMER.L	1315,66746	640,2
50	gi|15800457|ref|NP_286469.1| peptidoglycan-associated lipoprotein			18794,2
	4348	R.GTPEYNISLGER.R	1335,65392	420,6
51	gi|9911115|sp|P27307|YIJC_ECOLI Hypothetical transcriptional regulator yijC			
	3138	K.TAIIPGNVKDE.-	1156,62083	816,3
52	gi|1723853|sp|P25894|YGGG_ECOLI Putative metalloprotease yggG			
	2142	K.ATIAPANSEYAK.R	1235,62664	487,4
53	gi|15800772|ref|NP_286786.1| 30S ribosomal subunit protein S1			

	3143	K.SESAIPAEQFK.N	1206,60009	534,1

Sample 3 from April 12th 2006

	Reference			MW
	Scan(s)	Peptide	MH+	Sp
1	gi|15804440|ref|NP_290480.1| protoporphyrinogen oxidase			21194,9
	3599 - 3643	R.IEEPQWENYDR.V	1478,65465	970,6
	4933	R.EIASYLASELK.E	1223,65180	1050,5
	4935	K.TLILFSTR.D	950,56694	683,1
	5656	K.EVVYTDWEQVANFAR.E	1826,87079	2487,8
	7479	R.YGHYHSAFQEFVKK.H	1740,84927	1352,2
2	gi|15833970|ref|NP_312743.1| transcription termination factor Rho			46956,6
	7397	K.NTPVSELITLGENMGLENLAR.M	2271,16492	1315,6
	7821	K.SGEDIFGDGVLEILQDGFGFLR.S	2384,17687	2748,8
3	gi|15804576|ref|NP_290617.1| 50S ribosomal subunit protein L7/L12			12296,1
	6700	K.DLVESAPAALK.E	1113,61502	864,7
	6784	K.ALEEAGAEVEVK.-	1244,63687	1802,9
4	gi|16131180|ref|NP_417760.1| 50S ribosomal subunit protein L15			14981,3
	7092	K.VILAGEVTTPVTVR.G	1454,85771	1658,6
	7122	K.AANIIGIQIEFAK.V	1387,79438	1697,2
5	gi|16130579|ref|NP_417151.1| hypothetical protein			16064,0
	6612	K.ATVTGDGLSQEAK.E	1276,63794	1805,0
	6733	K.SGDTLSAISK.Q	978,51022	1195,5
6	gi|15804286|ref|NP_290325.1| heat shock protein			15746,1
	7291	R.IAIAVAGFAESELEITAQDNLLVVK.G	2614,43381	2474,8
7	gi|15802128|ref|NP_288150.1| 50S ribosomal subunit protein L20, and regulator			13497,9
	7486	K.ILADIAVFDKVAFTALVEK.A	2063,17871	1672,0
8	gi|15803764|ref|NP_289798.1| 30S ribosomal subunit protein S9			14857,1
	7643	R.QPLELVDMVEKLDLYITVK.G	2246,23523	1397,5

9	gi|15803845|ref|NP_289879.1| 50S ribosomal subunit protein L23			11200,0
	7240	K.LFEVEVEVVNTLVVK.G	1716,97821	1893,8
10	gi|16130123|ref|NP_416690.1| 50S ribosomal subunit protein L25			10694,4
	7206	K.AEFYSEVLTIVVDGK.E	1669,86833	2610,1
11	gi|15803210|ref|NP_289242.1| carbon storage regulator			
	7324	R.RVGETLMIGDEVTVTVLGVK.G	2116,16822	1973,9
12	gi|15803823|ref|NP_289857.1| 30S ribosomal subunit protein S4			
	7167	R.SDLSADINEHLIVELYSK.-	2046,03898	1703,4
13	gi|15803833|ref|NP_289867.1| 30S ribosomal subunit protein S8, and regulator			
	7083	K.VMAGLGIAVVSTSK.G	1332,75555	2625,3
14	gi|15834432|ref|NP_313205.1| 30S ribosomal subunit protein S18			
	7157	R.FTAEGVQEIDYKDIATLK.N	2041,04881	1364,0
15	gi|15800564|ref|NP_286576.1| global regulator, starvation conditions			
	7223	R.QVIQFIDLSLITK.Q	1517,89376	1274,9
16	gi|15804792|ref|NP_290833.1| 50S ribosomal subunit protein L9			
	7075	K.INALETVTIASK.A	1259,72054	1343,8
17	gi|16131470|ref|NP_418056.1| PTS system, mannitol-specific enzyme IIABC component			
	2738	R.FGEEEDDIAR.L	1180,51167	1220,3
18	gi|16128616|ref|NP_415166.1| RlpA			
	979	K.AEASTLQQR.L	1003,51670	1128,0
19	gi|16131771|ref|NP_418368.1| essential cell division protein			35753,4
	890	R.GAEQAETVR.A	960,47450	907,0
20	gi|133976|sp|P02358|RS6_ECOLI 30S ribosomal protein S6			15675,6
	6725	R.YTAAITGAEGK.I	1081,55242	1501,6
21	gi|15803566|ref|NP_289599.1| orf, hypothetical protein			
	7087	R.ISDDLYVFK.D	1099,56700	643,2
22	gi|15800357|ref|NP_286369.1| putative alpha helical protein			18767,4
	6671	R.TEVDELTR.A	962,47892	620,9
23	gi|15804102|ref|NP_290141.1| cold shock protein 7.4			7380,6
	6364	K.GPAAGNVTSL.-	886,46287	849,9
24	gi|15834020|ref|NP_312793.1| Sec-independent protein translocase			
	1457	K.TSQDADFTAK.T	1083,49529	1028,6
25	gi|16130441|ref|NP_417011.1| putative membrane protein			
	5869	R.LTLNAEQSPAQ.-	1171,59534	955,5
26	gi|15799860|ref|NP_285872.1| histone-like protein			17659,3
	1606	R.METDLQAK.M	935,45026	705,7

27	gi|15799862|ref|NP_285874.1| (3R)-hydroxymyristol acyl carrier protein dehydratase			
	7237	R.FPFLLVDR.V	1006,57203	653,9
28	gi|2506612|sp|P45571|YBCJ_ECOLI Hypothetical protein ybcJ			
	863	K.VDGAVETR.K	846,43157	984,8
29	gi|16131320|ref|NP_417905.1| hypothetical protein			
	6660	R.VLQSQPGER.N	1013,53743	473,8

Sample 4 from April 12th 2006

Reference			MW
Scan(s)	Peptide	MH+	Sp
1	gi|15800564|ref|NP_286576.1| global regulator, starvation conditions		
4724	R.YAIVANDVR.K	1020,54727	1319,4
5389	K.DDDTADILTAASR.D	1363,63358	2538,7
5633	K.ATNLLYTR.N	951,52581	1125,7
5671	K.ATVELLNR.Q	915,52581	1494,0
6049	R.AVQLGGVALGTTQVINSK.T	1755,99632	2437,4
6054	K.AIGEAKDDDTADILTAASR.D	1932,95089	1923,9
6240	K.KATVELLNR.Q	1043,62077	728,4
6840	R.QVIQFIDLSLITK.Q	1517,89376	1906,1
7047	K.FLWFIESNIE.-	1297,64632	1728,2
7368	R.DLDKFLWFIESNIE.-	1768,87923	777,3
2	gi|15804440|ref|NP_290480.1| protoporphyrinogen oxidase		21194,9
1028	R.TPQTNSYAR.K	1037,50105	710,3
3708	R.IEEPQWENYDR.V	1478,65465	864,0
5118	R.EIASYLASELK.E	1223,65180	946,8
6448	R.LNSMPSAFYSVNLVAR.K	1768,90507	1022,5
6471	K.EVVYTDWEQVANFAR.E	1826,87079	2874,8
6560	R.KEVVYTDWEQVANFAR.E	1954,96575	1146,7
6772	R.YGHYHSAFQEFVK.K	1612,75430	2140,2
6938	R.EIASYLASELKELGIQADVANVHR.I	2626,38351	2901,1
8683	R.YGHYHSAFQEFVKK.H	1740,84927	1762,4
3	gi|16130343|ref|NP_416912.1|		
863	K.SLVSDDKK.D	891,47819	502,7
5045	K.MVAPVDGTIGK.I	1087,58161	604,2
5690	K.LSGSVTVGETPVIR.I	1414,79002	904,1
6294	K.STLTPVVISNMDEIK.E	1646,86695	1200,4
6828	K.VGDTVIEFDLPLLEEK.A	1816,95787	2464,6
6883	R.VKVGDTVIEFDLPLLEEK.A	2044,12125	1353,2
7162	K.DTGTIEIIAPLSGEIVNIEDVPDVVFAEK.I	3083,60345	3197,2
4	gi|15834157|ref|NP_312930.1| protein chain elongation factor EF-Tu		
3206	K.ALEGDAEWEAK.I	1218,56371	1339,9
5909	K.VGEEVEIVGIK.E	1171,65688	1215,5

	6100	K.FESEVYILSK.D	1214,63033	863,3
	6499	R.TTDVTGTIELPEGVEMVMPGDNIK.M	2546,23643	2400,1
	6984	K.ILELAGFLDSYIPEPER.A	1962,02187	931,5
	7109	R.AIDKPFLLPIEDVFSISGR.G	2117,16412	1480,3
5	gi|10955180|ref|NP_052173.1| beta-lactamase			31477,2
	1805	R.VDAGQEQLGR.R	1072,53816	2022,6
	6065	R.VGYIELDLNSGK.I	1307,68416	1506,6
	6254	R.IHYSQNDLVEYSPVTEK.H	2021,98146	1847,0
	6481	R.SALPAGWFIADK.S	1275,67320	654,6
	6567	K.LLTGELLTLASR.Q	1286,76783	1492,8
6	gi|15800357|ref|NP_286369.1| putative alpha helical protein			18767,4
	2495	R.TEVDELTR.A	962,47892	621,6
	5685	R.DIDALVEQAR.E	1129,58478	1714,1
	6972	R.DLEEFAMSYEESLKEESDSVFMR.V	2771,20625	2815,4
	7203	K.ESLWQELADITDKTQLEWR.E	2361,17212	873,4
7	gi|16130187|ref|NP_416755.1| Ais			
	5673	K.VYLDGEFVNH.-	1192,56331	809,7
	6618	R.ELGNAFSADIPDFDLYSSNTVR.T	2431,14121	1124,9
	6646	R.DATFKPDYLDGLVMHVEK.G	2078,02630	2595,8
8	gi|15800320|ref|NP_286332.1| alkyl hydroperoxide reductase, C22 subunit			20730,4
	5951	K.YAMIGDPTGALTR.N	1365,68311	1081,5
	6532	K.EGEATLAPSLDLVGKI.-	1612,87923	794,3
	7497	R.ATFVVDPQGIIQAIEVTAEGIGR.D	2384,28200	1915,7
9	gi|15800563|ref|NP_286575.1| periplasmic glutamine-binding protein; permease			
	6415	K.NVDLALAGITITDER.K	1600,85408	1160,0
	6716	K.LVVATDTAFVPFEFK.Q	1683,89924	1437,9
	6763	R.ADAVLHDTPNILYFIK.T	1829,97961	1425,2
10	gi|15800464|ref|NP_286476.1| phosphoglyceromutase 1			
	867	K.YGDEQVK.Q	838,39412	720,2
	5757	R.YYLGNADEIAAK.A	1327,65286	1138,0
	6693	K.LLKEEGYSFDFAYTSVLK.R	2110,07430	1316,9
11	gi|15799860|ref|NP_285872.1| histone-like protein			17659,3
	1684	R.METDLQAK.M	935,45026	655,7
	5946	K.TGVSNTLENEFK.G	1338,65359	739,3
	6726	K.IAIVNMGSLFQQVAQK.T	1746,95710	1623,9
12	gi|15803692|ref|NP_289726.1| putative periplasmic protein			19997,7
	1063	K.AAADIASR.V	774,41044	940,5
	5911	K.VLLVGQSPNAELSAR.A	1553,86458	1362,7
	5995	R.SQLLTSDLVK.S	1103,63067	1002,4
13	gi|15803832|ref|NP_289866.1| 50S ribosomal subunit protein L6			
	1872	R.YADEVVR.T	851,42576	645,0
	2480	R.TLNDAVEVK.H	988,53095	604,8
	5589	K.APVVVPAGVDVK.I	1150,68304	862,7

14	gi|15803846|ref|NP_289880.1| 50S ribosomal subunit protein L4			
	7742	K.LKDMALEDVLIITGELDENLFLAAR.N	2802,49576	1971,1
	7790	K.DMALEDVLIITGELDENLFLAAR.N	2561,31673	3400,3
15	gi|15804576|ref|NP_290617.1| 50S ribosomal subunit protein L7/L12			
	3012	K.ALEEAGAEVEVK.-	1244,63687	1663,7
	8220	K.DQIIEAVAAMSVMDVVELISAMEEK.F	2721,33952	2579,4
16	gi|15801846|ref|NP_287864.1| thiol peroxidase			17806,2
	5986	K.DLSDVTLGQFAGK.R	1350,68997	2411,3
	6576	R.NAEFLQAYGVAIADGPLK.G	1876,98034	2505,6
17	gi|16130338|ref|NP_416907.1| ZipA			
	6758	K.LMLQSAQHIADEVGGVVLDDQR.R	2394,20818	1391,2
	6847	K.DFTTPGVTIFMQVPSYGDELQNFK.L	2734,30690	1970,6
18	gi|16131220|ref|NP_417800.1| 30S ribosomal subunit protein S7			
	6819	K.SELEAFEVALENVRPTVEVK.S	2259,18670	1285,2
	7031	K.STAESIVYSALETLAQR.S	1838,94943	1645,9
19	gi|30063856|ref|NP_838027.1| lipoprotein-34			36801,6
	1123	K.SATDAANAAQNR.A	1189,55560	1439,6
	1636	R.LDEDEQYR.G	1067,46399	1006,1
20	gi|16132194|ref|NP_418793.1| OsmY			
	2069	K.GVEGVTSVSDK.L	1077,54224	902,3
	5853	K.LLADDIVPSR.H	1098,61535	1141,5
21	gi|16131266|ref|NP_417847.1| DamX			
	1339	K.TAGNVGSLK.S	846,46796	541,0
	4718	K.AVSTLPADVQAK.N	1199,66303	558,8
22	gi|15803847|ref|NP_289881.1| 50S ribosomal subunit protein L3			
	6849	R.LAEGEEFTVGQSISVELFADVK.K	2368,19185	2909,5
23	gi|15802128|ref|NP_288150.1| 50S ribosomal subunit protein L20			
	7090	K.ILADIAVFDKVAFTALVEK.A	2063,17871	2125,4
24	gi|15804508|ref|NP_290548.1| triosephosphate isomerase			26936,8
	6719	K.TQGAAAFEGAVIAYEPVWAIGTGK.S	2407,22924	3021,3
25	gi|15803764|ref|NP_289798.1| 30S ribosomal subunit protein S9			
	7352	R.QPLELVDMVEKLDLYITVK.G	2246,23523	1458,4
26	gi|133976|sp|P02358|RS6_ECOLI 30S ribosomal protein S6			15675,6
	7227	K.AHYVLMNVEAPQEVIDELETTFR.F	2704,32869	1339,0
27	gi|15803836|ref|NP_289870.1| 50S ribosomal subunit protein L24			
	6247	K.EAAIQVSNVAIFNAATGK.A	1803,95994	1789,9
28	gi|15803726|ref|NP_289760.1| 50S ribosomal subunit protein L21			
	7029	K.LDIATGETVEFAEVLMIANGEEVK.I	2578,29566	1426,7
29	gi|15833970|ref|NP_312743.1|			46956,6

	7176	K.NTPVSELITLGENMGLENLAR.M	2271,16492	1520,6
30	gi|15804286|ref|NP_290325.1| heat shock protein			15746,1
	6744	R.GANLVNGLLYIDLER.V	1659,90645	2601,3
31	gi|15803848|ref|NP_289882.1|			11710,4
	7960	R.LDLAAGVDVQISLG.-	1370,75257	675,8
32	gi|15802817|ref|NP_288844.1|			11280,8
	7517	R.IDDDLTLLSETLEEVLR.S	1974,02774	1286,4
33	gi|15803833|ref|NP_289867.1| 30S ribosomal subunit protein S8			
	6215	K.VMAGLGIAVVSTSK.G	1332,75555	2710,4
34	gi|16131215|ref|NP_417795.1| bacterioferrin			
	6943	R.ILFLEGLPNLQDLGK.L	1669,95233	1612,4
35	gi|15834432|ref|NP_313205.1| 30S ribosomal subunit protein S18			
	6362	R.FTAEGVQEIDYKDIATLK.N	2041,04881	1198,2
36	gi|15802070|ref|NP_288092.1| superoxide dismutase			21234,5
	6352	K.DALAPHISAETIEYHYGK.H	2014,98688	876,9
37	gi|15803210|ref|NP_289242.1| carbon storage regulator			
	6807	R.RVGETLMIGDEVTVTVLGVK.G	2116,16822	1239,7
38	gi|15803825|ref|NP_289859.1| 30S ribosomal subunit protein S13			
	4778	K.AILAAAGIAEDVK.I	1241,70998	2391,8
39	gi|15803823|ref|NP_289857.1|			23436,6
	8635	R.SDLSADINEHLIVELYSK.-	2046,03898	1382,9
40	gi|15803877|ref|NP_289911.1| peptidyl-prolyl cis-trans isomerase A			20400,4
	6770	R.TADKDSATSQFFINVADNAFLDHGQR.D	2868,35473	1385,3
41	gi|2495538|sp|P77717|YBAY_ECOLI Hypothetical protein ybaY precursor			
	6656	K.VALPPDAVLTVTLSDASLADAPSK.V	2351,27043	1153,5
42	gi|15803725|ref|NP_289759.1| 50S ribosomal subunit protein L27			
	6359	R.FGGESVLAGSIIVR.Q	1404,78454	1610,3
43	gi|15803128|ref|NP_289159.1| 50S ribosomal subunit protein L19			
	6509	R.LQAFEGVVIAIR.N	1315,77325	1748,6
44	gi|16130123|ref|NP_416690.1| 50S ribosomal subunit protein L25			
	6866	K.AEFYSEVLTIVVDGK.E	1669,86833	1596,0
45	gi|16128561|ref|NP_415110.1| oxygen-insensitive NAD(P)H nitroreductase			
	2357	K.LVVDQEDADGR.F	1216,58042	978,4
46	gi|15800816|ref|NP_286832.1|			37159,7
	5579	K.DGSVVVLGYTDR.I	1280,64811	1535,4
47	gi|16131470|ref|NP_418056.1|			
	2828	R.FGEEEDDIAR.L	1180,51167	1196,1

48	gi|16131180|ref|NP_417760.1| 50S ribosomal subunit protein L15			
	6502	K.AANIIGIQIEFAK.V	1387,79438	1357,5
49	gi|16130441|ref|NP_417011.1| putative membrane protein			
	3436	R.LTLNAEQSPAQ.-	1171,59534	1253,9
50	gi|15833303|ref|NP_312076.1| protein chain initiation factor IF-2			
	986	R.LAAEEQAQR.E	1015,51670	1059,0
51	gi|16128119|ref|NP_414668.1| putative carbonic anhdrase			
	2400	R.DLDVTATNR.E	1004,50071	1195,1
52	gi|16130245|ref|NP_416813.1| ArgT			
	5916	K.GSPIQPTLDSLK.G	1255,68924	452,6
53	gi|15799694|ref|NP_285706.1| chaperone Hsp70			
	2189	K.ASSGLNEDEIQK.M	1290,61720	984,3
54	gi|16128616|ref|NP_415166.1| RlpA			
	1021	K.AEASTLQQR.L	1003,51670	1329,0
55	gi|134659|sp|P00448|SODM_ECOLI Superoxide dismutase [Mn] (MnSOD)			
	1959	K.LDQLPADK.K	899,48327	938,7
56	gi|15803639|ref|NP_289672.1| orf, hypothetical protein			
	1922	R.LGETGDAIAK.Q	974,51530	1267,7
57	gi|15800203|ref|NP_286215.1|			
	6742	K.LVTDELVIALVK.E	1312,80863	1643,4
58	gi|16128174|ref|NP_414723.1| UDP-N-acetylglucosamine acetyltransferase			
	1121	R.GTVQGGGLTK.V	917,50507	463,7
59	gi|15834020|ref|NP_312793.1| Sec-independent protein translocase			
	1555	K.TSQDADFTAK.T	1083,49529	858,5
60	gi|16128655|ref|NP_415205.1|			
	5771	K.IVVSPAAGTIVK.I	1154,71434	367,6

Appendix 2: Peptides found in LC-MS/MS of fractions from the overproduction of HemG in *Escherichia coli*.

Sample 1 from January 1st 2006

Reference			MW
Scan(s)	Peptide	MH+	Sp
1 gi|16131979|ref|NP_418578.1|FrdA			
3544	R.AAIAAAQANPNAK.I	1210,65386	1494,7
4857	R.AATAGNGNEAAIEAQAAGVEQR.L	2099,01120	2263,0
4567	R.ANAVVM*ATGGAGR.V	1190,59462	1721,4
4807	R.ANAVVMATGGAGR.V	1174,59972	1019,3
5858	R.GDVVYLDLR.H	1049,56259	865,8
5247	R.GEGGILVNK.N	886,49926	964,3

	5341	R.GLVAM*NM*M*EGTLVQIR.A	1810,88594	825,3
	3909	R.LAGEQATER.A	974,49015	763,3
	6541	R.LGSNSLAELVVFGR.L	1461,80600	799,4
	6428	R.RPDGSVNVR.R	999,53302	459,2
	5163	R.TPELM*QK.T	862,43387	319,0
	5292	R.YLQDYGM*GPETPLGEPK.N	1910,88404	1338,2
	5385	R.YLQDYGMGPETPLGEPK.N	1894,88914	1859,0
2	gi|15800816|ref|NP_286832.1| outer membrane protein 3a			
	4592	K.AQGVQLTAK.L	915,52581	273,6
	4849	K.DGSVVVLGYTDR.I	1280,64811	1361,3
	4799	K.GIKDVVTQPQA.-	1155,63681	800,2
	5538	R.IGSDAYNQGLSER.R	1409,66555	1356,5
	5850	K.SDVLFNFNK.A	1083,54694	838,0
3	gi|16130152|ref|NP_416719.1| outer membrane protein 1b			
	6441	R.DAGINTDNIVALGLVYQF.-	1922,98582	1442,0
	5336	K.FQDVGSFDYGR.N	1290,57494	368,0
	5812	K.INLLDDNQFTR.D	1348,68555	629,4
	4135	R.TDAQNTAAYIGNGDR.A	1566,71429	818,0
	5401	K.YVDVGATYYFNK.N	1439,68416	1334,0
4	gi|15830995|ref|NP_309768.1| CoA-linked acetaldehyde dehydrogenase			
	5736	R.EYASFTQEQVDK.I	1444,65907	356,3
	5383	K.IAELAGFSVPENTK.I	1475,77404	778,2
	6457	R.ILINTPASQGGIGDLYNFK.L	2021,07022	1145,8
5	gi|15804747|ref|NP_290788.1| fumarate reductase			
	4190	R.TADQGTNIQTPAQMAK.Y	1674,81156	987,2
	2945 - 3367	R.TADQGTNIQTPAQM*AK.Y	1690,80646	885,1
	6419	K.VEALANFPIER.D	1258,67901	876,2
6	gi|15800564|ref|NP_286576.1| global regulator			
	5397	R.AVQLGGVALGTTQVINSK.T	1755,99632	1257,4
	6538	R.QVIQFIDLSLITK.Q	1517,89376	1219,2
	6369	R.YAIVANDVR.K	1020,54727	930,6
7	gi|15802089|ref|NP_288111.1| murein lipoprotein			
	5592	K.IDQLSSDVQTLNAK.V	1531,79623	1217,2
	4781	K.VDQLSNDVNAMR.S	1361,64779	1441,3
	3971	K.VDQLSNDVNAM*R.S	1377,64269	1139,4
8	gi|15834157|ref|NP_312930.1| protein chain elongation factor EF-Tu			
	5668	R.AFDQIDNAPEEK.A	1376,63285	960,7
	5399	R.AGENVGVLLR.G	1027,58947	759,4
	5659	K.FESEVYILSK.D	1214,63033	485,4
9	gi|16130579|ref|NP_417151.1| hypothetical protein			
	4746	K.ATVTGDGLSQEAK.E	1276,63794	849,2
	5572	K.SGDTLSAISK.Q	978,51022	947,9
	6207	K.TATPATASQFYTVK.S	1485,75839	381,5
10	gi|15802193|ref|NP_288215.1| glyceraldehyde-3-phosphate dehydrogenase A			
	5098	R.GASQNIIPSSTGAAK.A	1401,73323	670,3
	5538	R.VPTPNVSVVDLTVR.L	1495,84787	1675,9

11	gi|16128752|ref|NP_415305.1| MoaD			
	5964	R.ELVGTDATEVAADFPTVEALR.Q	2204,10812	2112,1
12	gi|15802055|ref|NP_288077.1| putative outer membrane protein			
	4866	R.VVLASNGSQVTVSPR.-	1513,83328	295,9
13	gi|15803846|ref|NP_289880.1| 50S ribosomal subunit protein L4			
	4871	K.DAQSALTVSETTFGR.D	1582,77074	852,9
14	gi|15800563|ref|NP_286575.1| periplasmic glutamine-binding protein			
	4974	K.AVGDSLEAQQYGIAFPK.G	1793,90684	942,1
15	gi|15804792|ref|NP_290833.1| 50S ribosomal subunit protein L9			
	5084	R.DIADAVTAAGVEVAK.S	1429,75330	1172,6
16	gi|15804576|ref|NP_290617.1| 50S ribosomal subunit protein L7/L12			
	4873	K.ALEEAGAEVEVK.-	1244,63687	1173,5
17	gi|15804574|ref|NP_290615.1| 50S ribosomal subunit protein L1			
	5129	R.VAVFTQGANAEAAK.A	1376,71685	1633,6
18	gi|15804734|ref|NP_290775.1| GroES			
	5158	K.SAGGIVLTGSAAAK.S	1202,67393	651,3
19	gi|15832699|ref|NP_311472.1| putative formate acetyltransferase			
	4793	K.AGYAEDEVVAVSK.L	1337,65834	659,9
20	gi|16130649|ref|NP_417222.1| lipoprotein			
	5096	K.VIETFGASEGGNK.G	1308,64302	1169,0
21	gi|16130827|ref|NP_417401.1| phosphoglycerate kinase			
	5280	R.VATEFSETAPATLK.S	1464,75805	500,7
22	gi|33112659|sp|P21420|NMPC_ECOLI O			
	5401	K.YVDVGATYYFNK.N	1439,68416	1334,0
23	gi|16128548|ref|NP_415097.1| outer membrane protein 3b (a) protease VII			
	5166	R.VYLAEEGGR.K	993,49999	954,2
24	gi|15803871|ref|NP_289905.1| cyclic AMP receptor protein			
	5884	R.IAQTLLNLAK.Q	1084,67247	603,4
25	gi|16131220|ref|NP_417800.1| 30S ribosomal subunit protein S7			
	4587	R.LANELSDAAENK.G	1274,62229	635,9
26	gi|15804573|ref|NP_290614.1| 50S ribosomal subunit protein L11			
	4630	R.AQLQEIAQTK.A	1129,62116	431,9
27	gi|15799705|ref|NP_285717.1| 30S ribosomal subunit protein S20			
	5042	K.AFNEM*QPIVDR.Q	1335,63615	392,5
28	gi|133976|sp|P02358|RS6_ECOLI 30S ribosomal protein S6			
	4566	R.YTAAITGAEGK.I	1081,55242	892,4
29	gi|15804575|ref|NP_290616.1|			
	5568	R.LATLPTYEEAIAR.L	1447,77912	256,8
30	gi|15803832|ref|NP_289866.1| 50S			

	ribosomal subunit protein L6			
	4918	R.TLNDAVEVK.H	988,53095	398,2
31	gi|1169721|sp|P46009|FOCD_ECOLI			
	5812	K.SLTGSAGGGNNR.M	1090,52357	645,4
32	gi|16131619|ref|NP_418207.1| D-ribose periplasmic binding protein			
	5357	K.ELANVQDLTVR.G	1257,67974	144,4

Sample 2 from November 20th 2006

	Reference			MW
	Scan(s)	Peptide	MH+	Sp
1	gi|16131979|ref|NP_418578.1| FrdA			
	4715	R.AAIAAAQANPNAK.I	1210,65386	1404,7
	4845	R.AATAGNGNEAAIEAQAAGVEQR.L	2099,01120	3117,3
	5007	R.ANAVVM*ATGGAGR.V	1190,59462	1812,1
	5404	R.ANAVVMATGGAGR.V	1174,59972	1350,2
	6364	R.DADGTTRLEYSDVK.I	1569,73911	632,8
	5875	R.DDVNFLK.H	850,43051	678,3
	5194	K.DLVNQDGGENWAK.I	1445,66555	491,0
	7936	R.FDEHFVLDILVDDGHVR.G	2026,00287	2567,7
	3752	R.GDVVYLDLR.H	1049,56259	815,0
	5960	R.GEGGILVNK.N	886,49926	1129,7
	7734	R.GLVAMNM*MEGTLVQIR.A	1778,89614	2130,9
	7423	R.GLVAM*NM*M*EGTLVQIR.A	1810,88594	1027,5
	7456	R.GLVAM*NM*MEGTLVQIR.A	1794,89104	1998,9
	7391	R.GLVAMNM*M*EGTLVQIR.A	1794,89104	1772,8
	7734	R.GLVAM*NMMEGTLVQIR.A	1778,89614	1290,9
	7456	R.GLVAM*NMM*EGTLVQIR.A	1794,89104	2247,2
	7898	R.GLVAMNMMEGTLVQIR.A	1762,90124	2423,2
	7734	R.GLVAMNMM*EGTLVQIR.A	1778,89614	2414,4
	1374	K.ITTLPPAKR.V	996,62004	188,9
	7552	R.KGNTISTPR.G	973,54252	691,2
	3684	R.LAGEQATER.A	974,49015	722,8
	7886	R.LGSNSLAELVVFGR.L	1461,80600	1989,4
	7685	R.LKDLVNQDGGENWAK.I	1686,84457	1961,8
	7636	-.M*QTFQADLAIVGAGGAGLR.A	1891,96944	2093,8
	7272	R.RPDGSVNVR.R	999,53302	711,7
	3236	R.VYGGEADAADK.A	1095,49529	448,4
	6674	R.VYGGEADAADKAEAANK.K	1679,78712	1440,7
	7195	R.YLQDYGMGPETPLGEPK.N	1894,88914	2028,5
	7142	R.YLQDYGM*GPETPLGEPK.N	1910,88404	2076,9
2	gi|15830995|ref|NP_309768.1| CoA-linked acetaldehyde dehydrogenase			
	4589	R.AAALAAADAR.I	900,48976	1014,6
	7659	K.AADIVLQAAIAAGAPK.D	1479,85295	2609,0
	7269	R.AKDFEDAVEK.A	1151,55789	768,8
	2305	R.AVASVLMSK.T	905,51246	697,9
	3079	R.DYVEGETAAK.K	1082,50005	660,0
	6886	R.EAGVQEADFLANVDK.L	1605,77549	715,4
	5421	R.EYASFTQEQVDK.I	1444,65907	669,4
	7837	R.FATHGGYLLQGK.E	1291,67935	1398,4
	7168	K.IAELAGFSVPENTK.I	1475,77404	1245,8

7715	R.ILINTPASQGGIGDLYNFK.L	2021,07022	2069,5
5140	K.MAVAESGM*GIVEDK.V	1452,67088	746,8
5630	K.M*AVAESGMGIVEDK.V	1452,67088	2513,8
6378	K.MAVAESGMGIVEDK.V	1436,67598	2723,0
6361	K.M*AVAESGM*GIVEDK.V	1468,66578	1215,5
7832	R.NAIIFSPHPR.A	1151,63200	1277,5
3038	K.NGALNAAIVGQPAYK.I	1486,80125	816,5
7645	K.QILLDTYYGR.D	1241,65246	404,3
7750	R.YAEIADHLGLSAPGDR.T	1684,82892	2064,5
gi|16130152|ref|NP_416719.1| outer 3 membrane protein 1b			
8613 - 8665	R.DAGINTDNIVALGLVYQF.-	1922,98582	1243,5
6760	K.DGNKLDLYGK.V	1122,57896	502,2
3774	K.DVDGDQTYMR.L	1199,49973	581,0
3741	K.DVDGDQTYM*R.L	1215,49463	779,9
6518	K.FQDVGSFDYGR.N	1290,57494	1344,2
5892	R.GYDDEDILK.Y	1067,48915	617,1
7444	K.INLLDDNQFTR.D	1348,68555	1114,4
4522	K.NGNPSGEGFTSGVTNNGR.D	1764,78958	1410,7
4699	K.NM*STYVDYK.I	1136,49284	552,0
6100	K.NMSTYVDYK.I	1120,49794	609,9
6914	K.RTDAQNTAAYIGNGDR.A	1722,81540	1202,1
4118	R.TDAQNTAAYIGNGDR.A	1566,71429	1934,3
7314	R.VAFAGLK.F	705,42939	384,9
6910	R.VGSLGWANK.A	931,49959	670,7
7093	K.YDANNIYLAAQYTQTYNATR.V	2354,10476	2258,6
7307	K.YVDVGATYYFNK.N	1439,68416	1953,2

4	gi|15834157|ref|NP_312930.1| protein chain elongation factor EF-Tu			
	5215	R.AFDQIDNAPEEK.A	1376,63285	1024,8
	7279	R.AGENVGVLLR.G	1027,58947	874,0
	7948	R.AIDKPFLLPIEDVFSISGR.G	2117,16412	1299,8
	5997	K.ALEGDAEWEAK.I	1218,56371	1166,5
	7566	R.ELLSQYDFPGDDTPIVR.G	1964,96000	963,5
	7531	K.FESEVYILSK.D	1214,63033	1286,3
	7927	K.MVVTLIHPIAMDDGLR.F	1780,94482	1160,1
	7921	R.QVGVPYIIVFLNK.C	1489,87771	490,6
	7879	K.TTLTAAITTVLAK.T	1303,78314	1939,3
	6896	K.VGEEVEIVGIK.E	1171,65688	1401,5
5	gi|15800564|ref|NP_286576.1| global regulator			
	7449	K.AIGEAKDDDTADILTAASR.D	1932,95089	2768,6
	2298	K.ATNLLYTR.N	951,52581	1133,3
	6525	K.ATVELLNR.Q	915,52581	1249,1
	6903	R.AVQLGGVALGTTQVINSK.T	1755,99632	1154,4
	5070	K.DDDTADILTAASR.D	1363,63358	1271,2
	6521 - 7113	R.DLDKFLWFIESNIE.-	1768,87923	1298,6
	7900	R.QVIQFIDLSLITK.Q	1517,89376	1528,0
	6407	R.TALIDHLDTMAER.A	1485,73660	1701,6
	6163	R.YAIVANDVR.K	1020,54727	1095,5
6	gi|16129204|ref|NP_415759.1| OppA			
	5738	K.AQGNMPAYGYTPPYTDGAK.L	2001,90110	1134,3
	5208	K.AQGNM*PAYGYTPPYTDGAK.L	2017,89600	1163,0
	4183	K.DPLDNTYTR.N	1094,51128	560,3
	7673	R.HQGTFDVAR.A	1030,50647	535,1
	5063	K.IEGVPESNISR.D	1200,62189	267,1
	7752	K.LTQPEWFGWSQEK.R	1635,78018	441,6
	6744	K.SPAFDSIM*AETLK.V	1425,69299	1079,3
	7795	K.SPAFDSIMAETLK.V	1409,69809	1845,3
	7251	K.WTQPGNIVTNGAYTLK.D	1762,91226	766,5
7	gi|16128548|ref|NP_415097.1| outer membrane protein 3b (a) protease VII			
	4463	R.DDIGSFPNGER.A	1206,53856	716,7
	7820	K.GWLLNEPNYR.L	1261,63240	388,3
	7309	R.LGLMAGYQESR.Y	1224,60413	1208,0
	6032	R.LGLM*AGYQESR.Y	1240,59903	1502,4
	7738	K.MPYIGLTGSYR.Y	1257,62962	984,1
	7545	K.NGAGIENYNFITTAGLK.Y	1782,90209	1516,1
	5712	R.VYLAEEGGR.K	993,49999	777,4
	6884	K.VYVEGAWNR.V	1093,54252	788,1
	7447	R.YEDFELGGTFK.Y	1305,59976	1344,7
8	gi|15804747|ref|NP_290788.1| fumarate reductase			
	7869	K.DFLIATLKPR.-	1173,69902	964,6
	5316	K.DNLAPDLSYR.W	1163,56913	668,8
	7710	R.DYTDGMKVEALANFPIER.D	2069,00082	1680,1
	7605	R.DYTDGM*KVEALANFPIER.D	2084,99572	559,1
	7202	K.HVDPAAAIQQGK.V	1234,65386	1213,5
	4055	R.TADQGTNIQTPAQM*AK.Y	1690,80646	974,5
	4403	R.TADQGTNIQTPAQMAK.Y	1674,81156	1028,3

	7433	K.VEALANFPIER.D	1258,67901	1777,1
9	gi|15800816|ref|NP_286832.1| outer membrane protein 3a			
	4537	K.AQGVQLTAK.L	915,52581	605,8
	5724	K.DGSVVVLGYTDR.I	1280,64811	1300,8
	5450	K.GIKDVVTQPQA.-	1155,63681	978,6
	5854	R.IGSDAYNQGLSER.R	1409,66555	1346,0
	7743	K.LGYPITDDLDIYTR.L	1654,83228	961,2
	7883	R.RAQSVVDYLISK.G	1378,76889	1169,3
	7790	R.RVEIEVK.G	872,51999	350,2
	7601	K.SDVLFNFNK.A	1083,54694	1027,4
10	gi|16131619|ref|NP_418207.1| D-ribose periplasmic binding protein			
	6450	K.ELANVQDLTVR.G	1257,67974	426,7
	7260	K.FNVLASQPADFDR.I	1479,72267	523,3
	7538	K.ILLINPTDSDAVGNAVK.M	1739,95379	1015,3
	6805	K.LAATIAQLPDQIGAK.G	1509,86352	385,0
	7100	K.MANQANIPVITLDR.Q	1555,82609	851,0
	6424	K.SDVMVVGFDGTPDGEK.A	1652,74723	521,8
	6732	K.VIELQGIAGTSAAR.E	1385,77470	2150,4
11	gi|15802193|ref|NP_288215.1| glyceraldehyde-3-phosphate dehydrogenase A			
	7211	K.AGIALNDNFVK.L	1161,62625	853,9
	5131	R.FDGTVEVK.D	894,45672	852,0
	2010	R.GASQNIIPSSTGAAK.A	1401,73323	988,3
	6969	K.LVSWYDNETGYSNK.V	1675,75984	1239,3
	6690	K.VGINGFGR.I	819,44716	749,6
	7890	K.VLDLIAHISK.-	1108,67247	933,3
	7342	R.VPTPNVSVVDLTVR.L	1495,84787	1733,4
12	gi|15834378|ref|NP_313151.1|			
	7311	R.AAVEEGVVAGGGVALIR.V	1567,88023	1188,1
	5266	K.AIAQVGTISANSDETVGK.L	1760,90248	982,6
	6191	K.AVTAAVEELK.A	1030,57790	563,7
	5619	K.DTTTIIDGVGEEAAIQGR.V	1845,91886	1565,3
	3822	R.GQNEDQNVGIK.V	1201,58076	483,1
	2960	R.GVNVLADAVK.V	985,56767	544,6
13	gi|15802089|ref|NP_288111.1| murein lipoprotein			
	5816	K.IDQLSSDVQTLNAK.V	1531,79623	1515,7
	3580	R.LDNM*ATK.Y	808,38692	498,5
	3374	R.LDNMATK.Y	792,39202	515,0
	6336	R.SDVQAAKDDAAR.A	1246,60222	1328,4
	5528	K.VDQLSNDVNAM*R.S	1377,64269	1636,3
	5443	K.VDQLSNDVNAMR.S	1361,64779	1485,2
14	gi|15832893|ref|NP_311666.1| enolase			
	7703	K.AVAAVNGPIAQALIGK.D	1492,88459	1361,6
	6655	K.DAGYTAVISHR.S	1189,59601	1412,4
	6681	K.IM*IDLDGTENK.S	1264,60893	1383,2
	6653	K.IMIDLDGTENK.S	1248,61403	870,1
	7680	K.IQLVGDDLFVTNTK.I	1562,84245	1524,0
	7165	R.SGETEDATIADLAVGTAAGQIK.T	2118,05608	2969,9
15	gi|15833050|ref|NP_311823.1| fructose-bisphosphate aldolase class II			
	1440	R.AGQTSMIAR.L	934,47748	543,3

	1414	R.AGQTSM*IAR.L	950,47238	334,8
	2665	K.ANEAYLQGQLGNPK.G	1502,75978	1230,7
	7556	K.APVIVQFSNGGASFIAGK.G	1762,94865	1664,7
	2487	R.DSQEYVSK.K	955,43672	609,0
16	gi|16131180|ref|NP_417760.1| 50S ribosomal subunit protein L15			
	7286	R.GFEGGQMPLYR.R	1254,59357	347,6
	2562	R.GFEGGQM*PLYR.R	1270,58847	226,9
	4598	R.LNTLSPAEGSK.K	1116,58953	199,6
	6599	K.VEGGVVDLNTLK.A	1243,68924	1055,1
	7281	K.VILAGEVTTPVTVR.G	1454,85771	576,1
17	gi|15803853|ref|NP_289887.1| GTP-binding protein chain elongation factor EF-G			
	6971	K.GGVIPGEYIPAVDK.G	1414,75766	407,2
	6343	K.VEVETPEENTGDVIGDLSR.R	2058,98258	1524,2
	6630	R.VYSGVVNSGDTVLNSVK.A	1737,90176	1067,3
	6978	K.YLGGEELTEAEIK.G	1451,72642	1482,6
18	gi|15803830|ref|NP_289864.1| 30S ribosomal subunit protein S5			
	4972	R.ATIDGLENM*NSPEM*VAAK.R	1922,88337	897,9
	5749	R.ATIDGLENMNSPEM*VAAK.R	1906,88847	473,5
	2683	K.AYGSTNPINVVR.A	1290,68008	617,3
	7468	R.VFMQPASEGTGIIAGGAMR.A	1892,93571	1887,2
19	gi|15799694|ref|NP_285706.1| chaperone Hsp70			
	4148	K.ASSGLNEDEIQK.M	1290,61720	625,9
	7561	R.IINEPTAAALAYGLDK.G	1659,89521	1716,3
	7437	R.QAVTNPQNTLFAIK.R	1544,84312	882,6
	7407	K.SLGQFNLDGINPAPR.G	1598,82853	674,8
20	gi|16130827|ref|NP_417401.1| phosphoglycerate kinase			
	6891	R.ADLNVPVKDGK.V	1155,63681	649,9
	6609	K.SLYEADLVDEAK.R	1352,65800	801,6
	7729	K.SLYEADLVDEAKR.L	1508,75911	1740,5
	6322	R.VATEFSETAPATLK.S	1464,75805	1112,0
21	gi|16128870|ref|NP_415423.1| formate acetyltransferase 1			
	7514	R.DAIPTQSVLTITSNVVYGK.K	2006,08045	949,4
	7647	K.LATAWEGFTK.G	1123,57824	754,1
	6997	K.SGVLTGLPDAYGR.G	1305,67974	836,9
	7213	R.VDDLAVDLVER.F	1243,65286	1940,2
22	gi|15800772|ref|NP_286786.1| 30S ribosomal subunit protein S1			
	5679	K.AYEDAETVTGVINGK.V	1566,76459	894,7
	7130	R.DQLLENLQEGMEVK.G	1645,81016	658,9
	7542	K.GATVELADGVEGYLR.A	1549,78566	743,4
	5752	K.SESAIPAEQFK.N	1206,60009	349,4
23	gi|15802947|ref|NP_288976.1| cysteine synthase A			
	3945	K.AEEIVASNPEK.Y	1186,59501	625,7
	7297	K.ALGANLVLTEGAK.G	1256,72088	1197,4
	7288	K.NIVVILPSSGER.Y	1283,73178	555,7
	6520	K.VIGITNEEAISTAR.R	1473,79075	1214,3
24	gi|15804792|ref|NP_290833.1| 50S ribosomal subunit protein L9			
	5999	R.DIADAVTAAGVEVAK.S	1429,75330	617,7

	7069	K.INALETVTIASK.A	1259,72054	951,9
	2725	K.LAEVLAAANAR.A	1098,62658	1080,5
	6359	K.VANLGSLGDQVNVK.A	1413,76962	510,2
25	gi|30065018|ref|NP_839189.1| tryptophanase			
	7633	R.FAENAYFIK.Q	1102,55677	1036,8
	7811	R.GAEQIYIPVLIK.K	1343,79331	803,8
	6990	K.GNFDLEGLER.G	1149,55348	1133,9
	7121	R.SYYALAESVK.N	1130,57282	1194,0
26	gi|15834105|ref|NP_312878.1| glycerol kinase			
	6625	R.ATLESIAYQTR.D	1252,65319	412,9
	7407	R.SNTGLVIDPYFSGTK.V	1598,80606	744,1
	4084	R.SSEVYGQTNIGGK.G	1339,64883	321,2
	6181	K.YIVALDQGTTSSR.A	1410,72233	1459,5
27	gi|15803840|ref|NP_289874.1| 50S ribosomal subunit protein L16			
	7699	R.GLAQGTDVSFGSFGLK.A	1583,80640	2277,6
	7463	K.VLYEMDGVPEELAR.E	1620,79378	756,5
	6555	K.VLYEM*DGVPEELAR.E	1636,78868	366,0
28	gi|16128896|ref|NP_415449.1| outer membrane protein 1a			
	4558	R.TNLQEAQPLGNGK.K	1369,70702	657,8
	1448	R.VGGVATYR.N	822,44683	523,5
	6448	K.YDANNIYLAANYGETR.N	1847,85587	931,2
29	gi|15833433|ref|NP_312206.1| 30S ribosomal subunit protein S3			
	1528	R.LGGAEIAR.T	786,44683	718,2
	6812	K.LVADSITSQLER.R	1331,71652	1717,4
	7465	K.VVADIAGVPAQINIAEVR.K	1835,03852	545,4
30	gi|15832699|ref|NP_311472.1| putative formate acetyltransferase			
	5532	K.AGYAEDEVVAVSK.L	1337,65834	2166,2
	5478	R.FNSLTPEQQR.D	1219,60658	944,1
	7799	R.VEGGQHLNVNVLR.R	1434,78119	856,3
31	gi|15829780|ref|NP_308553.1|			
	6312	R.ALSNPDLYEGDGELR.V	1648,78131	846,2
	5231	R.EILQDSTVTR.N	1161,61099	864,2
	7237	R.GLIDSSDLPLNVSR.E	1485,79075	1078,2
32	gi|15803832|ref|NP_289866.1| 50S ribosomal subunit protein L6			
	6046	K.APVVVPAGVDVK.I	1150,68304	624,8
	5317	R.DGYADGWAQAGTAR.A	1438,63458	1314,5
	5325	R.TLNDAVEVK.H	988,53095	391,6
33	gi|15804574|ref|NP_290615.1| 50S ribosomal subunit protein L1			
	6319	K.AAGAELVGM*EDLADQIK.K	1746,85783	339,1
	5859	R.VAVFTQGANAEAAK.A	1376,71685	868,0
	7158	R.VVGQLGQVLGPR.G	1222,72663	1753,0
34	gi|15804575|ref|NP_290616.1| 50S ribosomal subunit protein L10			
	7170	K.AAAFEGELIPASQIDR.L	1687,86498	725,7
	7349	R.LATLPTYEEAIAR.L	1447,77912	364,3
	6522	K.QAIVAEVSEVAK.G	1243,68924	851,2
35	gi|16130476|ref|NP_417046.1| serine hydroxymethyltransferase			
	2482	K.SPFVTSGIR.V	963,52581	709,0

	1473	R.VM*QAQGSQLTNK.Y	1320,65761	406,2
	1451	R.VMQAQGSQLTNK.Y	1304,66271	566,0
36	gi|3915453|sp|P76335|YEDS_ECOL I			
	6760	K.DGNKLDLYGK.V	1122,57896	502,2
	6100	K.NMSTYVDYK.I	1120,49794	609,9
	4699	K.NM*STYVDYK.I	1136,49284	552,0
37	gi|16129338|ref|NP_415895.1| putative outer membrane protein			
	6760	K.DGNKLDLYGK.V	1122,57896	502,2
	6100	K.NMSTYVDYK.I	1120,49794	609,9
	4699	K.NM*STYVDYK.I	1136,49284	552,0
38	gi|16130649|ref|NP_417222.1| lipoprotein			
	5749	K.GQAIIATADGR.V	1072,57455	757,6
	5355	K.IATMGSTGTSSTR.L	1269,61034	664,8
	5302	K.IATM*GSTGTSSTR.L	1285,60524	460,8
39	gi|15799860|ref|NP_285872.1| histone-like protein			
	5759	R.M*ETDLQAK.M	951,44516	795,2
	5889	R.METDLQAK.M	935,45026	367,2
	6800	K.TGVSNTLENEFK.G	1338,65359	658,3
40	gi|15834164|ref|NP_312937.1| RNA polymerase beta subunit			
	5023	R.AVAVDSGVTAVAK.R	1187,66303	475,6
	7255	K.LGPEEITADIPNVGEAALSK.L	2024,05463	919,9
41	gi|33347763|ref|NP_417963.2| Slp			
	2548	K.GNNQPDIQK.S	1013,50105	294,9
	7781	K.SFVAVHNQPGLYVGQQAR.F	1971,01952	1374,2
42	gi|15803847|ref|NP_289881.1| 50S ribosomal subunit protein L3			
	7809	R.IFTEDGVSIPVTVIEVEANR.V	2188,14959	665,5
	6686	R.VTVQSLDVVR.V	1115,64190	1533,2
43	gi|16130342|ref|NP_416911.1|			
	5691	R.DALPTEEEQFAAYK.A	1611,75369	223,4
	4736	K.ISADQVDQEVER.F	1388,66521	1106,0
44	gi|15799705|ref|NP_285717.1| 30S ribosomal subunit protein S20			
	6849	K.AFNEMQPIVDR.Q	1319,64125	874,3
	5672	K.AFNEM*QPIVDR.Q	1335,63615	420,0
45	gi|15801645|ref|NP_287662.1|			
	6062	K.DGEDPGYTLYDLSER.L	1729,75515	1681,0
	2183	K.LQGIAQQNSFK.H	1233,65861	498,7
46	gi|16131389|ref|NP_417974.1| glutamate decarboxylase isozyme			
	6062	K.DGEDPGYTLYDLSER.L	1729,75515	1681,0
	2183	K.LQGIAQQNSFK.H	1233,65861	498,7
47	gi|15803846|ref|NP_289880.1| 50S ribosomal subunit protein L4			
	5710	K.DAQSALTVSETTFGR.D	1582,77074	663,7
	7589	R.DATGIDPVSLIAFDK.V	1561,81081	1296,9
48	gi|16129562|ref|NP_416121.1| hypothetical protein			
	5587	R.IVQSPDVIPADSEAGR.A	1653,84424	800,6
	4283	R.QIDANQGGNQR.I	1200,57159	170,5

49	gi|15804576|ref|NP_290617.1| 50S ribosomal subunit protein L7/L12			
	5602	K.ALEEAGAEVEVK.-	1244,63687	1095,7
	5544	K.DLVESAPAALK.E	1113,61502	603,8
50	gi|15800457|ref|NP_286469.1| peptidoglycan-associated lipoprotein			
	6146	R.GTPEYNISLGER.R	1335,65392	354,7
	6380	K.GVSADQISIVSYGK.E	1423,74274	1307,2
51	gi|15803823|ref|NP_289857.1| 30S ribosomal subunit protein S4			
	6023	K.AALELAEQR.E	1000,54219	687,8
	6651	R.LSDYGVQLR.E	1050,55784	1134,0
52	gi|16130437|ref|NP_417007.1| putative dehydrogenase			
	5824	R.GESAPTTAFGAAVVGGDNGR.V	1833,87258	751,6
	6209	R.IYLVDQNDR.V	1135,57421	475,4
53	gi|15799688|ref|NP_285700.1| transaldolase B			
	4787	K.ELAESEGAIER.K	1203,58517	355,3
	4717	K.LYNDAGISNDR.I	1237,58076	1345,0
54	gi|15803848|ref|NP_289882.1| 30S ribosomal subunit protein S10			
	6611	R.LIDQATAEIVETAK.R	1501,81081	954,2
	6441	R.LVDIVEPTEK.T	1142,63033	731,4
55	gi|15804334|ref|NP_290373.1| membrane-bound ATP synthase			
	6942	R.VNAEYVEAFTK.G	1270,63139	1285,3
	5782	R.VVNTLGAPIDGK.G	1183,66811	968,5
56	gi|15804573|ref|NP_290614.1| 50S ribosomal subunit protein L11			
	6048	K.AADMTGADIEAMTR.S	1452,64574	640,8
	5133	R.AQLQEIAQTK.A	1129,62116	669,5
57	gi|10955180|ref|NP_052173.1| beta-lactamase			
	7617	R.QIAEIGASLIK.H	1142,67795	343,8
	4803	R.VDAGQEQLGR.R	1072,53816	491,4
58	gi|15800566|ref|NP_286578.1| outer membrane protein X			
	5981	K.FQTTEYPTYK.H	1277,60484	395,9
	6688	K.NQYYGITAGPAYR.I	1473,71210	726,5
59	gi|2506315|sp|P11026|CYDA_ECOL I Cytochrome D ubiquinol oxidase subunit I			
	5878	R.YTPNVADATEAQIQQATK.D	1948,96106	2224,4
60	gi|15802055|ref|NP_288077.1| putative outer membrane protein			
	6534	K.TQGVELEIR.K	1044,56840	744,5
61	gi|16128752|ref|NP_415305.1| MoaD			
	7622	R.ELVGTDATEVAADFPTVEALR.Q	2204,10812	2094,4
62	gi|15804332|ref|NP_290371.1| membrane-bound ATP synthase			
	7584	R.QIASLGIYPAVDPLDSTSR.Q	2003,04440	1092,0